

Äspö Hard Rock Laboratory

Interpretation of conductive features at the -450 m level, Äspö

Ingemar Markström
Niklas Bockgård
Golder Associates

Carljohan Hardenby
Vattenfall Power Consultant

Peter Hultgren
Svensk Kärnbränslehantering AB

May 2010

Svensk Kärnbränslehantering AB

Swedish Nuclear Fuel
and Waste Management Co
Box 5864
SE-102 40 Stockholm Sweden
Tel. 80-459 84 00
+46 8 459 84 00
Fax 08-661 57 19
+46 661 57 19



**Äspö Hard Rock
Laboratory**

Report no.	No.
IPR-10-12	F69
Author	Date
Ingemar Markström	May 2010
Niklas Bockgård	
Carljohan Hardenby	
Peter Hultgren	
Checked by	Date
Leif Stenberg	2010-05-07
Approved	Date
Mats Ohlsson	2011-02-25

Äspö Hard Rock Laboratory

Interpretation of conductive features at the -450 m level, Äspö

Ingemar Markström
Niklas Bockgård
Golder Associates

Carljohan Hardenby
Vattenfall Power Consultant

Peter Hultgren
Svensk Kärnbränslehantering AB

May 2010

Keywords: Äspö HRL, Conductive features, RVS-models, GeoMod, APSE, Prototype, TRUE block scale.

This report concerns a study which was conducted for SKB. The conclusions and viewpoints presented in the report are those of the author(s) and do not necessarily coincide with those of the client.

Abstract

The interpretation of conductive features at the -450 m described in this report concerns a part of the tunnel system of the Äspö Hard Rock Laboratory (Äspö HRL). The result of the modelling work is presented as an RVS-model (Rock Visualization System). When drilling some bore holes for the Mini-Can Project in the NASA3384A niche at Äspö HRL some highly transmissive structures were penetrated. This gave a pressure drop response particularly in the Micobe experiment area (the end of TASJ-tunnel) but also in some adjacent areas at the same level. To better understand the complex hydraulic conditions of this part of the tunnel system it was understood that a new interpretation of conductive features was needed.

The length axis of the model volume runs along the TASA-tunnel from section 3/260-3/600 m (end of tunnel in the Prototype repository). Laterally the model volume reaches 80 m perpendicular to the length axis in both directions and vertically it reaches to the 350 m and 500 m level respectively.

All major water-bearing structures recorded by previously performed geological mapping of the tunnels and drifts (TASF, TASI, TASJ, TASG, TASQ and TASA) at this level of the Äspö HRL were considered and formed the base for the modelling work. Also some potentially water-bearing open fractures in the tunnels were taken into account. Structures considered as large are those that can be traced over most of a tunnel periphery. No particular concern has been taken about deformation zones unless they were water bearing or acted as hydraulic barriers.

A total of 212 cored boreholes penetrated or were identified close to the model volume. 39 of these were intersected by the modelled structures. Various features such as open fractures, fractures identified by bore hole radar, RQD, water inflow etc. were used in the modelling work. A number of earlier RVS-models such as the Geomod, the APSE, the Prototype, the TRUE BS model etc. that have been created within or close to the present model volume have also been considered in the modelling work. The modelled structures are classified as main or minor structures. Main structures in the model have been extended to the boundary of the model volume unless reasons have been found not to do so. Such reasons could be lack of identification in boreholes or tunnels intersecting the tentative path of the structure. In these cases the structure in question was terminated against another structure. Minor structures are generally terminated against intersecting structures and their vertical extension is limited to be roughly similar to the lateral extension.

In total, 38 structures have been modelled within this project. Structures that could be connected between several tunnels and/or boreholes were given a higher confidence than those that could not be connected. Hydraulic connectivity was given a high weight in the confidence assessment since the work concerned a hydro-structural model. All the modelled structures were classified according to a confidence classification system containing three confidence classes: possible, probable and certain. Even if the exact geometry and position of each individual structure sometimes can be somewhat uncertain, the over all pattern is well supported by all the observations in boreholes and tunnels and by hydraulic measurements.

The drilling of the new the Mini-Can bore holes affected not only the Microbe experiment area but also the inflow in the nearby TASF-tunnel. The distance between the Mini-Can site and the Microbe experiment site as well as the TASF is about 150 m in a WNW direction. This direction coincides well with the general picture of WNW trending hydraulic active structures in this part of the Äspö HRL. Earlier studies have shown that these structures commonly form clusters of steeply dipping sub-parallel fractures, so called fracture swarms. In the present model it is believed that the monitored pressure responses in the Microbe and the Mini-Can sites are transmitted via such sub-parallel structures. The general WNW to NW orientation of water-bearing steeply dipping structures is verified by previous observations in the Äspö HRL tunnels, such as the TASA- and the TASQ-tunnels within the model volume. Many of these WNW to NW oriented structures have been connected in the present model.

Water-bearing structures in one area that are hydraulically connected with structures found in another area, for example in two tunnels, may not always be continuous as individual structures. It may very well be that sub-parallel structures are connected by other vertical cross-cutting structures, horizontal fractures and/or bore holes. The interpretations made in this model are only valid within the model volume. Interpretations of common structures used in this model as well as in other models are discussed. Different combinations of observations have led to different interpretations in the various models. Regional structures have not been taken into account unless they actually intersect the model volume or are found in close vicinity. It could be interesting to review the interpretations of modelled structures in some of the already existing models in the area to see if new interpretations could be made based on both interpretations.

Sammanfattning

Denna rapport beskriver tolkning av konduktiva strukturer över en del av Äspölaboratoriets tunnelsystemet belägen på c:a -450 m nivå. Resultatet av modellarbetet presenteras i RVS (Rock Vizualisation System). När man borrade ett antal hål för det s.k. Mini-Can projektet i NASA3384A-nischen på Äspölaboratoriets -450 m nivå penetrerades ett antal starkt hydro-konduktiva strukturer. Detta orsakade ett tryckfall framför allt i området kring det s.k. Microbe-experimentet (slutet på TASJ-tunneln) men även i intilliggande delar av Äspötunnelsystemet. För att bättre förstå de ganska komplexa hydrauliska förhållandena i denna del av tunnelsystemet var en tolkning av konduktiva strukturer önskvärd. Modellens längdaxel löper längs TASA-tunneln från sektion 3/260-3/600 m (d.v.s. till slutet av Prototypförvaret). Åt sidorna sträcker sig modellen c:a 80 m vinkelrätt mot längdaxeln och i vertikal led uppåt till -350 m och neråt till -500 m nivån.

Alla större registrerade vattenförande strukturer/sprickor från tidigare utförda geologiska karteringar i tunnarna kring -450 m nivån (TASF, TASI, TASJ, TASG, TASQ and TASA) har utnyttjats och bildat stommen i modelleringsarbetet. Även en del större strukturer som kunde vara potentiellt vattenförande inkluderades i arbetet. Som stora strukturer definieras de som kan följas över större delen av tunnelperiferin. Hänsyn har tagits till deformationszoner endast om de varit vattenförande eller har fungerat som en hydraulisk barriär.

Totalt 212 kärnborrhål penetrerade modellvolymen eller befann sig i dess närhet. 39 av hålen genomkorsades av de modellerade strukturerna. Ett flertal parametrar såsom t.ex. öppna sprickor, sprickor identifierade med borrhålsradar, RQD, vatteninflöde etc. användes i modelleringsarbetet. Hänsyn har även tagits till ett flertal tidigare RVS-modeller som Geomod-, APSE-, Prototype- och TRUE BS-modellerna vilka har skapats inom eller nära den nu aktuella modellvolymen. De modellerade strukturerna klassificeras som huvudstrukturer (main) och mindre strukturer (minor). Huvudstrukturerna har dragits ut till modellvolymens ytterkanter såvida det inte har funnits goda skäl att avsluta dem tidigare. Sådana skäl kunde vara att en struktur inte kunde återfinnas i t.ex. borrhål eller tunnlar som skar den tänkta sträckningen av strukturen i fråga. Den aktuella strukturen avslutades då mot en annan struktur. De mindre strukturerna klipps i allmänhet mot första korsande struktur och deras utbredning i höjddled begränsas så den är ungefär lika stor som den laterala utbredningen.

Totalt modellerades 38 strukturer. Strukturer som kunde följas mellan flera tunnlar och eller borrhål gavs en högre förtroendegrad än de som inte kunde följas på detta sätt. Det sattes även en hög tillit till hydrauliska samband vid bedömningen av en struktur eftersom arbetet framför allt gick ut på att skapa en hydro-strukturell modell. Alla de modellerade strukturerna klassificerades enligt ett särskilt klassificeringssystem med tre tillförlitlighetsklasser: möjlig (possible), trolig (probable) och säker (certain). Även om inte alltid den exakta geometrin och läget för varje individuell struktur har varit helt säkert så är det generella mönstret väl underbyggt genom alla observationer i borrhål och tunnlar och genom utförda hydrauliska mätningar.

Borrningen av de nya hålen för Mini-Can-projektet påverkade inte bara trycket i området för Microbe-experimentet utan även inflödet till den närliggande TASF-tunneln. Avståndet från de senare till Mini-Can-området, samt TASF, är c:a 150 m i WNW-ESE-riktning. Denna riktning överensstämmer väl med den generella bilden av WNW-liga hydrauliskt aktiva strukturer i detta område av Äspölaboratoriets tunnelsystem. Tidigare studier har visat att dessa strukturer ofta bildar svärmar av brant stående sub-parallella sprickor, s.k. spricksvärmar. De registrerade tryckresponserna mellan Mini-Can- och Microbe-experimentområdena har i den nu aktuella modellen ansetts vara överförda via sådana sub-parallella strukturer. Den generella WNW till NW-liga orienteringen av vattenförande brantstående strukturer är verifierad genom tidigare observationer i Äspölaboratoriets tunnelsystem såsom i TASA- och TASQ-tunnlarna inom modellvolymen. Många av dessa WNW till NW-liga strukturer har knutits samman i den nu aktuella modellen.

Det kan påpekas att vattenförande strukturer som påträffats i ett område och som har ett hydrauliskt samband med strukturer i ett annat område (t.ex. två tunnlar) inte nödvändigtvis behöver vara exakt samma struktur hela vägen. Det kan mycket väl vara sub-parallella strukturer som förbinds av andra korsande branta strukturer, horisontella strukturer och/eller borrhål. Tolkningarna som har gjorts i denna modell gäller endast för området inom modellvolymen. Tolkningar av strukturer som är gemensamma för den nu aktuella modellen och andra modeller diskuteras. Olika kombinationer av observerade strukturer leder till olika tolkningar i de olika modellerna. Regionala storskaliga strukturer har inte tagits i beaktande såvida de inte skär modellvolymen eller befinner sig tätt intill.

Som en fortsättning på det nu utförda modelleringsarbetet kunde det vara intressant att göra en genomgång av tidigare tolkningar av vissa modellerade större strukturer i olika modeller för att se om nya tolkningar går att göra baserade på nya tolkningar.

Contents

1	Introduction - The assignment.....	11
1.1	Background.....	11
1.2	Objectives and scope	12
1.2.1	Objectives.....	12
1.2.2	Scope	12
1.3	Size and location of the model volume	12
2	Background data.....	15
2.1	Borehole data.....	15
2.1.1	Selection of boreholes	15
2.1.2	RVS borehole parameters from SICADA.....	16
2.2	Other data from SICADA, HMS and reports	17
2.3	Tunnel mapping.....	17
2.4	Groutings	18
2.5	Current RVS models in the area.....	18
2.5.1	GeoMod.....	19
2.5.2	APSE.....	19
2.5.3	Prototype	19
2.5.4	TRUE	19
2.5.5	HQ-3.....	20
2.5.6	LX_V.1.2.2_LOC_DZ	20
2.5.7	Review of current models	20
2.6	Compliation of background models and reference files.....	23
3	Modelling methodology	25
3.1	Concept of water bearing structures	25
3.2	WNW trending hydraulic connections at the 450-metre level	26
3.3	Interpolation, extrapolation and termination of structures	27
3.4	Confidence classification.....	29
4	The model of water-bearing structures at the -450 m level, Äspö	31
5	Discussion.....	37
5.1	The validity and limitations of the model.....	37
5.2	Comparison with other models.....	38
5.2.1	GeoMod.....	38
5.2.2	APSE.....	39
5.2.3	Prototype	40
5.2.4	TRUE	40
5.2.5	HQ-3.....	41
5.2.6	LX_V1.2.2_LOC_DZ, Local Laxemar deformation zone model.....	41
5.3	Review of NE-2.....	42
6	Acknowledgements	43
7	References	45
	Appendix A - Structure modelling	49

1 Introduction - The assignment

1.1 Background

While drilling the boreholes for the Mini-Can-experiment in the NASA3384A niche (Figure 1-1) some highly conductive structures were penetrated. At the same time, as the drilling took place, a pressure drop was discovered in the rock mass close to the Microbe experiment area /Pedersen 2005/. This observation indicate that both areas are directly connected by conductive structures. Some pressure drops, observed in the Prototype area, may be connected to the leakage in NASA3384A too. See Figure 1-1 and Figure 1-2 below.

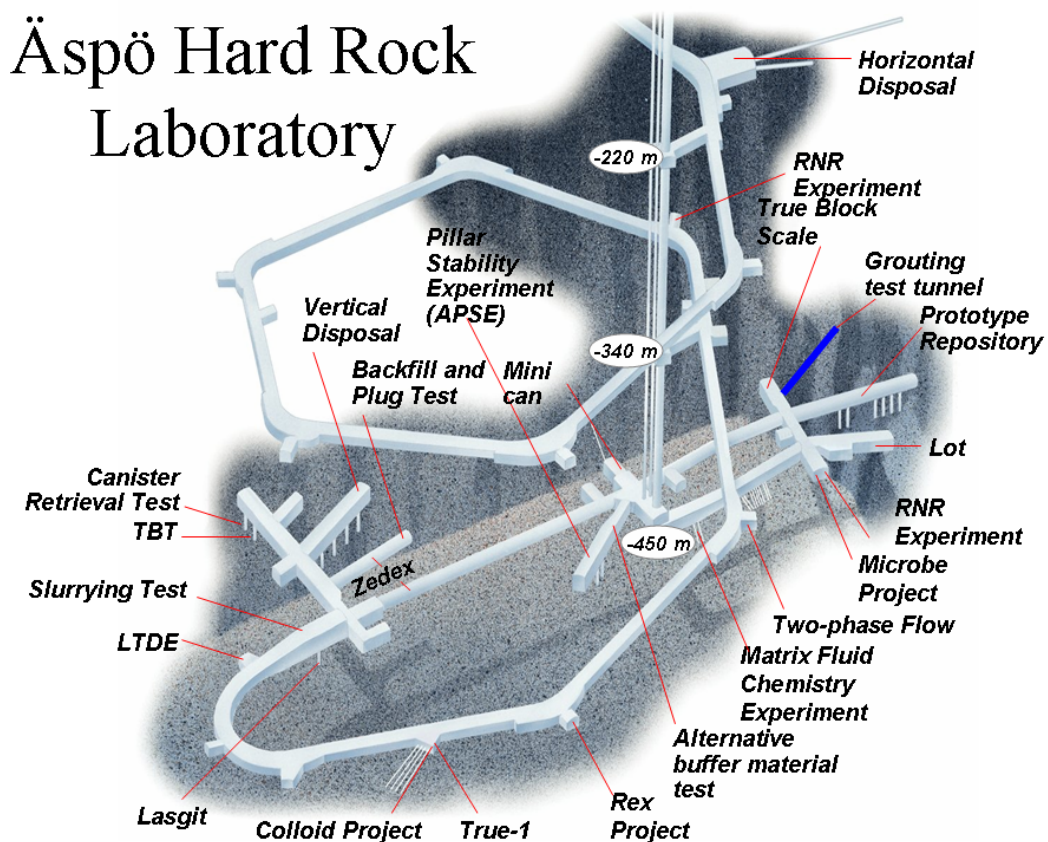


Figure 1-1. Experiment areas in Äspö HRL

Before new tunnels and experiment sites within the laboratory are located it is important to do predictions of the influence on other parts of the laboratory. Experience from the Äspö HRL shows that hydraulic responses may be very complex and therefore difficult to predict and understand. To improve the current understanding there is a need for more detailed hydro-structural modelling work, since the site-scale model, containing only major deformation zones, is at an inappropriate scale. The model scale should range from the so-called block scale to detailed site scale (from 10 m to some hundreds of metres).

As mentioned earlier, it was the observed hydraulic interference between the Mini-Can and the Microbe experiment sites at the 450-metre level that triggered the current modelling work. Moreover, the rationale of selecting the 450-metre level for the modelling exercise was that this level is the most prominent experiment area. This area was also suitable since there is a high concentration of background data.

1.2 Objectives and scope

1.2.1 Objectives

The objective of the work was to model potential water-bearing structures at the -450 m level, an area with many active experiments. The aim was to visualize how water-bearing structures may connect, in order to give a better understanding of the hydraulic connections in the area and the pressure responses monitored between different parts of the tunnel system. It is important to note that the intention is not to create a geological structural model describing e.g. deformation zones on the -450 m level but rather to interpret potentially water bearing structures from observed data. The modelling work was performed in SKB's Rock Visualization System (RVS), an application based on Bentley MicroStation[®]/Curtis et al. 2007/.

1.2.2 Scope

All major water-bearing structures from the TMS database (Tunnel Mapping System) in tunnels TASF, TASI, TASJ, TASG, TASQ and in TASA from section 3/280 to 3/530 were considered in the model. Some data for potentially water-bearing structures (e.g. open fractures and deformation zones) were also used. These were interpreted in conjunction with borehole information. The work was initiated by Björn Magnor and was carried out by Ingemar Markström (RVS modelling) assisted by Niclas Bockgård (hydrogeology), Peter Hultgren and Carljohan Hardenby (geology). Philip Curtis was involved in the initial study of NE-2.

The result of the work comprises an RVS model and this report.

1.3 Size and location of the model volume

The length axis of the model volume has a bearing of 68° from RT90 north and runs along the TASA-tunnel from section 3/260 m to 3/530 m (in the Prototype repository). The model volume has a width of 160 m, extending 80 m from the tunnel axis in both directions and a depth of 150 m, situated between the levels -350 m and -500 m.

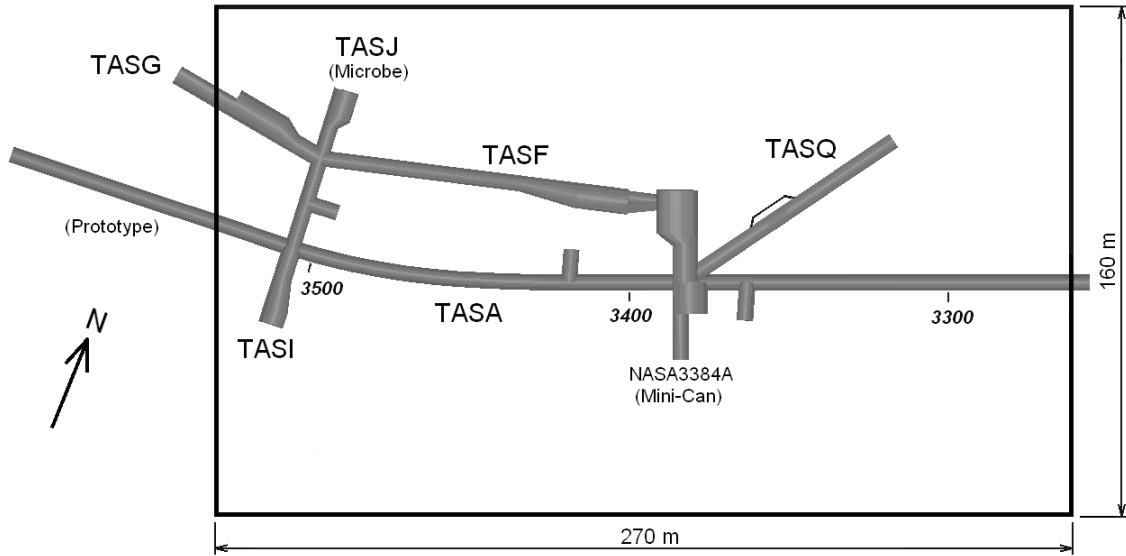


Figure 1-2. Top view of the model volume. Origin: Easting (x) = 1551265, Northing (y) = 6367676, Elevation (z) = -500 Extent: $dx = 270$ m, $dy = 160$ m, $dz = 150$ m. Y-axis bearing: 338° from RT90 north.

The model volume is considered to be large enough to give an idea of how structures interact with each other and across the various tunnels at and around the -450 masl level. Furthermore, it is considered to be small enough to give the modelled extent of the interpreted structures a reasonable degree of confidence. Although some of the structures could be traced outside the model volume it was decided to limit the volume to a size where most of the structures could be verified in the tunnels and boreholes of the volume.

2 Background data

2.1 Borehole data

2.1.1 Selection of boreholes

A total of 212 boreholes have been identified near or in the model volume. The modelled structures intersect 39 of these boreholes. In Tables 2-1 to 2-4 below these boreholes are written in bold.

Table 2-1. Cored boreholes in the A-tunnel (148).

KA2162B	KA3542G01	KA3551G06	KA3573A
KA2511A	KA3542G02	KA3551G07	KA3573C01
KA2563A	KA3543A01	KA3551G08	KA3574D01
KA2598A	KA3543G01	KA3551G09	KA3574G01
KA2599G01	KA3543I01	KA3551G10	KA3575G
KA3191F	KA3544G01	KA3552A01	KA3575G02
KA3375A01	KA3544G02	KA3552G01	KA3575G03
KA3375A02	KA3544G03	KA3552G02	KA3575G04
KA3375A03	KA3545G	KA3552G03	KA3575G05
KA3375A04	KA3545G02	KA3552G04	KA3575G06
KA3375A05	KA3545G03	KA3552H01	KA3575G07
KA3375G01	KA3545G04	KA3553B01	KA3576G01
KA3375G02	KA3545G05	KA3553G01	KA3577G01
KA3375G03	KA3545G06	KA3554G01	KA3578C01
KA3375G04	KA3545G07	KA3554G02	KA3578G01
KA3376A01	KA3545G08	KA3557G	KA3578G02
KA3376A01	KA3545G09	KA3563A01	KA3578H01
KA3377A01	KA3546G01	KA3563D01	KA3579D01
KA3377G01	KA3546G02	KA3563G	KA3579G
KA3378A01	KA3546G03	KA3563I01	KA3581G
KA3378G01	KA3546G04	KA3566C01	KA3584G01
KA3378G02	KA3548A01	KA3566G01	KA3586G01
KA3385A	KA3548D01	KA3566G02	KA3587G
KA3386A01	KA3548G01	KA3568D01	KA3588C01
KA3386A02	KA3548G02	KA3569G	KA3588D01
KA3386A03	KA3548G03	KA3569G02	KA3588G01
KA3386A04	KA3549G01	KA3569G03	KA3588I01
KA3386A05	KA3550G01	KA3569G04	KA3589G01
KA3386A06	KA3550G02	KA3569G05	KA3590G01
KA3510A	KA3550G03	KA3569G06	KA3590G02
KA3536C01	KA3550G04	KA3569G07	KA3592C01
KA3536C02	KA3550G05	KA3569G08	KA3592G01
KA3536D01	KA3551G	KA3569G09	KA3593G
KA3536D02	KA3551G01	KA3569G10	KA3597D01
KA3536H01	KA3551G03	KA3569G11	KA3597G01
KA3536H02	KA3551G04	KA3571G01	KA3597H01
KA3539G	KA3551G05	KA3572G01	KA3600F

Table 2-2. Cored boreholes from side tunnels (47).

KC0045F	KG0037G01	KJ0052F02	KQ0064A05
KF0051A01	KG0042G01	KJ0052F03	KQ0064A06
KF0066A01	KG0046G01	KQ0049A01	KQ0064B01
KF0069A01	KG0048A01	KQ0053A01	KQ0064B02
KF0093A01	KG0051G01	KQ0053A02	KQ0064B03
KG0010B01	KI0023B	KQ0053A03	KQ0064B04
KG0021A01	KI0025F	KQ0053A04	KQ0064B05
KG0023A01	KI0025F02	KQ0055A01	KQ0064B06
KG0027A01	KI0025F03	KQ0064A01	KQ0064B07
KG0032G01	KJ0044F01	KQ0064A02	KQ0065B01
KG0033A01	KJ0050F01	KQ0064A03	KQ0065B02
KG0033G01	KJ0052F01	KQ0064A04	

Note that short boreholes from the floor in the Q-tunnel have been omitted.

Table 2-3. Cored boreholes from the ground surface (3).

KAS02	KAS05	KAS06

Table 2-4. Probe holes from the A-tunnel (14).

SA3436B	SA3508F	SA3547F	SA3583F
SA3445A	SA3509F	SA3561F	SA3584F
SA3448F	SA3526F	SA3562F	
SA3454A	SA3546F	SA3572F	

2.1.2 RVS borehole parameters from SICADA

For the selected boreholes, shown in bold in Tables 2-1 to 2-4 above, the following parameters from SICADA have been visualized in the model. The order date for the data used in the modelling work is 2007-05-14.

Fract_core_ori_open

The parameter *fract_core_ori_open* comes from the SICADA parameter table *Fract_core* and lists all mapped fractures that are not classified as 'sealed', this means that unclassified fractures are also included. See description in Appendix B. The fracture parameter has been visualized as oriented disks along the boreholes.

Rqd_rqd

The parameter *rqd_rqd* is derived from the SICADA parameter table *Rqd*. It is a measure of rock quality. See description in Appendix C. The parameter has been visualised as cylinders along the boreholes where the radius is inversely proportional to the rock quality. Poorer rock (lower RQD) gives thicker cylinders.

Radar_direct_ori_x

The parameters *radar_direct_ori1* and *_ori2* are derived from the SICADA parameter table *Radar_direct* and show radar reflectors in two alternative directions. See description in Appendix D. The radar interpretations have been visualized as oriented disks along the boreholes.

Other RVS parameters

RVS parameters that have been assessed but not visualized are listed below.

- rock_alter-type (used to detect oxidation). See description in Appendix E.
- freq_1m-open_crush (for detecting crush). See description in Appendix F.
- freq_1m-petrocor_crush (for detecting crush). See description in Appendix G.
- fract_crush-pclen (for detecting crush). See description in Appendix H.
- fract_core-ori_broken (broken fractures). See description in Appendix B.
- fract_core-ori_all (all fractures). See description in Appendix B.
- freq_1m-total (fracture frequency). See description in Appendix F.
- freq_1m-open_total (open fracture frequency). See description in Appendix F.
- flow_logging-flow (inflow). See description in Appendix I.
- p_fract_core (SICADA parameter). See description in Appendix B.

2.2 Other data from SICADA, HMS and reports

Borehole data other than RVS parameters from SICADA have also been used in the modelling. These are mainly hydrogeological data and observations found in SICADA or found in official or internal SKB reports for example /Rhén and Forsmark 2001/ but not necessarily reported in SICADA. The data include drilling records and data from various types of flow logging, hydraulic tests, and interference tests. In addition some unpublished data on groundwater pressure responses from the hydro-monitoring system (HMS) have been utilized. The probe hole drilling were performed during the tunnel construction. No probe hole drilling protocols are available, instead measured values for inflow and transmissivity listed in the report SKB PR HRL-96-19 by /Markström I, Erlström M 1996/ have been used.

2.3 Tunnel mapping

All rock surfaces of the tunnels, niches etc at the Äspö Hard Rock Laboratory have been geologically mapped. Field maps have then been digitized and associated data fed into a database. For this work a MicroStation based 2D mapping application called TMS (Tunnel Mapping System) has been used. All geological features, such as fractures, rock types, rock boundaries etc., which appear on a digitized drawing have data attached to them. The database that is used is a Microsoft Access[®] database. The tunnel mapping from the TMS system has been attached to the model as 3D MicroStation[®] DGN files. Attached data have been read directly from the TMS database. Recent mapping work, performed after the conversion of the TMS files to 3D, have also been converted to 3D within this project and have been used as attached reference files. This includes the tunnels TASG, TASI, TASJ and TASQ. Fractures mapped and described in the so called "Fracture Catalogue" /Rhén and Stanfors 1995/ have been attached as a 3D reference file. Shaft mapping in 3D have been attached to the model as 3D MicroStation[®] DGN files.

2.4 Groutings

Inflows, volumes of grout and start sections for the pre-groutings have been obtained from SICADA, see Table 2-5. The lengths of the grouting curtains have been interpreted from the compilation of the tunnel mapping / Markström and Erlström 1996/. In the -450-model the pre-grouting has been visualized along the tunnel as cylinders of the type Fracture observations with a radius proportional to measured total inflow from the grouting holes. Screen 229 and 230 were visualized as one object.

Table 2-5. Pre-grouting.

Screen No.	Start section	Length (m)	Total inflow (l/min)
229	3/376	30	120
230	3/376	30	207
231	3/435	20	52
232	3/455	24	14
233	3/471	25	7.5
234	3/481	35	13.5
235	3/526	22	44

For the complimentary groutings there are no data concerning volumes of grout or inflows. Consequently, these have not been visualized in the model.

2.5 Current RVS models in the area

A number of RVS models have been created in or close to the current project's model volume, see Figure 2-1. Presently, there is no complete model bank where the models can be retrieved and the models, in most cases, were provided by the different modellers. These have been reviewed as reference during the modelling work. The different model volumes are shown below with the exception of GeoMod which covers the entire Äspö island and LX_V.1.2.2_LOC_DZ which covers a much larger area.

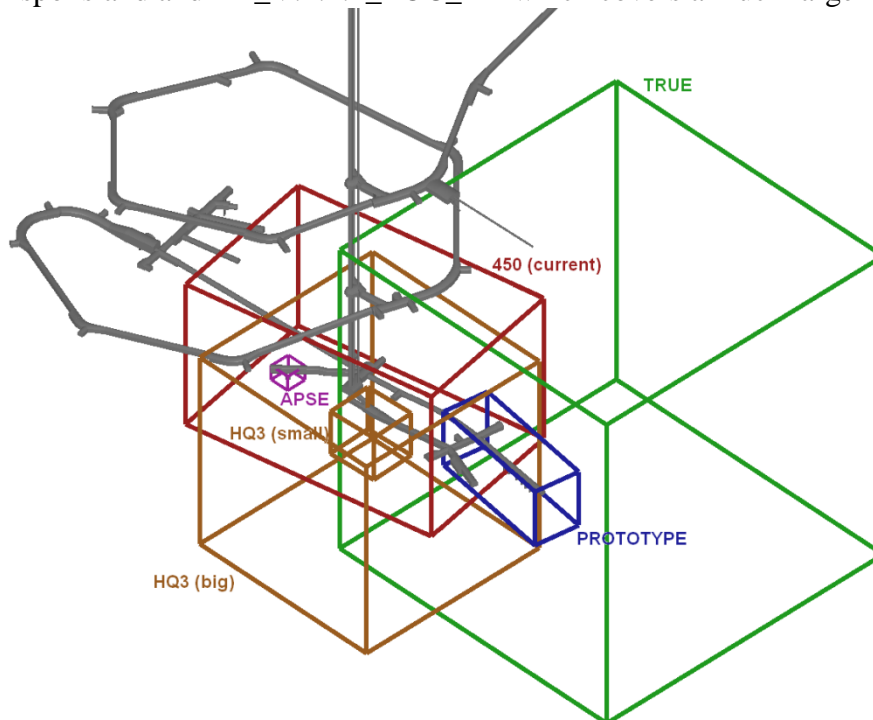


Figure 2-1. RVS model volumes around the Äspö tunnel.

2.5.1 GeoMod

The GeoMod model covers an area of 1000*1000 m, essentially covering southern Äspö, and goes down to a depth of -1000 m. The main purpose of the GeoMod project, was to update the previous geoscientific model of Äspö (Äspö96), mainly by incorporate additional data collected after 1995.

This model can be found in the SIMON Site Model Manager. The model is imported as a RVS background model. The model description can be found in the report by/Berglund et al. 2005/.

2.5.2 APSE

The APSE model covers an area of 20*20 m in the inner part of the Q-tunnel on a depth between -440 to -455 m including the rock volume that will host an experimental pillar between two deposition holes. The aim of the project was 1) to derive material properties for numerical modelling and 2) to ensure that the pillar location is suitable from a structural and rock mechanical point of view. Three fracture sets were modelled in TASQ where the major fracture set is sub-vertical and trending NW. It is also water bearing. The model has been delivered as a MicroStation® DGN file and is attached as a reference file. The model description can be found in the report by /Staub et al. 2004/.

2.5.3 Prototype

The Prototype model covers an area of 130*45 m between approximately -420 to -478 m depth, essentially covering the lowest part of the A-tunnel (after 3/550) and the southern part of the I-tunnel. The model was created in an earlier version of RVS and thus cannot be directly imported to the present version of RVS 3. Therefore, the model has been saved as a MicroStation® DGN file and is attached as a reference file. The model description can only be found in a draft report delivered to SKB by Patel S 2003.

2.5.4 TRUE

The TRUE Block Scale model covers an area of 320*320 m at a depth between approximately -290 to -610 m, covering the lowest part of the A-tunnel, the I-tunnel and an area SW of these tunnels. The general objectives of the TRUE Block Scale Project were to 1) increase understanding of tracer transport in a fracture network and to improve predictive capabilities, 2) assess the importance of tracer retention mechanisms (diffusion and sorption) in a fracture network, and 3) assess the link between flow and transport data as a means for predicting transport phenomena. It was concluded that the conductive geometry of the investigated rock block is made up of steeply dipping deterministic NW structures and NNW structures. The model is imported as an RVS background model. The model description can be found in the report by /Andersson et al. 2002/. The TRUE BS model (a.k.a. the March -00 model) is documented in the report by /Hermanson and Doe 2000/. An older model, covering a larger model volume at the -450 m level is presented in the report by /Hermanson 1998/.

2.5.5 HQ-3

The HQ-3 model covers two areas, a 50 m scale structural model of the HQ-3 Area, with connections to surrounding structures via a 200 m scale model. The aim of the work was to present a 50 m scale structural model of the HQ-3 Area, to the North of the F-tunnel. The larger model volume is 200*200 m between -150 to -350 m depth. The southern part of the model volume covers the J-tunnel, the F-tunnel and the A-tunnel between changes 3/350-3/550 m. The smaller model volume is 50*50 m and goes between -385 to -430 m depth north of the F- tunnel. A dominant structure, Zone Z4, and a water-bearing fracture swarm, NW-hyd intersects the models. The model was created in an earlier version of RVS and thus cannot be directly imported to the present version of RVS 3. Therefore, the model has been saved as a MicroStation® DGN file and is attached as a reference file. The model description can be found in the report by /Hansen and Hermansson 2002/.

2.5.6 LX_V.1.2.2_LOC_DZ

LX_V.1.2.2_LOC_DZ is the official site descriptive deformation zone model for the Laxemar v1.2 local model area. The model with an area of 7800*3200 m covers Laxemar in the western part along with the Simpevarp peninsula, the islands of Ävrö, Hålö, Bockholmen and the main part of the island of Äspö. The model volume reaches down to -1,100 m depth. It can be noted that from v2.2 onwards the local model area will not cover the islands in the east. The model was downloaded from SIMON and imported as an RVS background model. The model description can be found in the report SKB 2006.

2.5.7 Review of current models

Of the existing detailed RVS models the TRUE BS model and the HQ-3 model are of the same scale and cover a larger part of the model volume. The APSE model is very local, centred on the Q-tunnel, and the Prototype model is mainly an extrapolated visualization of mapped structures, Figure 2-1. There also exist a number of earlier conceptual structural models of the modelled volume. The model in Figure 2-2 is based on mapped large single open water-bearing fractures in the A-and F-tunnels, whereas the simple model in Figure 2-3 is based on observed inflow point in boreholes and on pressure responses.

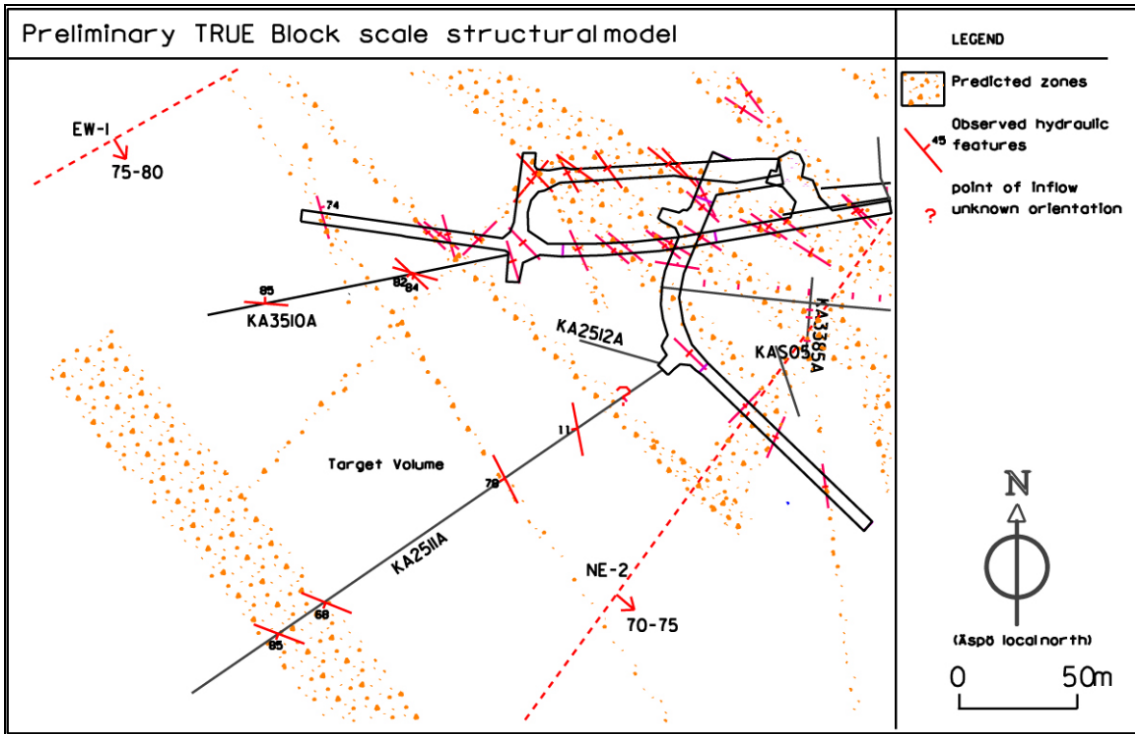


Figure 2-2. A preliminary structural model of the proposed experimental area for the TRUE Block Scale experiment. From /Andersson et al. 2002/.

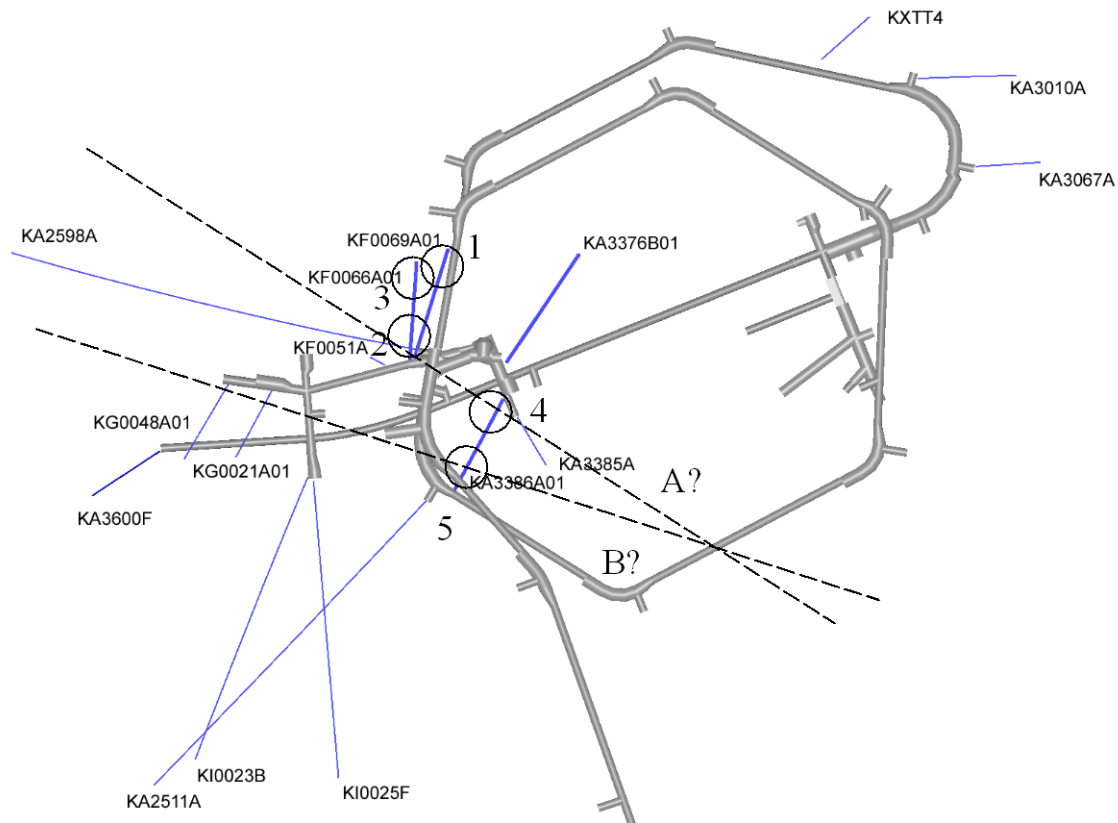


Figure 2-3. Locations of larger inflows (1)–(5) along boreholes KF0069A01, KF0066A01, and KA3386A01. A? and B? represent possible NW trending water-bearing features based on pressure responses. From /Fransson 2003/.

The most detailed hydro-structural model in the Äspö HRL was developed in the TRUE Block Scale project. The iterative modelling methodology can be described as follows: 1) Possible hydraulic structures were identified by inflow records and pressure responses during drilling. 2) Conductors were verified through flow logging. 3) The flow anomalies were associated with geologic features using BIPS and BOREMAP corelog. 4) A feature was designated as a structure in the hydro-structural model if it was associated with anomalies in more than one borehole. 5) The existing model was used to predict intercepts of structures along a given new borehole.

The modelling methodologies used for the APSE and HQ-3 models were similar. As a fracture observation in a tunnel represents a much larger exposed trace than an observation in a borehole, tunnel mapping was primarily used to define structures. Joints with the same orientation indicate that they may not just be more frequent but also more persistent than fractures with random orientation. They were therefore interpreted as more continuous and persistent than other observations. Observations that could be related between two or more boreholes were interpreted as the same structure. The closer the observations were, the higher was the confidence of the interpretation of the potential structure.

2.6 Compilation of background models and reference files

Table 2-6. Background models.

Model	Contents
True_BS_2004-JHE_2005	True Block Scale model, section 2.5.4
LX_V.1.2.2_Hydro_DV-PV	PLU local def. zone model Laxemar, section 2.5.6
Äspö_02_v2	Geomod, model over Äspö island, 2.5.1

Table 2-7. Reference files.

DGN-file	Contents
IS geologimodell APSE.dgn	The APSE model, section 2.5.2
Prototyp_v8.dgn	The Prototyp model, section 2.5.3
HQ-3-restored-v7-cut.dgn	The HQ-3 model, section 2.5.5
Official_tunnel_V3(MS_V8_cd).dgn	The Äspö tunnel, geometry and chainage
LMAT.dgn	Chainage c/c 10m, TASA-tunnel
TK1FR3D.dgn	3D fracture mapping TASA, 0/000-0/750 m
TK2FR3D.dgn	3D fracture mapping TASA, 0/750-1/470 m
TK3FR3D.dgn	3D fracture mapping TASA, 1/0-2/265 m
TK4FR3D.dgn	3D fracture mapping TASA, 2/265-2/875 m
TK5FR3D.dgn	3D fracture mapping TASA, 2/875-3/190 m
TKTBMFR3D.dgn	3D fracture mapping TASA, 3/190-3/600 m
TKZFR3D.dgn	3D fracture mapping TASZ
FRZON3D.dgn	3D deformation zone mapping TASA, 0/000-3/600 m
PCU-1.dgn	3D fracture mapping Elevator shaft
TASG_V1_Comp.dgn	3D fracture mapping TASG (walls+ceiling)
TASG_Golv_V1_Comp.dgn	3D fracture mapping TASG (floor)
TASI_V1_Comp.dgn	3D fracture mapping TASI
TASJ_V1_Comp.dgn	3D fracture mapping TASJ
TASQ_V1_Comp.dgn	3D fracture mapping TASQ

3 Modelling methodology

No specific field investigations have been made in this modelling work. Previous recorded data from SICADA database and TMS (Tunnel Mapping System) have been used. All used observations have been double checked with the BIPS image where available see Appendix A. The modelled structures and all indications used to model each structure are presented in detail in Appendix A.

3.1 Concept of water bearing structures

The term structure as used in this report generally refers to water-bearing features such as observed single water-bearing fractures. In some cases, however, a set of fractures which were closely spaced, have been regarded as a single feature. Large features are those that can be traced over most of the periphery of a tunnel. In the rest of this report, these features are referred to as “structures”.

It should be understood that a clear hydrological response between two structures, in for example two separate tunnels, does not necessarily mean that they represent one single and continuous structure. They may very well be a number of sub-parallel structures as well as splays that are connected (Figure 3-1). In the model they have, however, been drawn as a single structure that thus represents a possible and generalized water path.

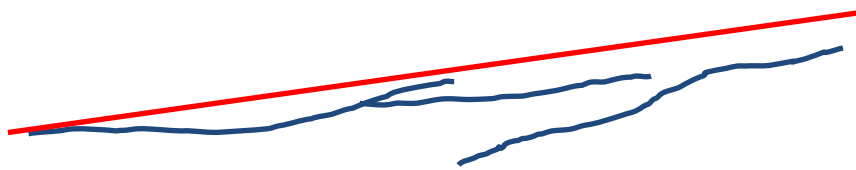


Figure 3-1. The blue lines illustrate fractures and the red line illustrates a possible generalised path for water.

The concept is such as it is believed that there are a number of more persistent structures feeding surrounding minor structures and splays, creating clusters of waterbearing fractures. The most significant modelled water bearing structures have been selected to be presented as main. In this case, it was decided that to be classified as a main structure, it must be detected in at least five evident points whereof at least four must be water bearing. Structures that are not identified in all intersecting tunnels or boreholes in the model volume were omitted as main. In a swarm of structures, only the most significant was selected as main. All other modelled structures are considered as minor structures or splays. In the current project deformation zones are defined as structures in which the number of fractures are too many to be handled separately; where the rock mass is more or less crushed or where the rock mass is more or less sheared and mylonitized. No particular concern has, however, been taken about deformation zones unless they act as a water barrier or if they are water bearing. Hence, the present model of the -450 m level is not a structural model showing various zones of deformation but shows interpreted single, often generalized water paths/water bearing structures.

3.2 WNW trending hydraulic connections at the 450-metre level

The drilling of the new boreholes for the Mini-Can experiment in spring 2005 resulted in an increased inflow in the niche NASA3384A, Figure 1-2, of between 50 l/min (with open boreholes) and 30 l/min (boreholes closed). This in turn resulted in a fast groundwater pressure drop of 3–5 bars in the boreholes in the Microbe experiment area. The inflow to the F-tunnel also shows a clear correlation to the groundwater pressure in the Mini-Can area. Between December 2005 to February 2006, when the pressure in borehole KA3386A01 was temporarily increased by about 15 bars by insertion of packers, the inflow in the measured upper 61 m of the F-tunnel instantaneously increased by 25%. The distance between the Mini-Can and the Microbe sites is about 150 m in a WNW direction. This hydraulic connection agrees with the general picture of WNW-trending hydraulically active structures in the area (cf. Figure 2-2). These structures are formed of clusters of sub-parallel single open fractures, so called fracture swarms /Rhén et al. 1997/. Statistical analysis of the mapping data from the whole tunnel length also shows that both fractures with grout and the dominant set of hydraulically active fractures are steep, strike WNW (around 300° RT90) and are generally longer than other fractures /Munier 1995 and Rhén et al. 1997/.

The modelling work was started with a review of the presumed water-bearing structures, A and B, indicated in Figure 2-3. Intersecting tunnels and boreholes were investigated for indications of any water-bearing structure. The basis for the hypothetical structure A in Figure 2-3 was the significant pressure responses monitored between KA3386A01 (10–11 m BH length), KA3385A, KF0066A01 (8 m BH length) and KA2598A. This implies a structure with a strike of approximately 130° (RT90). However, on closer investigation we found that the water-bearing structures in KF0066A01 are sub-horizontal and an analysis of the mapped tunnels between the boreholes and observations in other intersecting boreholes (see below) indicated structures striking more WNW, around 116° (RT90). The monitored pressure responses are probably transmitted via connected sub-parallel structures. The sub-parallel structures may be connected by shorter cross cutting steep fractures, by sub-horizontal fractures as noted by /Hermanson 1998/, and also by open boreholes which may effectively hydraulically connect structures. It should be noted that the frequency of sub-horizontal fractures is underestimated from the tunnel mapping due to the sampling bias resulting from the fact that these fractures are sub-parallel to the tunnels.

Several different observations contribute to the general picture of NW to WNW striking waterbearing structures at the 450-metre level. Most important are the distinct NW-SE striking water-bearing fractures visible all the way round the walls of the TBM-tunnel (TASA) (Figure 3-2 and Figure 3-3) and the precision-mapped water-bearing structures in the Q-tunnel (Figure 3-4). Both have a mean strike of approximately 110°-120° (RT90). Also for example the large amount of mapped open fractures, many of which are water bearing, in borehole KA3386A01 roughly confirm this picture (mean strike of approximately 279° and/or 99° (RT90)).

3.3 Interpolation, extrapolation and termination of structures

Large water bearing structures with similar orientations identified in two tunnels were regarded to be connected and were modelled as one structure. The intercepts with cross-cutting boreholes were predicted, and various kinds of borehole data (geological, hydrological as well as geophysical) were used to either confirm or restrict the extension of the structure.

All main structures have been drawn to the model boundary except when good reasons have been found to terminate a particular structure against another one. A structure was cut if it could not be identified in boreholes or tunnels on the other side of the intersecting structure.

Minor structures are always terminated against intersecting structures except when they are identified on both sides of the intersecting structure. The vertical extension of the minor structures is limited to be roughly similar to the lateral extension. Sometimes, however, structures were allowed to continue beyond a certain borehole where they had not been identified. In these cases the structures were believed to be identified in the tunnels or boreholes beyond the borehole that was lacking correlation. This is often related to structures intersecting short borholes at a very small angle. Here the actual position of the intersection point is uncertain. Even a slight change of orientation of the modelled structure can make it miss the borehole completely. In some cases, non water-bearing sections of crushed rock, low RQD or just open fractures have been used as an indication of an in other places water-bearing structure.

Since the tunnels within the model volume are situated more or less at the same level it has sometimes been difficult to secure the dip and dip direction of a structure unless it with certainty could be extrapolated to a borehole at another level in the rock mass of the Äspö HRL. Sometimes a mapped structure could show one dip on the drawing from the tunnel mapping and another one in the TMS database. This indicates that the orientations in the TMS sometimes are approximate. If enough evidence of the structure could be found elsewhere within the model volume the modelled dip of the structure has been used in the description of the structure. Even if a perfect fit for a possible structure could not be obtained between observations in boreholes and tunnels it was sometimes regarded as a single structure and was considered to undulate.

As the model is based on structures found by the tunnel mapping the further away from a tunnel a structure is extrapolated the less reliable the extension of the structure will be. Structures that could be connected between several tunnels or boreholes were given higher confidence. Information of hydraulic connectivity had a high weight in the confidence assessment since the model is a hydro-structural model. Only existing data were used in this work and no field investigations were done.

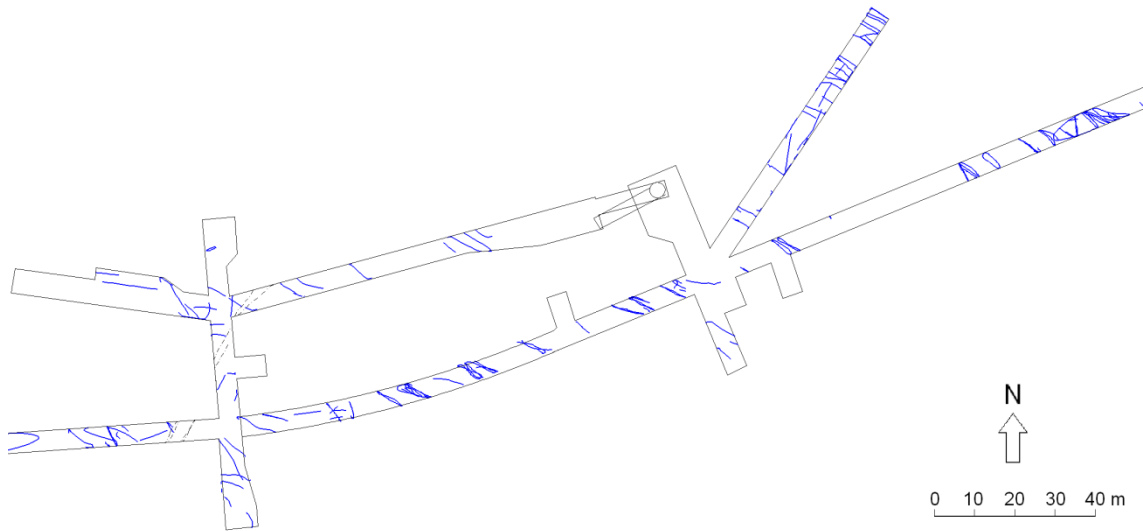


Figure 3-2. Tunnel mappings from the TMS system. Only water-bearing structures are shown (in blue).

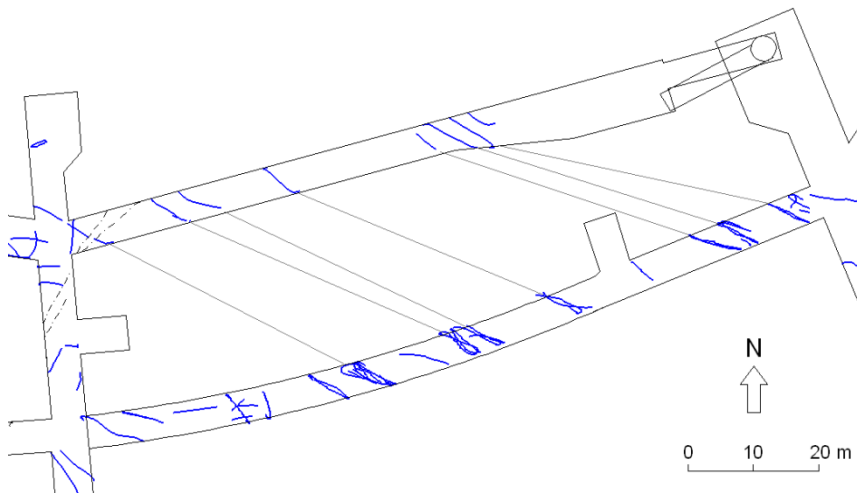


Figure 3-3. Connecting some observations of water-bearing structures in the A- and F-tunnels with an assumed strike of approximately 110-115°.

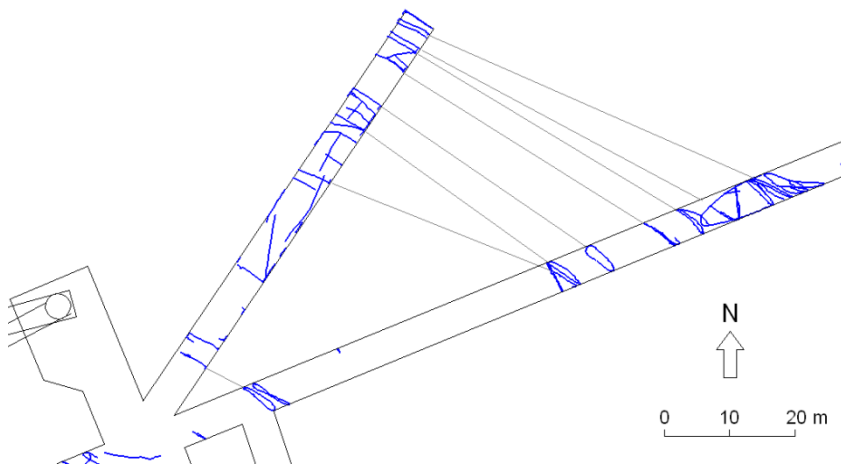


Figure 3-4. Connecting some observations of water-bearing structures in the A- and Q-tunnels with an assumed strike of approximately 115-120°.

3.4 Confidence classification

All modelled structures have been confidence classed. The confidence classification of the structures is largely based on the one found in /Rhén at al. 1997/ and is described in Table 3-1.

Table 3-1. Description of structure confidence classes.

Confidence class	Description
Possible	Increased fracture intensity in a section of a drill core, interpolation between at least two boreholes with sections of increased fracture intensity or open fractures and/or cuts the larger part of one or two tunnels. Water must be present in at least one of the observations.
Probable	Interpolated structures with some unique characteristics (geophysical, hydro-geological or geochemical) observed in two boreholes or a borehole and a tunnel or two tunnels. Water shall be present but hydraulic contact need not to be proven. The structure may intersect a borehole or a tunnel with increased fracture intensity or open fractures without water situated between two waterbearing observations.
Certain	Structure with unique characteristics observed in two or more boreholes and/or tunnels where hydraulic contact can be proven by interference or tracer tests. The structure may intersect a borehole or a tunnel with increased fracture intensity or open fractures without water situated between two waterbearing observations.

4 The model of water-bearing structures at the -450 m level, Äspö

The model is created by connecting all water-bearing fractures mapped in the tunnels at the -450 m level and analyzing the intersections between the extrapolated fractures and the boreholes in the area. Significant observations in the surrounding boreholes have been the main basis for the final interpretation and modelling of the structures. For a closer description of the modelling of each individual structure see Appendix A. The NW-SE strike is predominant for the modelled water-bearing structures. This corresponds well with the observed pattern in the mapped tunnels as well as with earlier models of Äspö /Rhén at al. 1997; Berglund et al. 2005/. The tunnel directions at the 450-level, mainly WSW, will however cause structures with a sub-parallel strike to be underrepresented in the mappings and hence also in the model. To some extent, this is true also for sub-horizontal structures since the tunnels are only gently inclined in the investigated area. A number of sub-horizontal fractures have, however been observed in the tunnel ceiling and in the vertical elevator shaft.

The modelled structures are classified as main or minor structures as described in section 3.1. Main structures are extrapolated to the model area boundaries, except in those cases where correlation is clearly missing in intersecting tunnels or boreholes. Minor structures are generally terminated against intersecting structures and their vertical extension is limited to be approximately equal to the lateral extension. See the individual notes for each modelled structure for information regarding extent in Appendix A.

Most modelled structures are sub-parallel but with slight variations in both strike and dip. This means that the structures intersect each other creating a hydraulic network with contact between the modelled structures. This is in good agreement with the actual conditions in the rock where the water-bearing structures are connected into a hydraulic network.

In this project a total of 37 structures have been modelled (Figure 4-1 and Figure 4-2). In Table 4-1 the confidence and classification of each modelled structure is presented. It is, however, important to note that even if the exact geometry and position of each individual structure can be rather uncertain, the overall pattern is well supported by all observations in boreholes and tunnels and by hydraulic measurements.

Table 4-1. Table of modelled structures.

Structure	Strike	Dip	Obs. points	Confidence	Class
FASEW001	111	78	7	probable	minor
FASEW002a	105	86	8	probable	minor
FASEW002b	107	86	4	probable	minor
FASEW002c	108	86	9	probable	main
FASEW002d	108	86	4	probable	minor
FASEW003	314	40	3	possible	minor
FASNS001	351	88	4	possible	minor
FASNS002	12	74	9	probable	main
FASNW001	133	83	3	possible	minor
FASNW002	115	86	5	probable	main
FASNW003	119	89	5	probable	main
FASNW004	121	89	4	probable	minor
FASNW005	303	89	5	probable	main
FASNW006	126	83	5	probable	minor
FASNW007	304	84	6	probable	main
FASNW008	295	87	6	probable	main
FASNW009	332	89	6	probable	main
FASNW010	311	85	6	probable	minor
FASNW011a	114	87	3	probable	minor
FASNW011b	307	82	2	possible	minor
FASNW011c	295	90	1	possible	minor
FASNW012	115	84	7	probable	minor
FASNW013	293	85	7	probable	main
FASNW014a	295	86	5	probable	minor
FASNW014b	296	87	7	probable	main
FASNW014c	298	87	6	probable	minor
FASNW015	297	87	7	probable	main
FASNW016	116	82	4	possible	minor
FASNW017	322(142)	90	2	possible	minor
FASNW018	116	87	7	probable	main
FASNW019n	329	86	2	possible	minor
FASNW019s	151	86	4	possible	minor
FASNW020	129	90	4	possible	minor
FASNW021a	114	8	10	probable	main
FASNW021b	111	81	8	probable	minor
FASNW021c	112	81	9	probable	minor
FASSH001	16	10	2	possible	minor

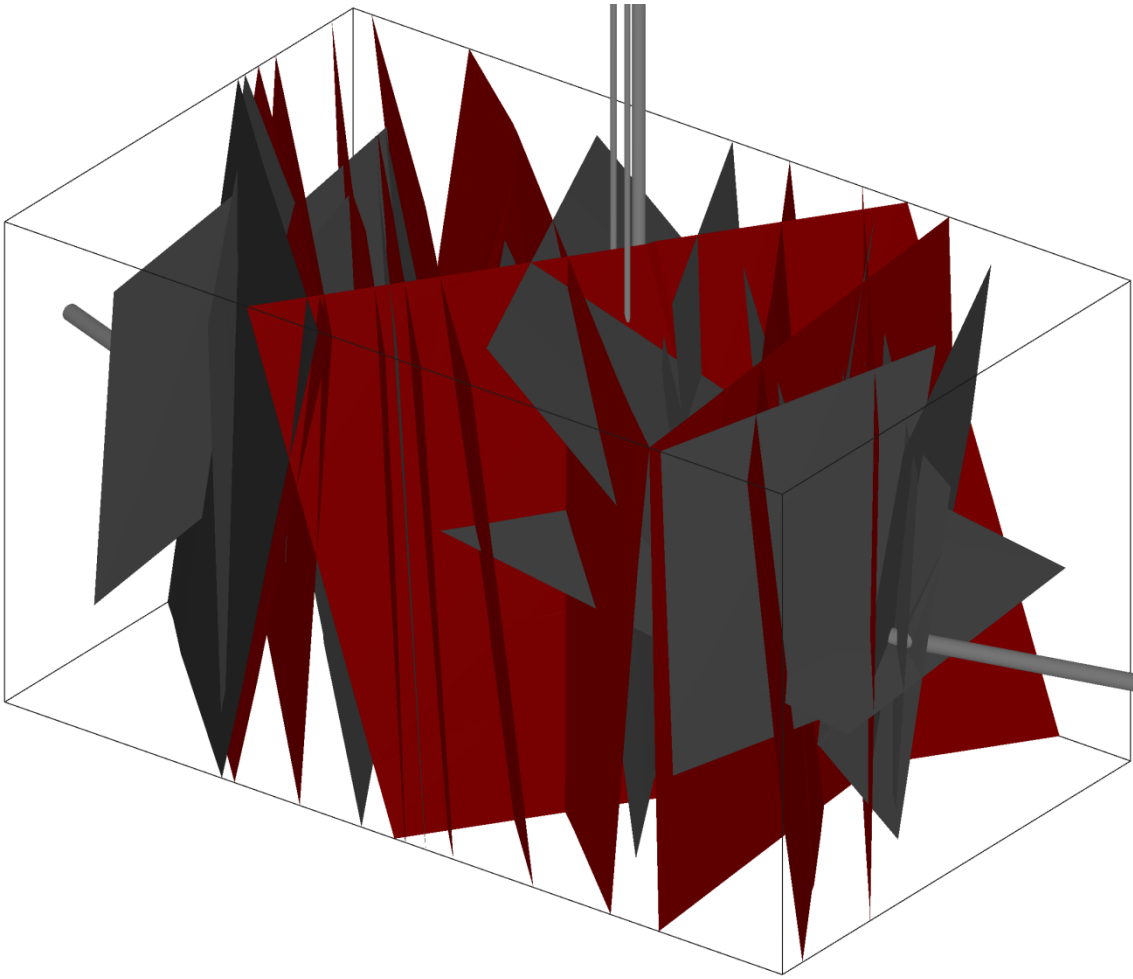


Figure 4-1. 3D view of all modelled structures at the -450 level. Each structure is presented and visualized individually in Appendix A.

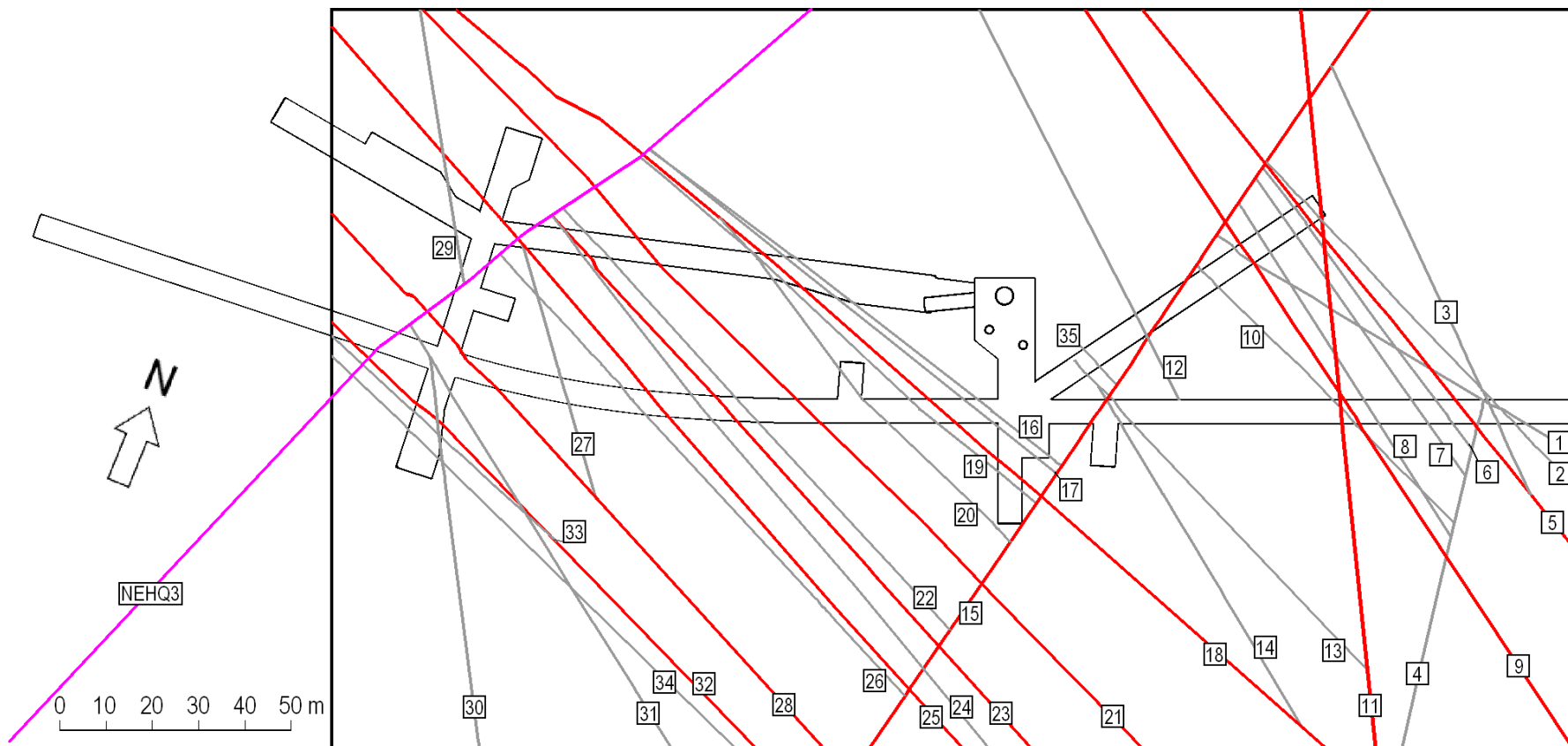


Figure 4-2. Modelled structures/generalized water paths (cf. Figure 3-1) intersection with a plane sloping 2° from east to west, as the tunnel. In the east Z=-440, in the west z=-450 m. The structures classified as main in Table 4-1 are marked with a red line and those classified as minor are marked with a grey line. The structure NEHQ3 is marked with a purple line. 1= EW001, 2=NW002, 3=NW001, 4=NS001, 5=NW003, 6=NW004, 7=NW005, 8=NW006, 9=NW007, 10=NW008, 11=NW009, 12=NW010, 13=NW011a, 14=NW011b, 15=NS002, 16=EW002a, 17=EW002b, 18=EW002c, 19=EW002d, 20=NW012, 21=NW013, 22=NW014a, 23=NW014b, 24=NW014c, 25=NW015, 26=NW016, 27=NW017, 28=NW018, 29=NW019n, 30=NW019s, 31=NW020, 32=NW021a, 33=NW021b, 34=NW021c, 35=NW011c. SH001 and EW003 are not visible in this section. The structure names here shown without the prefix “FAS”.

5 Discussion

5.1 The validity and limitations of the model

Most of the groundwater in the Äspö rock volume is transported in the major deformation zones and in some more or less open fractures. The rock mass outside the major deformation zones is normally not very hydraulically conductive. Earlier made estimates for blocks of homogeneous and only faintly tectonically affected rock, in 5x5x5 m scale, indicate the following geometric mean hydraulic conductivity for the various rock types at Äspö /Wikberg ed 1991/:

- Fine grained granite, $K=7.9 \times 10^{-10}$ m/s
- Ävrö (Småland) granite, $K=1.2 \times 10^{-10}$ m/s
- Äspö diorite, $K=5.2 \times 10^{-11}$ m/s
- Undifferentiated mafic rocks (previously called Greenstones), $K=5.2 \times 10^{-11}$ m/s
- Mylonites, $K=1 \times 10^{-10}$ m/s

The somewhat higher hydraulic conductivity in the fine grained granites is largely due to their higher fracture frequency. If this type of rock is present it may act as a hydraulic conductor within the host rock in which it appears. Commonly the boundaries between the rock types are sealed and hence do not act as hydraulic conductors. In general, due to the relatively low values and the normally sealed boundaries, no assessment has been made of how hydraulic conductivity varies specifically with rock type. Instead the work has concentrated on structures resulting from deformation of the rock mass.

The purpose of this particular model is to visualize how water-bearing structures can interact between themselves, tunnels and boreholes around the -450 m level of the Äspö HRL. It should be noted that it is not meant to be a geological structural model and hence doesn't consider various deformation zones unless they have any obvious affect on the water flow within the model volume.

The confidence of the extrapolation of single waterbearing structures, for example, between two tunnels, may not always be high. When the structures, as is often the case, appear in sets of many sub-parallel structures the confidence level is, however, considered to increase since they represent bigger structures that are easier to follow. To illustrate this, the most significant structure in a set is classified as the main structure of the set and the others as minor with less extension.

Earlier in the report it has been mentioned that even if there is a clear response between water-bearing structures in different parts of the model volume this does not necessarily mean that there is a continuous discrete structure all the way between the observations. It may very well be splays or two or more sub-parallel structures that have been connected by another structure. In the model they have, however, been modelled as one structure.

The model is only valid within the rock volume which it covers. If it is to be used in a broader setting, reference has to be taken about larger structures. These have not been considered here unless they actually intersect the model volume or appear in close vicinity of the model or for reasons mentioned above. One obvious area of application of the model is the implementation of the modelled structures into the Äspö groundwater flow model. These structures should then be compared to and interpreted together with the structures that were modelled in the groundwater flow model development project Äspö Models 2005 /Svensson et al. 2008/.

5.2 Comparison with other models

In the following section the present model is compared to the interpretations of the GeoMod model and the overlapping volumes in the TRUE Block Scale model and the HQ-3 model.

5.2.1 GeoMod

Deformation Zones

EW-1A and B

The deformation zone EW-1 touches the north-western corner of our model volume. Since it does not intersect the tunnel it is not included in our modelling work. It is oriented at an almost perpendicular angle to the main orientation of our modelled structures and hence intersects most structures. Since EW-1 is hydraulically active /Vidstrand 2003/ it can serve as a connection between the current modelled structures and also feed our structures with water.

NEHQ3

NEHQ3 is also oriented at an almost perpendicular angle to the main orientation of our modelled structures; the orientation for NEHQ3 is $32^{\circ}/70^{\circ}$ (RT90). It is clearly visible in the tunnel but since it is dry it is not included in our model. It is probable that this zone intersects the water-bearing structures NW014a, -b, -c, NW016, NW017 and NW019n and -s. This is supported by the following quote from the GeoMod report /Berglund et al. 2005/:

“The zone is mapped as dry in the tunnel, but there are a few water bearing fractures associated with the zone. All of these fractures end towards the zone or close to the zone boundary. No water bearing fractures crosscut the zone or are parallel to it according to the TMS mapping of the tunnel intersections.”

We have, however, found a few water-bearing structures that we judge pass through NEHQ3, e.g. EW002c. This is supported by the observed significant pressure response between the MiniCan and Microbe experiments that in fact gave the input for the current project. Other structures that are judged to pass through NEHQ3 are NW013, NW015, NW018, and NW021a. For NW015 this is clearly seen in TMS data.

NE-2

NE-2 is also oriented almost perpendicular to the main orientation of our modelled structures; the orientation of NE-2 is 21°/77.5° (RT90). NE-2 is modelled as water-bearing. We have not been able to find evidence at the -450 masl level that would motivate the modelling of a water-bearing structure with corresponding orientation and position. In the GeoMod report it is concluded that it is difficult to detect this zone at this level /Berglund et al. 2005/:

“The zone appears to vanish towards depth. The four intersections in the lower parts of the tunnel system are all judged as possible and the tunnel intersections here are very narrow (less than 0.5 m). There are no good alternative intersections here, but one alternative solution for the zone geometry would be that it ended already at a higher level.”

We have, however, a sub-parallel structure in FASNS002. This is oriented 12°/74° (RT90) and is on the -450 masl level positioned approximately 30 metres from NE-2. This could be a branch of NE-2 as indicated in the GeoMod report /Berglund et al. 2005/:

“There are several intersections of zones in the tunnel system that show the same orientation as NE2, but these are too far offset from certain intersections to be considered as possible intersections of the zone. However, the zone does undulate or splay significantly. It has not been possible to distinguish between undulations or splay geometries. The undulating character shown in the model is chosen because it is the simplest solution.”

Fractures

In the GeoMod model there are numerous objects modelled as ‘Fractures’ and a number as ‘Watercourse’. All these are modelled as disks around tunnel observations. None of the ‘Fracture’ objects coincide with any of our modelled structures, this is as expected since we only have modelled water-bearing structures and all water-bearing fracture objects in the GeoMod model are typed as ‘Watercourse’. Consequently, for the Watercourse objects there is good correspondence with our model, all observations in the tunnel we have used for modelling are also modelled as Watercourse in the GeoMod model.

5.2.2 APSE

Three of our modelled structures intersect the core volume of the APSE model; FASEW001, FASNW006 och FASNW007. FASEW001 and FASNW007 are close to a structure called 19_sec_45-60 and FASNW006 is close to a structure called NW_struct_1. This indicates that the expected orientations of the fractures are similar. However, the significant difference in model scale between the models makes it hard to make any further comparisons.

5.2.3 Prototype

Seven of our modelled structures intersect the Prototype model volume; FASNW018, FASNW019s+n, FASNW020 and FASNW021a+b+c. FASNW018 intersects the tunnel at the same position as the WTRSTD4 water bearing structure of the Prototype model. The strike is similar 116° for FASNW018 and 292° (112°) for WTRSTD4 but FASNW018 dips 87° to the west and WTRSTD4 82° to the east. The difference in dip is, however, not more than 11°. They are two different interpretations of the same water-bearing fracture in the A-tunnel, mapped with an orientation of 118°/82° (RT90). FASNW021a is in good correspondence with the saved HYDCE_211 structure in the Prototype model. FASNW021a is oriented 114°/81° (RT90) and the HYDCE_211 structure is oriented 115°/76°. It is, however, unclear what the HYDCE_211 structure represents. FASNW021b corresponds with both the non water-bearing structure STD13 and the water-bearing structure WTRSTD7 in the Prototype model. FASNW021b is oriented 111°/81° (RT90), STD13 is oriented 107°/86° (RT90) and WTRSTD7 is oriented 118°/66° (RT90). Both STD13 and WTRSTD7 are modelled from mapped fractures in the A-tunnel. For FASNW019s+n, FASNW020 and FASNW021c no corresponding modelled zones were found in the Prototype model.

5.2.4 TRUE

The involved structures in the TRUE BS model are structures 1–4 /Hermanson and Doe 2000/, Figure 2-1.

TRUE BS #1 is modelled from the same large steep water-bearing fractures in the F-tunnel as the structures FASEW002a–d and FASNW012. Instead of connecting it to fractures at 3,385–3,420 m in the A-tunnel, #1 is connected to the fractures around 3,430 m (here associated with FASNW013). This makes the #1 striking much more northerly (about 040°) than the FASEW002a–b group. The #1 structure is also associated with an intercept in KA2563A with the same orientation, but there is no other evidence of the #1 structure. It is considered that the FASEW002a–d group and FASNW012 structure honour the mapped orientations of the fractures in the tunnels better.

TRUE BS #2 is a modelled fracture zone that seems to be associated to the same water-bearing fractures in the I-tunnel as FASNW021a–b. The structures are also modelled from the same observation in KA2563A. However, #2 does not seem to be modelled from exactly the same point in KA3510A, even if this is stated as being so in the model report /Hermanson 1998/. This may be the reason that #2 is more southerly oriented and steeper than FASNW021a–b. TRUE BS #2 and FASNW021a–b should be regarded as alternative representations of the same structure. It may be possible to resolve this by a more thorough analysis of the boreholes surrounding the Prototype tunnel.

TRUE BS #3 and FASNW021c are sub-parallel structures crossing the I-tunnel at about the same location. TRUE BS #3, defined as a crush zone, is however associated with a non water-bearing fracture that was not used in the current modelling. TRUE BS #3 and FASNW021c may therefore be regarded as two co-existing structures. New data on these structures will be available from the new TASS-tunnel.

TRUE BS #4 is modelled from an observation in KA2563A (same as structure FASNW019s) and a possible intercept with KA3510A. There is, however, no mapped water-bearing fracture at the intercept with the I-tunnel. New data on this structure will also be available from the S-tunnel.

5.2.5 HQ-3

The structures in HQ-3 are modelled from mapped water-bearing structures in the F- and A-tunnels, but only a few structures have been modelled. The only modelled water-bearing structure crossing the current model volume is NW-HYD, modelled as two parallel surfaces representing the outer boundaries of the structure.

The western boundary of HQ-3 NW-HYD, with strike/dip = $302^{\circ}/87^{\circ}$, connects the same observations in the A- and F-tunnels as FASNW012, with strike/dip = $115^{\circ}/84^{\circ}$, and has approximately the same strike but dips steeply to the east whereas FASNW012 is dipping steeply to the west. The small difference in dip between the two structures may be due to the fact that the NW-HYD structure was modelled from the tunnel mapping only, while more observations were used for the FASNW012 structure. The tunnel observations are both vertical and are slightly more north striking which is a bit closer to the NW-HYD interpretation. FASNW012 is, however, connected to borehole observations in the MiniCan niche, which is in very good agreement with the overall hydrological pattern of the model.

The eastern boundary of HQ-3 NW-HYD, with strike/dip = $302^{\circ}/87^{\circ}$, uses the same observation in TASA as FASEW002d, with strike/dip = $108^{\circ}/86^{\circ}$. In the F-tunnel, the eastern boundary of HQ-3 NW-HYD intersects an area that is not mapped, so supporting evidence is lacking. The tunnel observation used in the A-tunnel has an orientation of $281^{\circ}/86^{\circ}$ which indicates a strike direction closer to that of FASEW002d. This structure is also supported in the F-tunnel, it is in agreement with the overall pattern of the surrounding modelled structures and with the overall hydrological pattern of the model.

5.2.6 LX_V1.2.2_LOC_DZ, Local Laxemar deformation zone model

Only one zone lies partly within our model volume. The local major deformation zone ZSMNE006A touches the SE corner of the model volume but does not intersect the tunnel and does not coincide with any of the modelled structures in this project. The strike direction 228° (RT90) is more or less perpendicular to the predominant direction of the modelled structures in our model and hence it can be suspected that they are hydraulically connected. This zone is the same as the NE-1 zone of the Geomod model, but the NE-1 is modelled as a much thinner zone and hence does not intersect our model volume.

5.3 Review of NE-2

A test to correlate NE-2 with observation SZ_W in TASQ would be an interesting task. Hence, a preliminary review of NE-2, including a site visit, was carried out in 2006 by Björn Magnor, Philip Curtis, Niklas Bockgård and Ingemar Markström. It is, however, a complicated matter to start to alter the interpretation of NE-2. This must be done on site and in full cooperation with the site geologist. Different hypotheses must be checked concerning expected intersections with tunnels, shafts and boreholes.

Furthermore, from a strictly geometrical point of view, SZ_W in TASQ corresponds better with an extrapolation downwards of the structure NEHQ3-top from the GeoMod model. This is also an interesting hypothesis to try. However, such an investigation is beyond the scope of the current project and should involve a complete analysis of all data from tunnels, shafts and boreholes. This work falls within the scope of an overall revision of the Äspö-model, a separate project.

6 Acknowledgements

We greatly acknowledge Pär Kinnbom for having converted a number of 2D TMS mapping files to 3D-format. We also want to express our appreciation to Phil Curtis for his review of the original draft of this report.

7 References

Andersson P, Byegård J, Dershowitz B, Doe T, Hermanson J, Merier P, Tullborg E-L, Winberg A (ed), 2002. Final report of the TRUE Block Scale project. 1. Characterisation and model development. SKB TR-02-13, Svensk Kärnbränslehantering AB.

Berglund J, Curtis P, Eliasson T, Olsson T, Starzec P, Tullborg E-L, 2005. Äspö Hard Rock Laboratory. Update of the geological model 2002. SKB IPR-03-34, Svensk Kärnbränslehantering AB.

Curtis P, Elfström M, Markström I, 2007. Rock Visualization System. Technical description (RVS version 4.0). SKB R-07-44, Svensk Kärnbränslehantering AB.

Emmelin A, Eriksson M, Fransson Å, 2004. Characterisation, design and execution of two grouting fans at 450 m level, Äspö HRL. SKB R-04-58, Svensk Kärnbränslehantering AB.

Forsmark T, Rhén I, 2000. Prototype Repository. Hydrogeology drill campaign 3A and 3B. SKB IPR-00-08, Svensk Kärnbränslehantering AB.

Forsmark T, Rhén I, 2001. Prototype Repository. Hydrogeology – Deposition- and lead-through boreholes: Inflow measurements, hydraulic responses and hydraulic tests. SKB IPR-00-33, Svensk Kärnbränslehantering AB.

Fransson Å, 2003. Äspö Hard Rock Laboratory. Äspö Pillar Stability Experiment. Core boreholes KF0066A01, KF0069A01, KA3386A01 and KA3376B01: Hydrogeological characterization and pressure responses during drilling and testing. SKB IPR-03-06, Svensk Kärnbränslehantering AB.

Hansen L, Hermansson J, 2002. Local model of geological structures close to the TASF-tunnel. SKB IPR-02-15, Svensk Kärnbränslehantering AB.

Hermanson J, Doe T, 2000. Äspö Hard Rock Laboratory. TRUE Block Scale Project. Tracer test stage. March`00 structural and hydraulic model based on borehole data from KI0025F03. SKB IPR-00-34. Svensk Kärnbränslehantering AB.

Hermanson J, 1998. Äspö Hard Rock Laboratory. TRUE Block Scale projekt Preliminary characterisation stage. September 1998 structural model; update using characterisation data from KI0023B. SKB IPR-01-42. Svensk Kärnbränslehantering AB.

Markström I, Erlström M, 1996. Äspö Hard Rock Laboratory. Overview of documentation of tunnels, niches and core boreholes. SKB PR-HRL-96-19, Svensk Kärnbränslehantering AB.

Munier R, 1995. Studies of geological structures at Äspö. Comprehensive summary of results. SKP PR-25-95-21, Svensk Kärnbränslehantering AB.

Olsson O, Stanfors R, Ramqvist G, Rhén I, 1994. Localization of experimental sites and layout of turn 2 - Results of investigations. SKB HRL Progress Report 25-94-14, Svensk Kärnbränslehantering AB.

Pedersen K, 2005. MICROBE. Analysis of microorganisms and gases in MICROBE groundwater over time during MINICAN drainage of the MICROBE water conducting zone. SKB IPR-05-29, Svensk Kärnbränslehantering AB.

Pusch R, Ramqvist G, 2007. Cleaning and sealing of borehole. Report of sub-project 2 on plugging of 5 m boreholes at Äspö. SKB IPR-06-29, Svensk Kärnbränslehantering AB.

Pöllänen J, Rouhiainen, 2002. Difference flow measurements in boreholes KA3386A01, KF0066A01 and KF0069A01 at the Äspö HRL. SKB IPR-02-55, Svensk Kärnbränslehantering AB.

Pöllänen J, Rouhiainen, 2003. Difference flow measurements in boreholes KA3386A01, KF0066A01 and KF0069A01 at the Äspö HRL. SKB IPR-03-07, Svensk Kärnbränslehantering AB.

Rhén I, Gustafson G, Stanfors R, Wikberg P, 1997. Äspö HRL – Geoscientific evaluation 1997/5. Models based on site characterization 1986–1995. SKB TR-97-06, Svensk Kärnbränslehantering AB.

Rhén I, Forsmark T, 2001. Prototype Repository. Hydrogeology. Summary report of investigations before the operations phase. SKB IPR-01-65, Svensk Kärnbränslehantering AB.

Rhén I, Stanfors R, 1995. Äspö Hard Rock Laboratory. Supplementary investigations of fracture zones in Äspö tunnel. SKB PR HRL 25-95-20, Svensk Kärnbränslehantering AB.

Rhén I, Stanfors R, Wikberg P, Forsmark T, 1995. Comparative study between the cored test borehole KA3191F and the first 200 m extension of the TBM tunnel. SKB PR-25-95-09, Svensk Kärnbränslehantering AB.

Rouhiainen P, Heikkinen P, 2002. TRUE Block Scale project. Difference flow measurements in boreholes KA2563A and KA2511A at the Äspö HRL. SKB IPR-01-48, Svensk Kärnbränslehantering AB.

Rouhiainen P, Heikkinen P, 2003. Flow measurements in boreholes KA3510A and KA2598A at the Äspö HRL. SKB IPR-01-68, Svensk Kärnbränslehantering AB.

Staub I, Andersson C, Magnor B, 2004. Äspö Pillar Stability Experiment. Geology and mechanical properties of the rock in TASQ. SKB R-04-01. Svensk Kärnbränslehantering AB.

SKB, 1994. Supplementary investigations of fracture zones in the tunnel. Hydrogeology. Compilation of technical notes. Measurements performed during construction of section 1475-2265 M. SKB HRL Progress Report 25-94-06. Svensk Kärnbränslehantering AB 1994

SKB, 2006. Preliminary Site description, Laxemar sub-area version 1.2. R 06-10. Svensk Kärnbränslehantering AB.

Svensson, U (ed), Vidstrand, P, Neretnieks, I, Wallin B, 2008. Towards a new generation of flow and transport models for the Äspö Hard Rock Laboratory. Main results from the project Äspömodels 2005. SKB R-08-74, Svensk Kärnbränslehantering AB.

Vidstrand P, 2003. Äspö Hard Rock Laboratory. Update of the hydrogeological model 2002. SKB IPR-03-35, Svensk Kärnbränslehantering AB.

Wikberg ed. 1991. Äspö Hard Rock Laboratory. Evaluation and conceptual modelling based on the pre-investigations 1986-1990. SKB Technical Report 91-22, Svensk Kärnbränslehantering AB.

Appendix A - Structure modelling

General

In this appendix, all modelled structures are presented individually. For each structure, the basis for the interpretation is presented and all observation points used are listed in a point table.

Key to the point table columns

ID	Observation point number referring to the text description above the table
Object	Tunnel or borehole ID
Section	For tunnel = mapcell ID + fracture ID, for borehole = borehole BH length (m)
Water	Indication of water. 0 = not water bearing, - = not measured. The labels v, vv, and vvv were used when tunnel mapping where v = moisture, vv = drip and vvv = wet to flow. "Infl" denotes recorded inflow, see point list above table for reference. "Wloss" denotes water loss. "PFL" inflow from Posiva Flow Log. "Cond" denotes high hydrolic conductivity.
Fract	Mapped fracture with Strike/Dip in RT90-RHB70 from TMS or SICADA. Bold text indicates open fracture. '-' = not measured. SICADA parameters fract_core-ori_all, fract_core-ori_open.
Mineral	Mapped fracture minerals/fillings from TMS or SICADA. The abbreviations are mostly from TMS: Ep = Epidote, Kl = Chlorite, Ka = Calcite, My = Mylonite, Ij = Grout, He = Hematite, Py = Pyrite, Go = Gouge, Pr = Prehnite, Cy = Clay, Fl = Fluorite/fluorspar, Qz = Quartz, At = Aplite, Xz = Filling could exist. '-' = not measured. SICADA parameters frac_core-minx, fract_crush-minx.
Width	Mapped fracture width in mm from TMS or SICADA. '-' = not measured. SICADA parameter fract_core-width.
RQD	Mapped Rock Quality Designation (%) from SICADA. '-' = not measured. Sicada parameter rqd_rqd. Some RQD values are very high (90-100%, excellent rock) but the fact that RQD drops from 100% means that the core is broken and may indicate the presence of not sealed fractures, which is significant when modelling single water-bearing fractures.
Freq	Fracture frequency from SICADA, as fractures/m. Format: A/B where A is total fractures and B is natural or open fractures. '-' = not measured 1) freq_1m_petrocor-total / freq_1m_petrocor-natural 2) freq = freq_1m-total / freq_1m-open_frac.
Crush	Crush from SICADA as number of fractures in crush (parameter 1 and 2) or average core piece length in crush (parameter 3). '-' = not measured 1) freq_1m_petrocor-crush. 2) freq_1m-open_crush. 3) fract_crush-pclen.
Radar	Radar reflector with interpreted Strike/Dip from SICADA. '-' = not measured. SICADA parameters radar_direct-ori1 and -ori2.
Oth	Other information. Ox = Oxidation, or see footnote below table. Oxidation information is from the SICADA parameter rock_alter-type. BIPS = Indication found in BIPS

A description of the modelling procedure is given in chapter 3. In this appendix, the interpretation and supporting evidence used to define each modelled structure are presented.

Structure FASEW001

The basis of the interpretation of FASEW001 was connecting the mapped water-bearing fractures in the TBM-tunnel (TASA) and tunnel TASQ.

Structure FASEW001 was modelled with an orientation of $111^{\circ}/78^{\circ}$ (RT90).

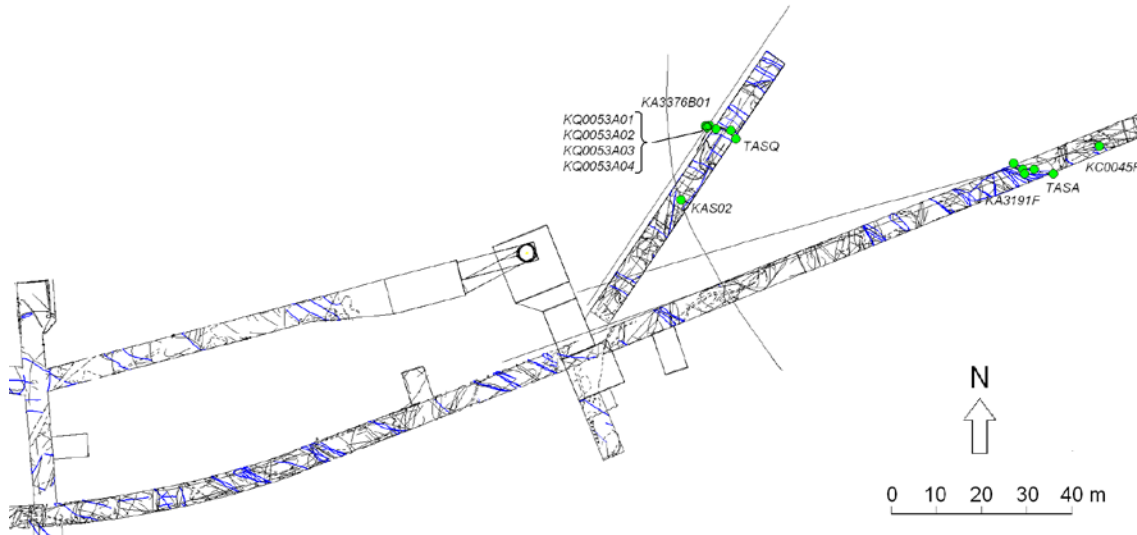


Figure A 1. Observation points used to model FASEW001 in tunnels and boreholes.

The indications used to model structure FASEW001 were:

1. Tunnel mapping, water-bearing fracture 3280.2-05 in TASA (the TBM-tunnel). Mapped with an orientation of RT90: $087^{\circ}/80^{\circ}$ ($085^{\circ}/80^{\circ}$ to magnetic north) /TMS/.
2. Tunnel mapping, water-bearing fracture 60-19 in TASQ mapped with an orientation of RT90: $095^{\circ}/80^{\circ}$ ($093^{\circ}/80^{\circ}$ to magnetic north) /TMS/.
3. Borehole KC0045F at 131 m BH length. Reduced RQD value (51%) at BH length 131-132 m /rqd_rqd, SICADA/. Crush between 131.5-131.7 m BH length /fract_crush-pklen, SICADA/. No measured inflow /Olsson et al. 1994/.
4. Borehole KA3376B01 at 47.66 m BH length. Mapped open fracture at BH length 47.66 m oriented RT90: $126^{\circ}/83^{\circ}$ ($138^{\circ}/83^{\circ}$ Äspö96) /fract_core-ori_open, SICADA/. Inflow at 45.6 and 47.7 m BH length /Pöllänen and Rouhiainen, 2003/.
5. In the boreholes KQ0053A01-04 there are no inflows detected, however no measurements were made where the modelled structure intersects. There are mapped open fractures at 6-7 m BH length in the boreholes 01, 02, 03 and 04, these points are included in the modelling /fract_core-ori_open, SICADA/.
6. Borehole KA3191F at 85 m BH length. Slightly reduced RQD value (94%) at BH length 85-86 m (declining from 94 at 85 m to 71 at 87 m) /rqd_rqd, SICADA/. A mapped fracture 'broken' at BH length 85.03 m oriented $300^{\circ}/77^{\circ}$ (Äspö96) (RT90: $288^{\circ}/77^{\circ}$) /fract_core-ori_broken SICADA/. A radar reflector at BH length 85 m oriented $127^{\circ}/77^{\circ}$ (RT90) /radar_direct-ori1, (Oxidation at 87 m BH length /rock_alter-type, SICADA/.)

This structure is classified as **probable**.

FASEW001 100°/78° (probable) - point table

ID	Object	Section (m)	Water	Fract RT90	Mineral	Width (mm)	RQD (%)	Freq (fr/m)	Crush	Radar RT90	Oth
1	TASA	3280-05	vvv	87/80	Ka/My	-	-	-	-	-	
2	TASQ	60-19	vv	95/80	Ka/lj	0,5	-	-	-	-	
3	KC0045F	131	0	-	-	-	51	32/9 ¹	23 ¹	(130+132)	
4	KA3376B01	47.7	Infl	126/83	Kl/Ka	1	92	5/3 ²	0 ²	-	BIPS
5	KQ0053A01	6	-								
	KQ0053A02	6	-								
	KQ0053A03	6	-								
	KQ0053A04	6	-								
6	KA3191F	85		288/77	0	0	94	5/3 ¹	0 ¹	127/77	

The modelled structure also intersects KF0066A01 and KF0069A01 but no evidence to support its existence was identified in these holes. It is therefore terminated against FASNW010 in the north.

Structure FASEW001 is trimmed towards FASNS002 in the NW. It is modelled only between z= -380 – -480 m.

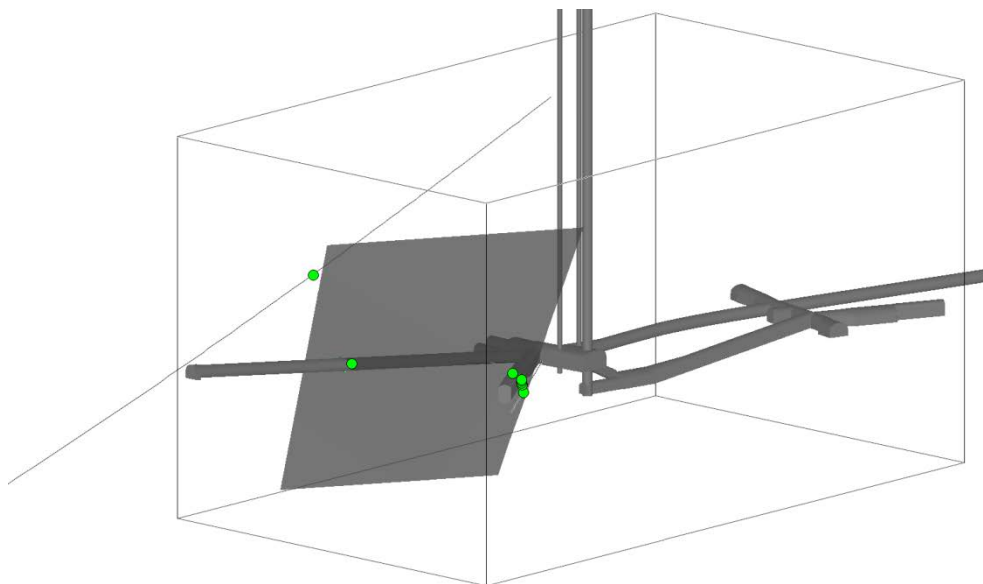


Figure A 2. 3D view of FASEW001 with observation points in green. View from NE.

The modelled structure, if extrapolated upwards, does not correlate with the mapping in the tunnels above.

Structure FASEW002a

A steeply dipping structure with an orientation of $105^{\circ}/86^{\circ}$ (RT90) was modelled. The basis of the interpretation for this structure were the tunnel mappings in TASA and TASF sub-parallel to the modelled main structure of FASEW002 in combination with borehole observations.

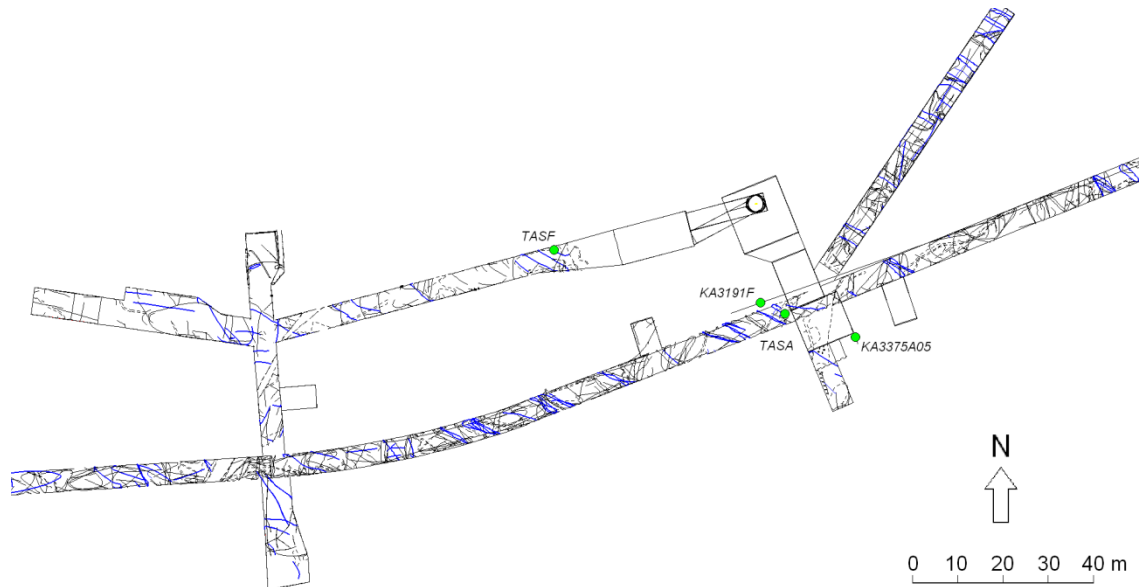


Figure A 3. Observation points used to model FASEW002a in tunnels and boreholes.

The indications used to model structure FASEW002a were:

1. Tunnel mapping, water-bearing fracture 3393.6-11 in TASA (the TBM-tunnel). Mapped with an orientation of RT90: $292^{\circ}/86^{\circ}$ ($290^{\circ}/86^{\circ}$ to magnetic north) /TMS/.
2. Tunnel mapping, water-bearing fracture 75-09 i TASF tunnel. Mapped with an orientation of RT90: $113^{\circ}/85^{\circ}$ ($111^{\circ}/85^{\circ}$ to magnetic north) /TMS/.
3. Borehole KA3191F at BH length 203.45 m. A mapped, open, fracture at BH length 203.45 m oriented RT90: $312^{\circ}/67^{\circ}$ ($324^{\circ}/67^{\circ}$ Äspö96) /fract_core-ori_open, SICADA/. Slightly reduced RQD value (88%) at BH length 204-205 m /rqd_rqd, SICADA/.
4. Borehole KA3375A05 at BH length 2.8 m. Increased fracturing at about 2.5–2.9 m /Pusch and Ramqvist, 2007/. A mapped, open, fracture at BH length 2.77 m oriented RT90: $089^{\circ}/66^{\circ}$ ($101^{\circ}/66^{\circ}$ Äspö96) /fract_core-ori_open, SICADA/.

In addition, FASEW002a and FASEW002b (below) intersects borehole KA2162B at a BH length between 110-130 m where there are a number of radar indicated fractures and areas with reduced RQD. These observations are, however, outside the modelled volume and are not included in the modelling of the structures.

This structure is classified as **probable**.

FASEW002a 105°/86° (probable) - point table

ID	Object	Section (m)	Water	Fract RT90	Mineral	Width (mm)	RQD (%)	Freq (fr/m)	Crush	Radar RT90	Oth
1	TASA	3393-11	vvv	292/86	Ka/lj	-	-	-	-	-	
2	TASF	75-09	vv	113/85	Kl/Ka	-		-	-	-	
3	KA3191F	203.5	0	312/67	Ep/Ka	4	88	5/4 ¹	0 ¹	0	
4	KA3375A05	2.8	-	89/66	Ka/	1	100	1/1 ²	0 ²	-	BIPS

Structure FASEW002a is trimmed by FASNS002 in the SE and NEHQ3 in the NW. It is modelled only between z= -380 – -490 m.

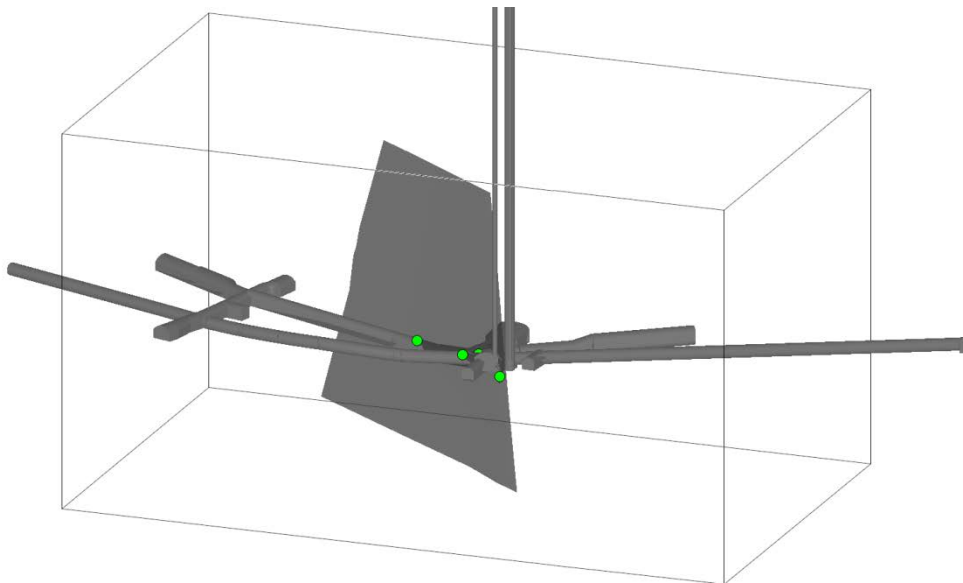


Figure A 4. 3D view of FASEW002a with observation points in green. View from SE.

The strike of 105 degrees was calculated from the observations. Since these are located on more or less the same z-depth, it is difficult to estimate the dip in a larger scale. Hence, the dip was locked to 86 degrees, guided by the main structure FASEW002c.

For intersections with the tunnel above, see Structure FASEW002c.

Structure FASEW002b

A steeply dipping structure with an orientation of 106°/86° (RT90) was modelled. The basis of the interpretation for this structure was the tunnel mappings in TASA and TASF sub-parallel to the modelled main structure of FASEW002 in combination with borehole observations.

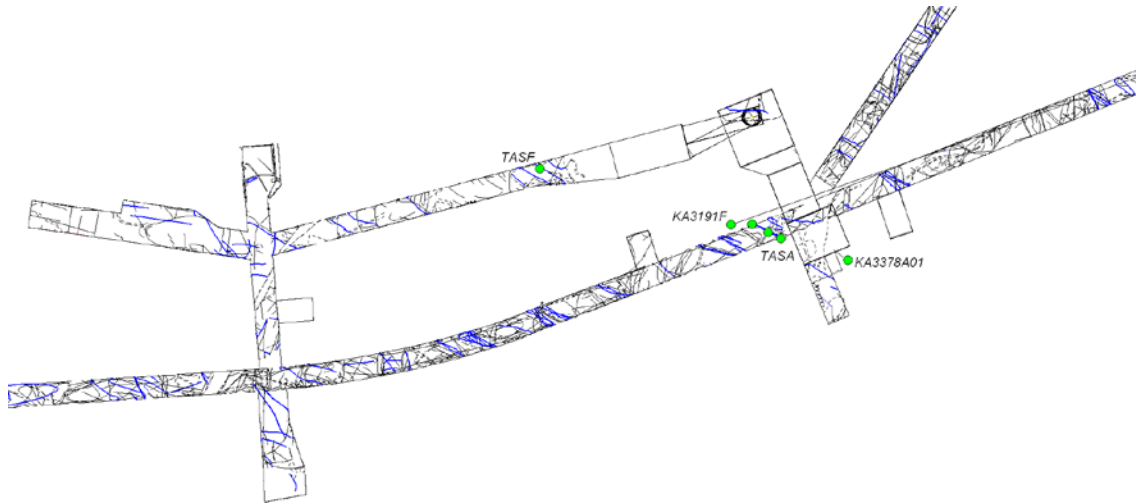


Figure A 5. Observation points used to model FASEW002b in tunnels and boreholes.

The indications used to model structure FASEW002b were:

1. Tunnel mapping, water-bearing fracture 3393.6-15 in TASA (the TBM tunnel). Mapped with an orientation of RT90: 284°/52° (282°/52° to magnetic north) /TMS/.
2. Tunnel mapping, water-bearing fracture 75-10 in the TASF tunnel. Mapped with an orientation of RT90: 295°/88° (293°/88° to magnetic north) /TMS/.
3. Borehole KA3378A01 at BH length 4.6 m. A mapped, open, probably hydraulically active /Pusch and Ramqvist, 2007/ fracture at BH length 4.61 m oriented RT90: 082°/84° (094°/84° Äspö96) /fract_core-ori_open, SICADA/. Oxidation at 4.2 m BH length /rock_alter-type, SICADA/.
4. Borehole KA3191F at BH length 209.52 m. A mapped, open, fracture at BH length 209.52 m oriented RT90: 318°/69° (330°/69° Äspö96) /fract_core-ori_open, SICADA/. Reduced RQD value (83%) at BH length 209-210 m /rqd_rqd, SICADA/.

This structure is classified as **probable**.

FASEW002b 106°/86° (probable) - point table

ID	Object	Section (m)	Water	Fract RT90	Mineral	Width (mm)	RQD (%)	Freq (fr/m)	Crush	Radar RT90	Oth
1	TASA	3393-15	vv	284/52	lj	-	-	-	-	-	
2	TASF	75-10	vv	295/88	Kl/Kl	-	-	-	-	-	
3	KA3378A01	4.6	Ja	082/84	Ka	1		4/2 ²	0 ²	-	Ox, BIPS
4	KA3191F	209.5	0	318/69	Ka/Ep/Kl	3	83	8/5 ¹	0 ¹	0	

The dip was locked to 86 degrees guided by the main structure FASEW002c.

Structure FASEW002b is trimmed by FASNS002 in the SE and NEHQ3 in the NW. It is modelled only between z= -380 – -490 m.

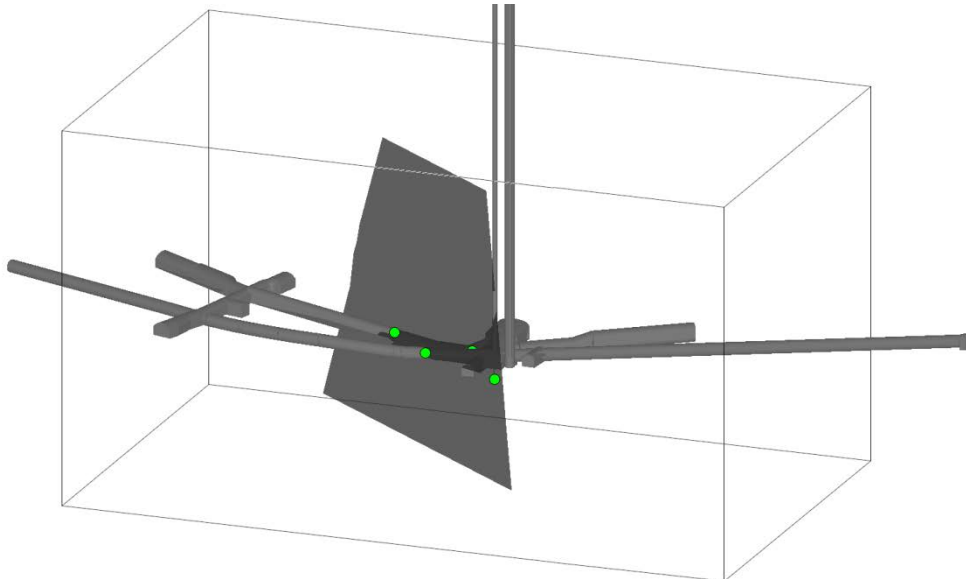


Figure A 6. 3D view of FASEW002b with observation points in green. View from SE.

For intersections with the tunnel above, see Structure FASEW002c.

Structure FASEW002c

A swarm of steeply dipping structures with an overall orientation of $108^{\circ}/86^{\circ}$ (RT90) were identified and modelled. These were modelled as separate structures but were named FASEW002a, b, c and d to indicate that they are interpreted as being part of a coherent swarm or "zone". FASEW002c is the most distinct main fracture and is governing the interpretation of the other fracture planes.

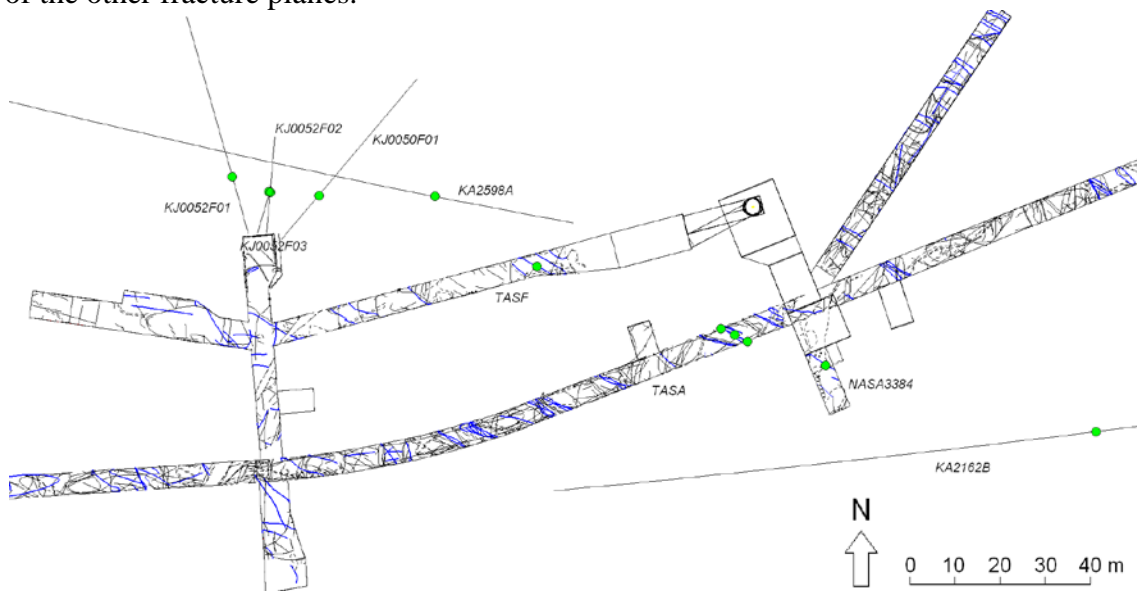


Figure A 7. Observation points used to model FASEW002c in tunnels and boreholes.

The basis of the interpretation was the tunnel mapping in NASA3384A, TASA and TASF that corresponds with the inferred strike of 110° (RT90). This interpretation also corresponds well with the position of the pressure drops in the KJ holes, KA2598A and KA2162B that were monitored when drilling the KA3386Axx holes at the Minican experiment.

The indications used to model structure FASEW002c were:

1. Tunnel mapping, water-bearing fracture 22 in NASA3384A (Minican). Mapped with an orientation of RT90: 305°/85° (303°/85° to magnetic north) /TMS/.
2. Tunnel mapping, water-bearing fracture 3408.4-08 in TASA (the TBM-tunnel). Mapped with an orientation of RT90: 106°/90° (104°/90° to magnetic north) /TMS/.
3. Tunnel mapping, water-bearing fracture 75-12 in the TASF-tunnel. Mapped with an orientation of RT90: 123°/86° (121°/86° to magnetic north) /TMS/.
4. Borehole KJ0050F01 at BH length 12.7 m. Water chemistry: Substantially increased salinity and a different population of microbes registered in fracture at 12.7 m BH length /Pedersen, 2005/. A mapped open fracture at BH length 12.73 m oriented RT90: 109°/75° (121°/75° Äspö96) /fract_core-ori_open, SICADA/. Pressure drop in the borehole when drilling in NASA3384 (Mini-Can) /Pedersen, 2005/. Slightly reduced RQD value (97%) at BH length 12-13 m /rqd_rqd, SICADA/.
5. Borehole KJ0052F02 at BH length 9.1 m. Distinct pressure drop in fracture at BH length 9 m and significantly altered water chemistry when drilling in NASA3384 (Mini-Can) /Pedersen, 2005/. A mapped open fracture at BH length 9.08 m with unknown strike and a dip of 75° /fract_core-ori_open, SICADA/, the BIPS image shows that the fracture intersects the borehole at an angle of approximately 90° which coincides well with the modelled strike. Slightly reduced RQD value (92%) at BH length 9-10 m /rqd_rqd, SICADA/.
6. Borehole KJ0052F03 at BH length 9.2 m. Distinct pressure drop in fracture at BH length 9 m and significantly altered water chemistry when drilling in NASA3384 (Mini-Can) /Pedersen, 2005/. A mapped open fracture at BH length 9.23 m with unknown strike and a dip of 75° /fract_core-ori_open, SICADA/. Reduced RQD value (83%) at BH length 9-10 m /rqd_rqd, SICADA/.
7. (weak) Borehole KJ0052F01 at BH length 12.9 m. A mapped open fracture at BH length 12.89 with unknown strike and a dip of 70° /fract_core-ori_open, SICADA/. Slightly reduced RQD value (90%) at BH length 11-12 m and (95%) at BH length 12-13 m /rqd_rqd, SICADA/. There was no water-bearing fracture on this BH length but an overall pressure drop in the borehole was observed when drilling in NASA3384 (Mini-Can) /HMS, unpublished data/.
8. Borehole KA2598A at BH length 37.1 m. Pressure response in the borehole when drilling in NASA3384 (Mini-Can) /HMS, unpublished data/. Significant inflow at BH length 37.4 and 37.0 m /Rouhiainen and Heikkinen, 2003/. A mapped open fracture at BH length 37.11 m with a mapped orientation of RT90: 325°/76° (337°/76° Äspö96) /fract_core-ori_open, SICADA/.
9. Borehole KA2162B at BH length approximately 163 m. Pressure response in the borehole when drilling in NASA3384 (Mini-Can) /HMS, unpublished data/, however largest below 202 m. Inflow of 34 l/min at BH length about 165 m during drilling. Mapped crush (71 fractures) on section 163-164 m /freq_1m-petrocor_crush, SICADA/. Very low RQD value (18%, very poor rock) at BH length 162-164 m /rqd_rqd, SICADA/.

The modelled position of the fracture can be connected to observations in all intersecting boreholes and tunnels.

This structure is classified as **probable**.

FASEW002c 108°/86° (probable) - point table

ID	Object	Section (m)	Water	Fract RT90	Mineral	Width (mm)	RQD (%)	Freq (fr/m)	Crush	Radar RT90	Oth
1	NASA3384A	24.1-22	vv	305/85	Ka/lj	-	-	-	-	-	
2	TASA	3408-08	vv	106/90	Ka	-	-	-	-	-	
3	TASF	75-12	vv	123/86	Ka/Kl	-	-	-	-	-	
4	KJ0050F01	12.7	a)	109/75	Ka	1	97	1/1 ²	0 ²	-	b), BIPS
5	KJ0052F02	9.1	a)	??/75	Ka/Kl	2	92	1/1 ²	0 ²	-	b), BIPS
6	KJ0052F03	9.2	a)	??/75	Ka	1	83	1/1 ²	0 ²	-	b), BIPS
7	KJ0052F01	12.9	0	??/70	Kl	-	95	0/0 ²	0 ²	-	BIPS
8	KA2598A	37.1	a) Infl	325/76	Ka	-	100	4/2 ¹	0 ¹	0	
9	KA2162B	163	a)	-	-	-	18	74/3 ¹	71 ¹	0	

a) Pressure response in the borehole when drilling in NASA3384 (Mincan)

b) Significantly altered water chemistry /Pedersen, 2005/.

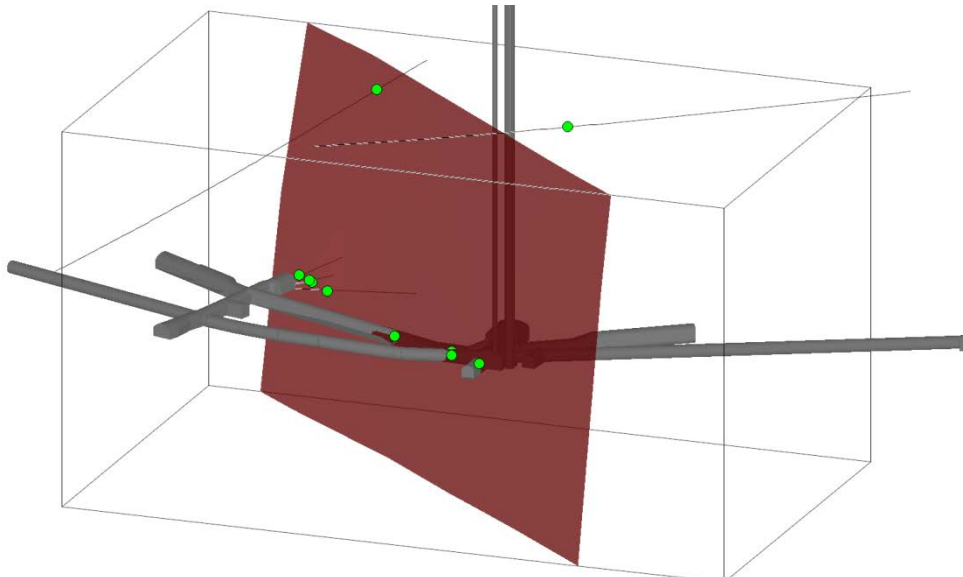


Figure A 8. 3D view of FASEW002c. with observation points in green. View from SE.

The fracture is modelled with an upper limitation at Z=-350 m, which is the upper boundary of the model volume. If the modelled fracture is extrapolated upwards, it will intersect the spiral tunnel TASA at approximately 2/592 and 1/671.

Between sections 2/590-2/610 there is a mapped fracture zone and before this, at section 2/580-2/590, there is a number of water-bearing fractures sub-parallel to the modelled fracture.

Between sections 1/670-1/700 there is a set of water-bearing fractures sub-parallel to the modelled fracture.

This shows that in both levels in the spiral tunnel TASA above the modelled volume there are water-bearing fractures corresponding well to the geometry and position of the modelled fracture. But since these observations are outside the modelled volume, no further analyses have been done.

Structure FASEW002d

A steeply dipping structure with an orientation of 108°/86° (RT90) was modelled. The basis of the interpretation for this structure were the tunnel mappings in NASA3384A, TASA and TASF sub-parallel to the modelled main structure of FASEW002.

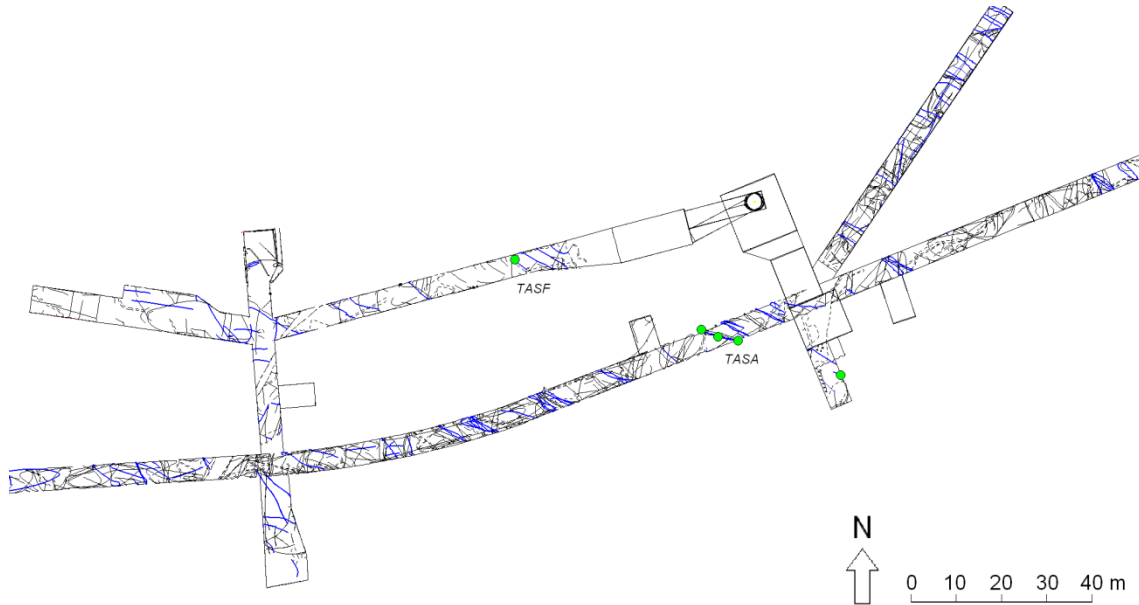


Figure A 9. Observation points used to model FASEW002d in tunnels and boreholes.

The indications used to model structure FASEW002d were:

1. Tunnel mapping, water-bearing fracture 3408.4-14 in TASA (the TBM tunnel). Mapped with an orientation of RT90: 281°/86° (279°/86° to magn north) /TMS/.
2. Tunnel mapping, water-bearing fracture 21 i NASA3384A (Minican). Mapped with an orientation of RT90: 295°/88° (293°/88° to magnetic north) /TMS/.
3. Tunnel mapping, water-bearing fracture 60-16 in the TASF tunnel. Mapped with an orientation of RT90: 127°/90° (125°/90° to magnetic north) /TMS/.

This structure is classified as **probable**.

FASEW002d 108°/86° (probable) – point table

ID	Object	Section (m)	Water	Fract RT90	Mineral	Width (mm)	RQD (%)	Freq (fr/m)	Crush	Radar RT90	Oth
1	TASA	3408-14	vv	281/86	Ep/Ka/Kl	-	-	-	-	-	Ox
2	NASA3384A	21	v	295/88	lj	-	-	-	-	-	
3	TASF	60-16	vv	127/90	Kl	-	-	-	-	-	a)

a) Only mapped in the tunnel ceiling

Structure FASEW002d is trimmed by FASNS002 in the SE and NEHQ3 in the NW. It is modelled only between $z = -380 - -490$ m.

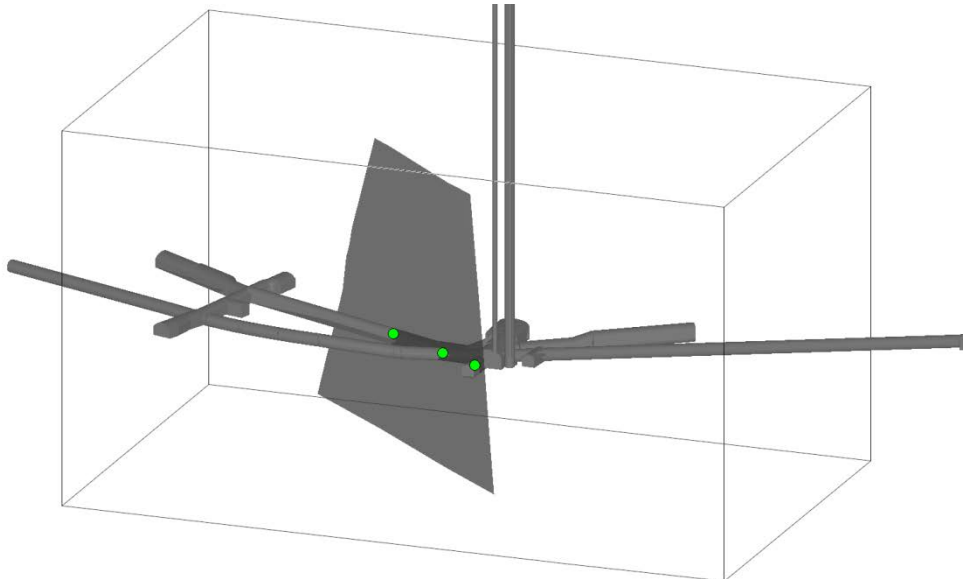


Figure A 10. 3D view of FASEW002d with observation points in green. View from SE.

The strike of 108 degrees was calculated from the observations. Since these are located on more or less the same z -depth, it is difficult to estimate the dip in a larger scale. Hence, the dip was locked to 86 degrees, guided by the main structure FASEW002c. For intersections with the tunnel above, see Structure FASEW002c.

Structure FASEW003

The basis of the interpretation of FASEW003 was a mapped water-bearing fracture in the Elevator shaft. The structure does not intersect any tunnel in the model area. Structure FASEW003 was modelled with an orientation of $314^{\circ}/40^{\circ}$ (RT90).

The indications used to model structure FASEW003 were:

1. Elevator shaft (TASH) mapping, water-bearing fracture -400-11 in the elevator shaft. Mapped with an orientation of RT90: $302^{\circ}/40^{\circ}$ ($300^{\circ}/40^{\circ}$ to magnetic north) /TMS/.
2. (Weak) Borehole KAS02 at 404.9 m BH length. Reduced RQD value (55%, fair rock) at BH length 404-405 m /rqd_rqd, SICADA/. Mapped fracture 'broken' at BH length 404.9 m oriented RT90: $294^{\circ}/38^{\circ}$ ($306^{\circ}/38^{\circ}$ Äspö96) /fract_core-ori_broken, SICADA/.
3. Borehole KA2162B at 224 m BH length. Reduced RQD value (52%) at BH length 224-225 m /rqd_rqd, SICADA/. Crush (open) between 223.8-224.3 m /fract_crush-plen, SICADA/. Oxidation between 223.1-224.5 m /rock_alter-type, SICADA/.

This structure is classified as **possible**.

FASEW003 314°/40° (possible) - point table

ID	Object	Section (m)	Water	Fract RT90	Mineral	Width (mm)	RQD (%)	Freq (fr/m)	Crush	Radar RT90	Oth
1	TASH (elev)	-400-11	-	302/40	KI	-	-	-	-	-	
2	KAS02	405		294/38	KI/He	-	55	16/16	0	-	
3	KA2162B	224		Crush	KI/Ka/Ep	-	52	23/4	17 ³	0	Ox

The structure is trimmed towards FASNW009 and only exists above TASA. The lateral extent is limited to 120 m.

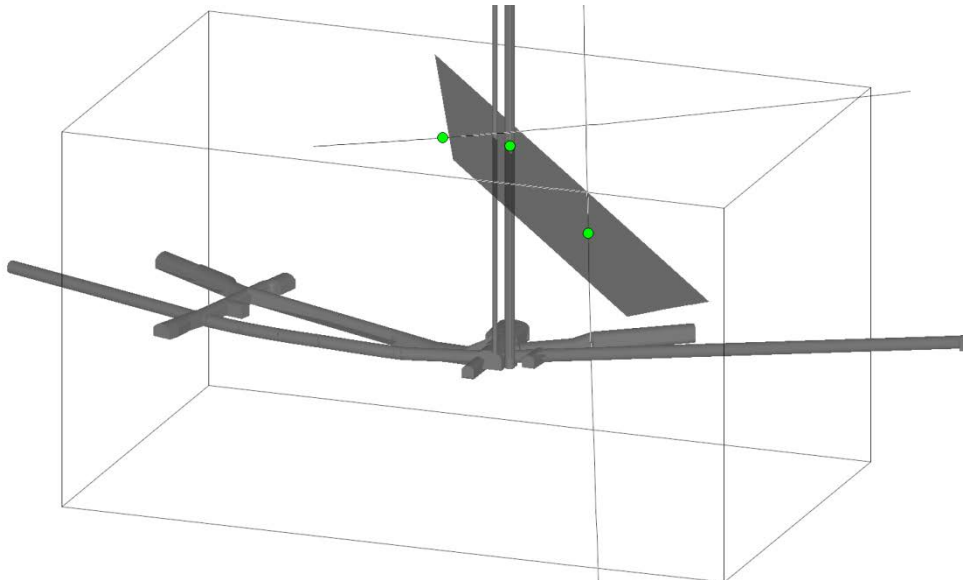


Figure A 11. 3D view of FASEW003 with observation points in green. View from SE.

If extrapolated upwards, in the west, the modelled structure intersects TASA at section approximately 2/580 – 2/585 m in the lower tunnel turn. Here there are two mapped water-bearing fractures 2578-06 (304°/68°) and 2582-06 (290°/56°) with good correspondence.

Structure FASNS001

The basis of the interpretation of FASNS001 was a mapped water-bearing fracture in the TBM-tunnel (TASA). The structure does not intersect TASQ.
Structure FASNS001 was modelled with an orientation of 351°/88° (RT90).

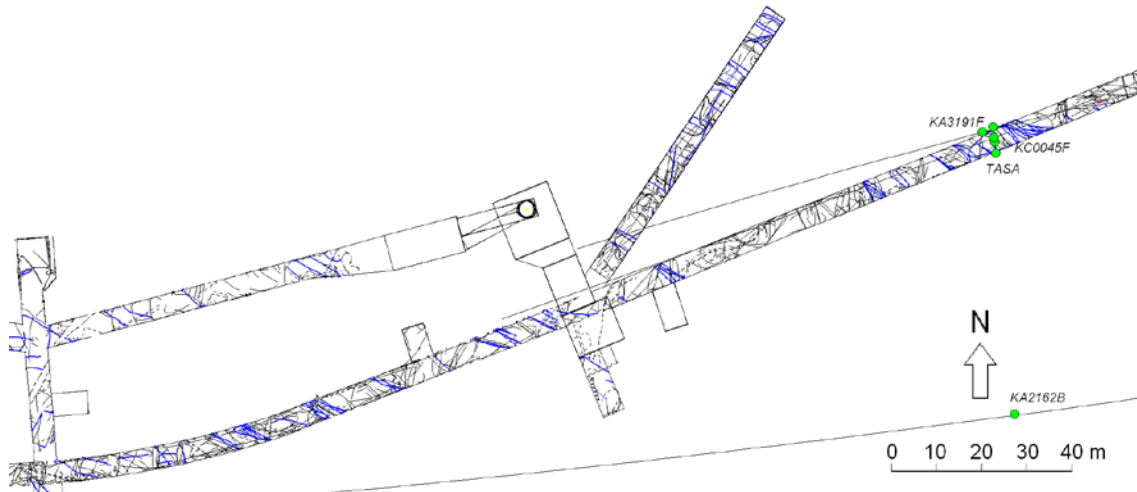


Figure A 12. Observation points used to model FASNS001 in A tunnel and boreholes.

The indications used to model structure FASNS001 were:

1. Tunnel mapping, water-bearing fracture 3290.0-05 in TASA (the TBM tunnel). Mapped with an orientation of RT90: 352°/90° (350°/90° to magnetic north) /TMS/.
2. Borehole KC0045F at 102 m BH length. Low RQD value (31%, poor rock) at BH length 101-102 m /rqd_rqd, SICADA/. A radar reflector at BH length 103 m oriented RT90: 324°/69° /radar_direct-ori1, SICADA/. Inflow between 99-105 m BH length (210 l/min) /Olsson et al. 1994/. Crush at 101 m /fract_crush-pclen, SICADA/.
3. Borehole KA2162B at 129 m BH length. Reduced RQD value (65%) at BH length 129-130 m /rqd_rqd, SICADA/. Increased fracture frequency (12) between 129-130 m /freq_1m-total, SICADA/. A radar reflector at BH length 129 m oriented RT90: 141°/68° /radar_direct-ori1, SICADA/. Crush at 129 m /fract_crush-pclen, SICADA/.
4. Borehole KA3191F at 92 m BH length. Reduced RQD value (79%) at BH length 91-92 m /rqd_rqd, SICADA/. Oxidation at 91 m and 92.2 m /rock_alter-type, SICADA/. Large inflow on flow logging between 91.5-92.5 m /flow_logging-flow, SICADA/. Mapped fracture at BH length 93.6 m oriented RT90: 005°/60° (017°/60° Äspö96) /fract_core-ori_all, SICADA/.

This structure is classified as **possible**.

FASNS001 351°/88° (possible) - point table

ID	Object	Section (m)	Water	Fract RT90	Mineral	Width (mm)	RQD (%)	Freq (fr/m)	Crush	Radar RT90	Oth
1	TASA	3290-05	v	352/90	Ep/Ka/Kl	-	-	-	-	-	
2	KC0045F	102	Infl	Crush	Ka/Kl	-	31	15/7 ¹	8 ¹	(103)	
3	KA2162B	129		Crush	Kl/Ka		65	17/5 ¹	12 ¹	141/68	
4	KA3191F	92	Infl	(005/60)	(Kl)	0	79	13/8 ¹	0 ¹	(94)	Ox

The structure is trimmed by FASEW001 in the N. It is modelled only between $z = -350 - -450$ m.

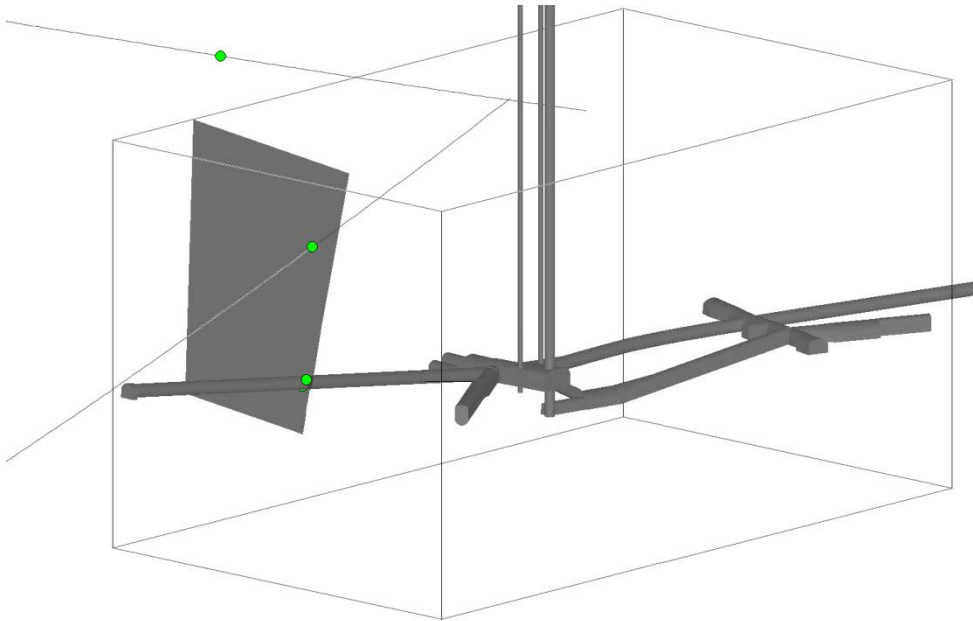


Figure A 13. 3D view of FASNS001 with observation points in green. View from NE.

If extrapolated upwards, in the south, the modelled structure intersects TASA at section approximately 2/347 m. At 2/338 and 2/351 m there are mapped sub-parallel water-bearing fractures corresponding well.

In the north, the modelled structure intersects TASA at section approximately 2/820 m in the lower tunnel turn in a mapped zone with high transmissivity. In the level above the structure intersects at approximately 1/870, where there is a mapped water-bearing fracture, however with a different orientation.

Structure FASNS002

The basis of the interpretation of FASNS002 was connecting the mapped water-bearing fractures in the TBM-tunnel (TASA) and tunnel TASQ.

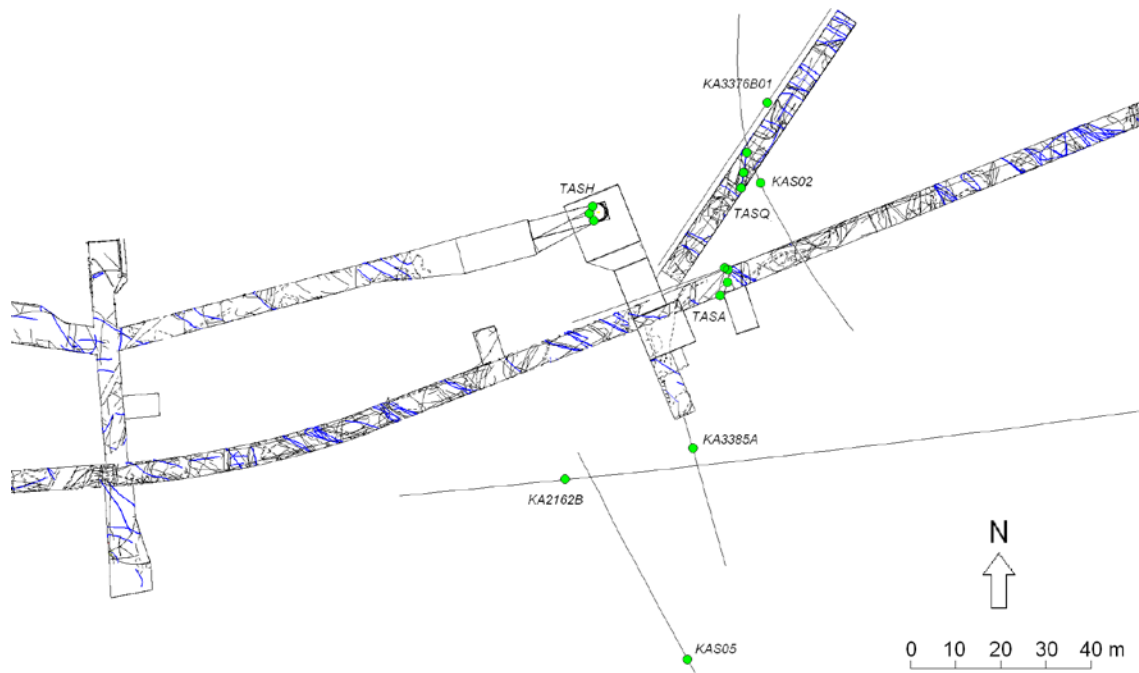


Figure A 14. Observation points used to model FASNS002 in tunnels and boreholes.

Structure FASNS002 was modelled with an orientation of $012^{\circ}/74^{\circ}$ (RT90).

The indications used to model structure FASNS002 were:

1. Tunnel mapping, water-bearing fracture 35-06 in TASQ mapped with an orientation of RT90: $018^{\circ}/76^{\circ}$ ($016^{\circ}/76^{\circ}$ to magnetic north) /TMS/.
2. Tunnel mapping, fracture 3378.8-01 in TASA (the TBM tunnel). Mapped with an orientation of RT90: $011^{\circ}/75^{\circ}$ ($009^{\circ}/75^{\circ}$ to magnetic north) /TMS/. NOTE, not mapped as water bearing.
3. Elevator shaft mapping, fracture -350-11. Mapped with an orientation of RT90: $003^{\circ}/75^{\circ}$ ($001^{\circ}/75^{\circ}$ to magnetic north) /TMS/.
4. Borehole KA3376B01 at BH length 43.4 m. Fracture with an inflow at BH length 43.4 m /Posiva Flow Log, SICADA/. Reduced RQD (73%) at BH length 43-44 m /rqd_rqd, SICADA/. There is, however, no mapped fracture at this BH length with corresponding orientation.
5. Borehole KAS02 at BH length 464 m. Reduced RQD (87%) at BH length 464-465 m /rqd_rqd, SICADA/. Mapped fracture 'broken' at 464 m BH length with an orientation of RT90: $038^{\circ}/65^{\circ}$ ($050^{\circ}/65^{\circ}$ Äspö96) /fract_core-ori_broken, SICADA/. Oxidation at 464 m BH length /rock_alter-type, SICADA/.
6. Borehole KA3191F at BH length 174 m. Reduced RQD value (65%) at BH length 173-174 m /rqd_rqd, SICADA/. Mapped fracture 'broken' at 172.3 m BH length oriented RT90: $016^{\circ}/63$ ($028^{\circ}/63^{\circ}$ Äspö96) /fract_core-ori_broken, SICADA/. Inflow at approximately 175 m BH length /Rhen et al., 1995/. Oxidation at 173-17.5 m BH length /rock_alter-type, SICADA/. Increased fracture frequency (1 fracture) between 173-174 m BH length /freq_1m-open_total, SICADA/.
7. Borehole KA3385A at BH length 7 m. A radar reflector at 7 m BH length oriented RT90: $193^{\circ}/87^{\circ}$ RT90 /radar_direct-ori1, SICADA/. Reduced RQD value (88%) at BH length 7-8 m /rqd_rqd, SICADA/. Same as FASNW012, point 7.
8. (Weak) Borehole KAS05 at BH length 491 m. Reduced RQD (83%) at BH length 490-491 m /rqd_rqd, SICADA/. Mapped fracture 'broken' at 490.3 m with an orientation of RT90: $017^{\circ}/46^{\circ}$ (measured in RT38) /fract_core-ori_broken, SICADA/.

9. (Weak) Borehole KA2162B at BH length 252 m. Pressure response in the borehole, mainly at BH length >200m when drilling in NASA3384 (Mini-Can) /HMS, unpublished data/. Water inflow between 252-254 m /SICADA/. Slightly reduced RQD value (92%) at BH length 251-252 m /rqd_rqd, SICADA/. Same as FASNW013, point 5.

This structure is classified as **probable**.

FASNS002 012°/74° (probable) - point table

ID	Object	Section (m)	Water	Fract RT90	Mineral	Width (mm)	RQD (%)	Freq (fr/m)	Crush	Radar RT90	Oth
1	TASQ	35-06	v	018/76	Ep/Kl/Ka	0	-	-	-	-	Ox
2	TASA	3378-01	-	011/75	Ep/Ka/Kl	-	-	-	-	-	Ox
3	TASH (elev)	-350-11	Y	003/75	Kl	-	-	-	-		
4	KA3376B01	43.4	Infl a)	0	-	-	73	11/0 ²	0 ²	-	BIPS
5	KAS02	464	0	038/65	Ka	-	87	10/3 ¹	0 ¹	-	Ox
6	KA3191F	174	Infl	016/63	Kl	0	65	8/8 ¹	0 ¹	0	Ox
7	KA3385A	7	0	-	-	-	88	3/3 ¹	0 ¹	193/87	Ox
8	KAS05	491	0	017/46	Kl/Ka/Py	0	83	9/5 ¹	0 ¹	-	
9	KA2162B	252	Wloss	-	-	-	92	2/2 ¹	0 ¹	0	

a) Posiva flow log

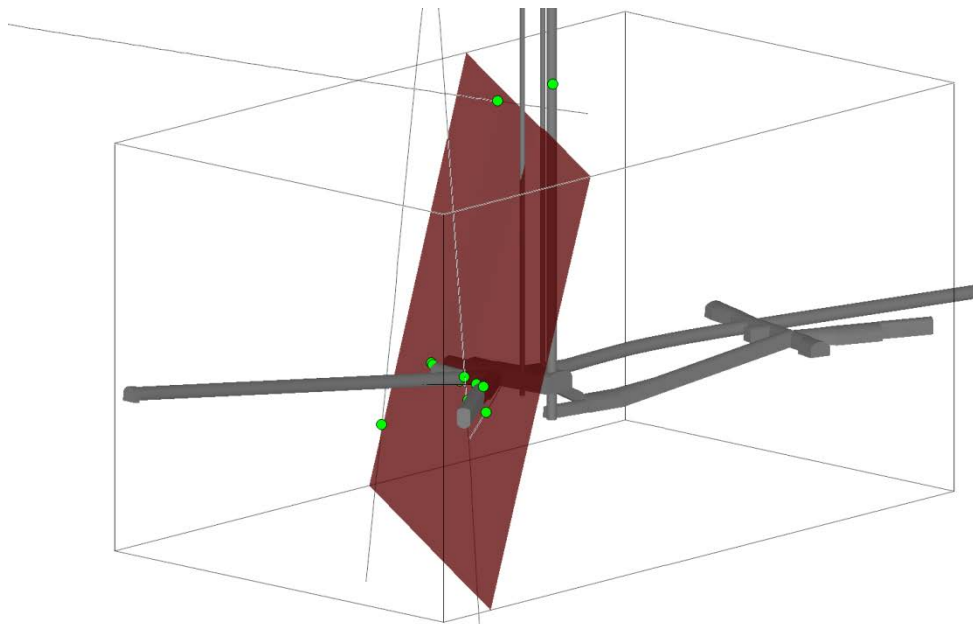


Figure A 15. 3D view of FASNS002 with observation points in green. View from NE.

If extrapolated upwards, in the south the structure intersects TASA at section approximately 2/500 in the lower tunnel turn. Here there is a smaller water-bearing fracture. In the level above the structure follows the tunnel direction. There is no corresponding mapped fracture but it should be noted that a slight change of the interpreted dip makes a big difference. In the north the modelled structure intersects the tunnel at approximately 2/770. There are water-bearing fractures at 2/767 and 2/775. The probe drillings showed big inflows between 2/750-2/770 m.

Structure FASNW001

The basis of the interpretation of FASNW001 was a mapped water-bearing fracture in the TBM-tunnel (TASA). The structure does not intersect TASQ.

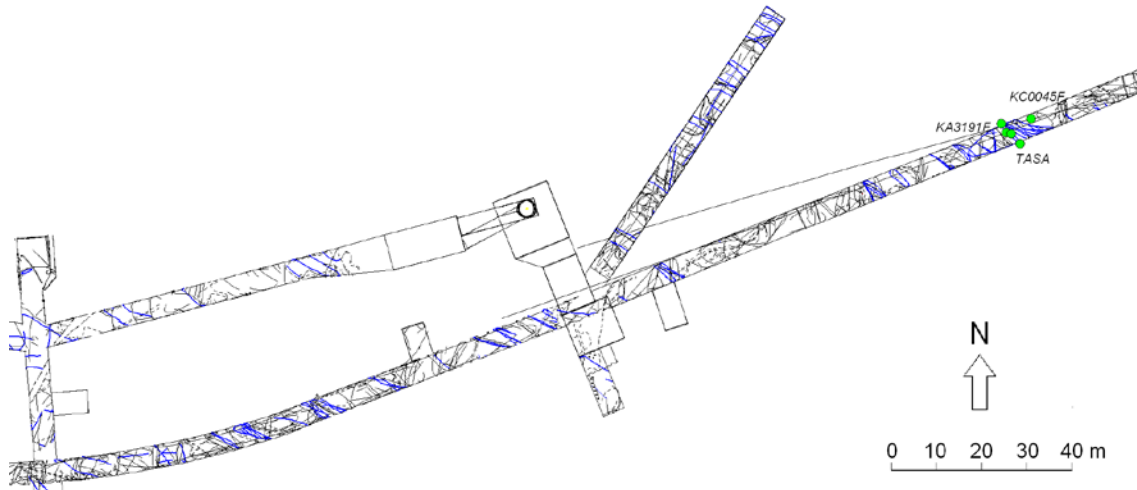


Figure A 16. Observation points used to model FASNW001 in A tunnel and boreholes.

Structure FASNW001 was modelled with an orientation of $133^{\circ}/83^{\circ}$ (RT90).

The indications used to model structure FASNW001 were:

1. Tunnel mapping, water-bearing fracture 3280.2-12 in TASA (the TBM tunnel). Mapped with an orientation of RT90: $127^{\circ}/90^{\circ}$ ($125^{\circ}/90^{\circ}$ to magnetic north) /TMS/.
2. Borehole KA3191F at 89 m BH length. Reduced RQD value (73%) at BH length 88-89 m /rqd_rqd, SICADA/. Mapped fracture ‘broken’ at BH length 88.77 m oriented RT90: $161^{\circ}/82^{\circ}$ ($173^{\circ}/82^{\circ}$ Åspö96) /fract_core-ori_broken, SICADA/. A radar reflector at BH length 89 m oriented RT90: $134^{\circ}/71^{\circ}$ /radar_direct-ori1, SICADA/.
3. Borehole KC0045F at 114 m BH length. Reduced RQD value (73%) at BH length 113-114 m /rqd_rqd, SICADA/. Water inflow between 112-117 m (145 l/min) /Olsson et al. 1994/.

This structure is classified as **possible**.

FASNW001 $133^{\circ}/83^{\circ}$ (possible) - point table

ID	Object	Section (m)	Water	Fract RT90	Mineral	Width (mm)	RQD (%)	Freq (fr/m)	Crush	Radar RT90	Oth
1	TASA	3280-12	vv	127/90	Ep/Ka	-	-	-	-	-	Ox
2	KA3191F	89		161/82	Kl/Ep	0	73	10/6 ¹	0 ¹	134/71	Ox
3	KC0045F	114	Infl	-	-	-	73	4/4 ¹	0 ¹	0	

The structure is trimmed by FASNS002 in the NW and FASNW003 in the SE. It is modelled only between $z = -360 - -490$ m.

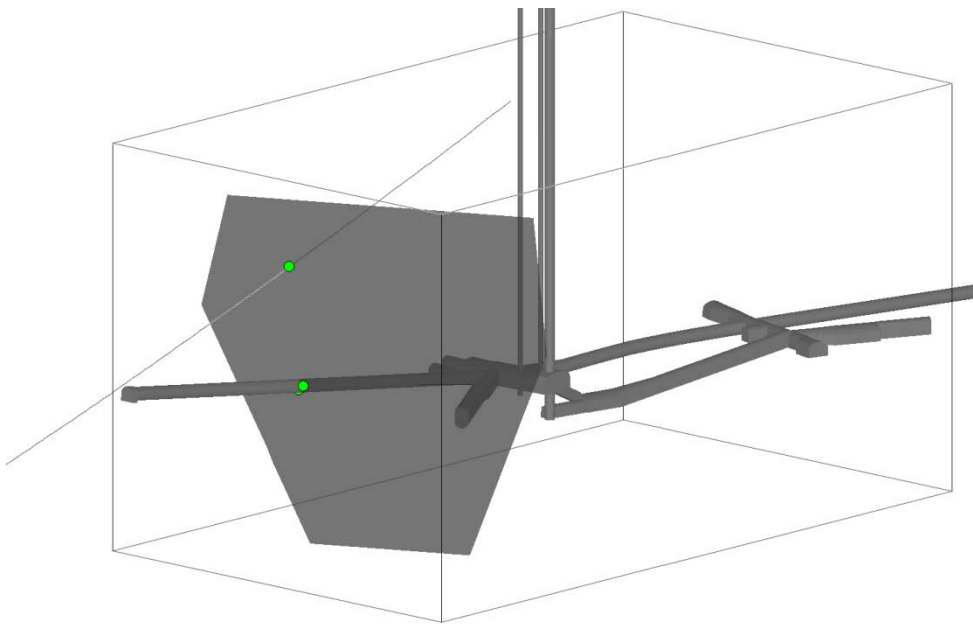


Figure A 17. 3D view of FASNW001 with observation points in green. View from NE.

If extrapolated upwards, in the north the modelled structure intersects TASA immediately outside the model area. In the south the modelled structure intersects TASA far outside the model area.

Structure FASNW002

The basis of the interpretation of FASNW002 was connecting the mapped water-bearing fractures in the TBM-tunnel (TASA) and tunnel TASQ. Structure FASNW002 was modelled with an orientation of 115°/86° (RT90).

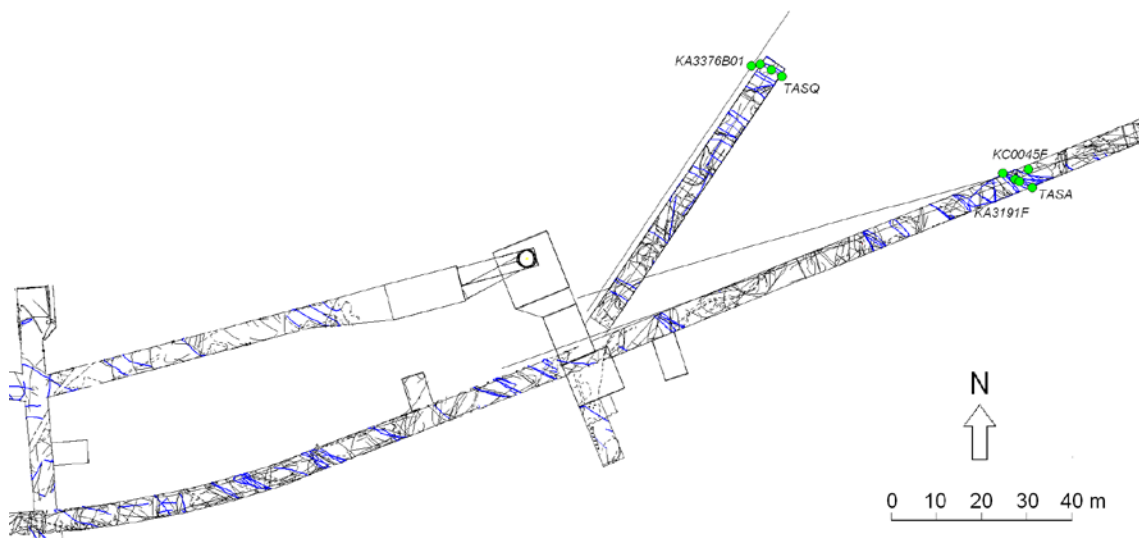


Figure A 18. Observation points used to model FASNW002 in tunnels and boreholes.

The indications used to model structure FASNW002 were:

1. Tunnel mapping, water-bearing fracture 3280.2-09 in TASA (the TBM tunnel). Mapped with an orientation of RT90: 110°/88° (108°/88° to magnetic north) /TMS/.
2. Tunnel mapping, water-bearing fracture 80-10 i TASQ mapped with an orientation of RT90: 114°/90° (112°/90° to magnetic north) /TMS/.
3. Borehole KA3191F at 87 m BH length. Reduced RQD value (71%) at BH length 87-88 m /rqd_rqd, SICADA/. Oxidation between 86.8-87.3 m /rock_alter-type, SICADA/. A mapped fracture 'broken' at BH length 87,04 m oriented RT90: 137°/61° (149°/61° Äspö96) /fract_core-ori_broken, SICADA/.
4. Borehole KC0045F at 113 m BH length. Reduced RQD value (73%) at BH length 113-114 m /rqd_rqd, SICADA/. Water inflow between 112-117 m (145 l/min) /Olsson et al. 1994/.
5. Borehole KAS3376B01 at BH length 65.6 m. Here there are a number of fractures with inflow measured at flow logging, the highest transmissivity is at 65.6 m /Pöllänen and Rouhiainen, 2003/. Mapped open fracture at BH length 65.48 m oriented RT90: 130°/86° (142°/86° Äspö96) /fract_core-ori_open, SICADA/.

This structure is classified as **probable**.

FASNW002 115°/86° (probable) - point table

ID	Object	Section (m)	Water	Fract RT90	Mineral	Width (mm)	RQD (%)	Freq (fr/m)	Crush	Radar RT90	Oth
1	TASA	3280-09	vv	110/88	Ka	-	-	-	-	-	
2	TASQ	80-10	v	114/90	Ep/Ka/Kl	0.5	-	-	-	-	
3	KA3191F	87		137/61	Cy/Kl/Ka	0	71	12/8 ¹	0 ¹	(85)	Ox
4	KC0045F	113	Infl	-	-	-	73	7/7 ¹	0 ¹	0	
5	KAS3376B01	65.6	Infl	130/86	Ka/Kl	1	87	7/4 ²	0 ²	-	BIPS

The structure is trimmed by FASNS002 in the NW. It is modelled only between z= -370 -- 470 m.

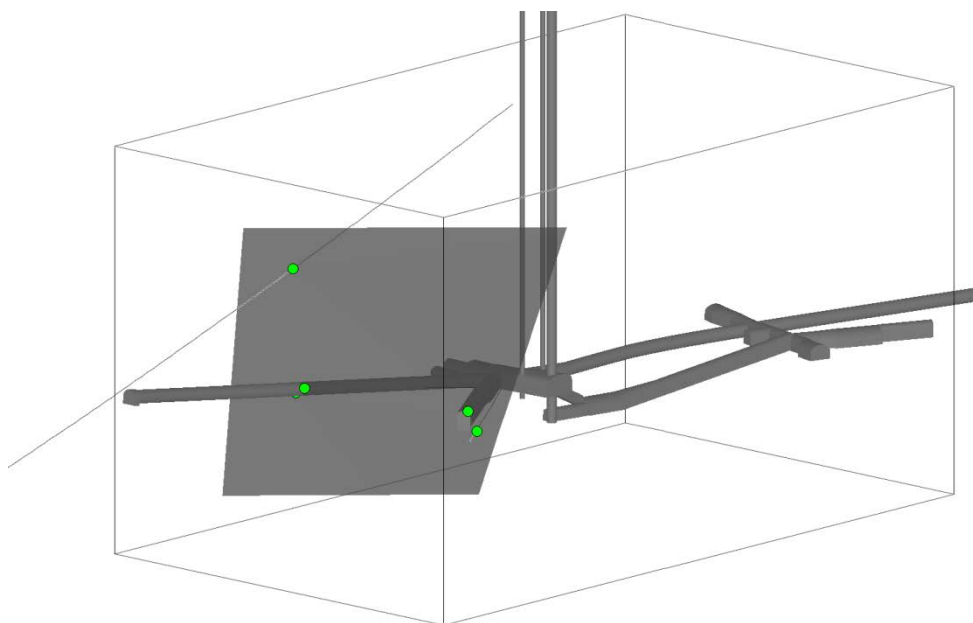


Figure A 19. 3D view of FASNW002 with observation points in green. View from NE.

In the north the modelled structure intersects TASA at section approximately 2/685 m in the lower tunnel turn in a mapped zone with high transmissivity. Same as FASNW006, FASNW005 and FASNW004. In the level above the structure intersects at approximately 1/766, where there is a mapped water bearing zone (Z7).

Structure FASNW003

The basis of the interpretation of FASNW003 was connecting the mapped water-bearing fractures in the TBM-tunnel (TASA) and tunnel TASQ.

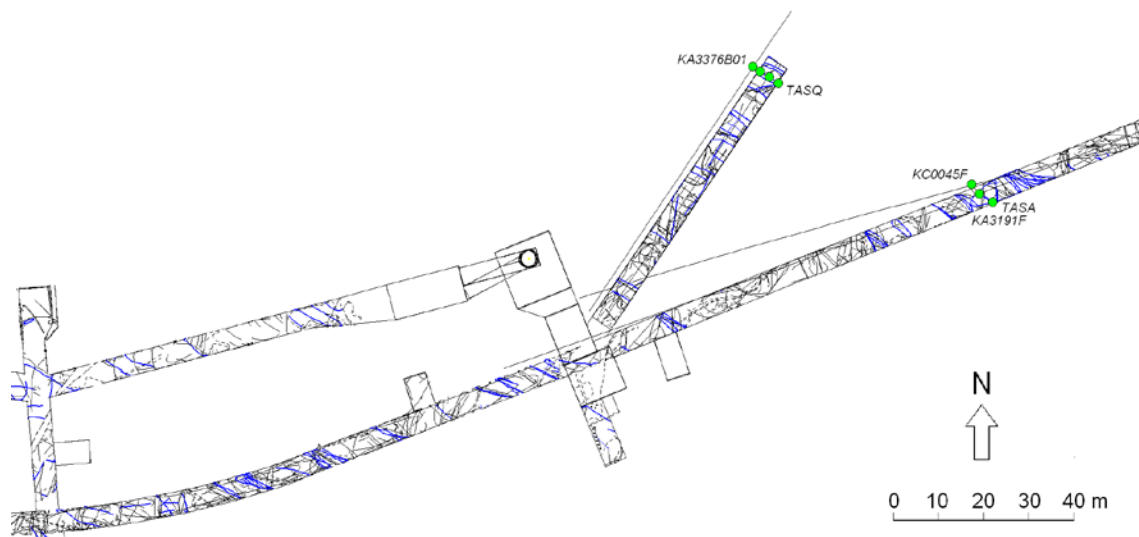


Figure A 20. Observation points used to model FASNW003 in tunnels and boreholes.

Structure FASNW003 was modelled with an orientation of $119^{\circ}/89^{\circ}$ (RT90).

The indications used to model structure FASNW003 were:

1. Tunnel mapping, water-bearing fracture 3290.0-11 in TASA (the TBM tunnel). Mapped with an orientation of RT90: $110^{\circ}/90^{\circ}$ ($108^{\circ}/90^{\circ}$ to magnetic north) /TMS/.
2. Tunnel mapping, water-bearing fracture 80-08 i TASQ mapped with an orientation of RT90: $116^{\circ}/90^{\circ}$ ($114^{\circ}/90^{\circ}$ to magnetic north) /TMS/.
3. Borehole KA3376B01 at BH length 65 m. Reduced RQD value (87%) at BH length 65-66 m /rqd_rqd, SICADA/. Increased fracture frequency (7) between 65-66 m /freq_1m-total, SICADA/. Mapped open fracture at BH length 65.15 m oriented RT90: $148^{\circ}/82^{\circ}$ ($160^{\circ}/82^{\circ}$ Äspö96) /fract_core-ori_open, SICADA/. Inflow on flow logging at 65.2 and 65.6 m /Pöllänen and Rouhiainen, 2003/.
4. Borehole KC0045F at 99 m BH length. Reduced RQD value (63%) at BH length 98-99 m /rqd_rqd, SICADA/. Crush between 98.7-99.2 m /fract_crush-pclen, SICADA/. Increased fracture frequency between 98-99 m (9) and 99-100 m (11) /freq_1m- total, SICADA/. Inflow between 99-105 m BH length (210 l/min) /Olsson et al. 1994/.
5. Borehole KA319F at 96 m BH length. Slightly reduced RQD value (91%) at BH length 96-97 m /rqd_rqd, SICADA/. A radar reflector at BH length 95 m oriented RT90: $143^{\circ}/56^{\circ}$ /radar_direct-ori1, SICADA/.. Mapped fracture 'broken' at BH length 96.78 m oriented RT90: $153^{\circ}/73^{\circ}$ ($168^{\circ}/73^{\circ}$ Äspö96) /fract_core-ori_broken, SICADA/.

This structure is classified as **probable**.

FASNW003 119°/89° (probable) - point table

ID	Object	Section (m)	Water	Fract RT90	Mineral	Width (mm)	RQD (%)	Freq (fr/m)	Crush	Radar RT90	Oth
1	TASA	3290-11	vv	110/90	Ka/lj	-	-	-	-	-	
2	TASQ	80-08	v	116/90	Ka	0	-	-	-	-	
3	KA3376B01	65	Infl	148/82	Ka/Kl	2	87	7/0 ²	0 ²	-	BIPS
4	KC0045F	99	Infl	Crush	Kl/Ka	-	63	14/3 ¹	11 ¹	0	
5	KA3191F	96		153/73	Kl/Ep	0	91	5/5 ¹	0 ¹	143/56	

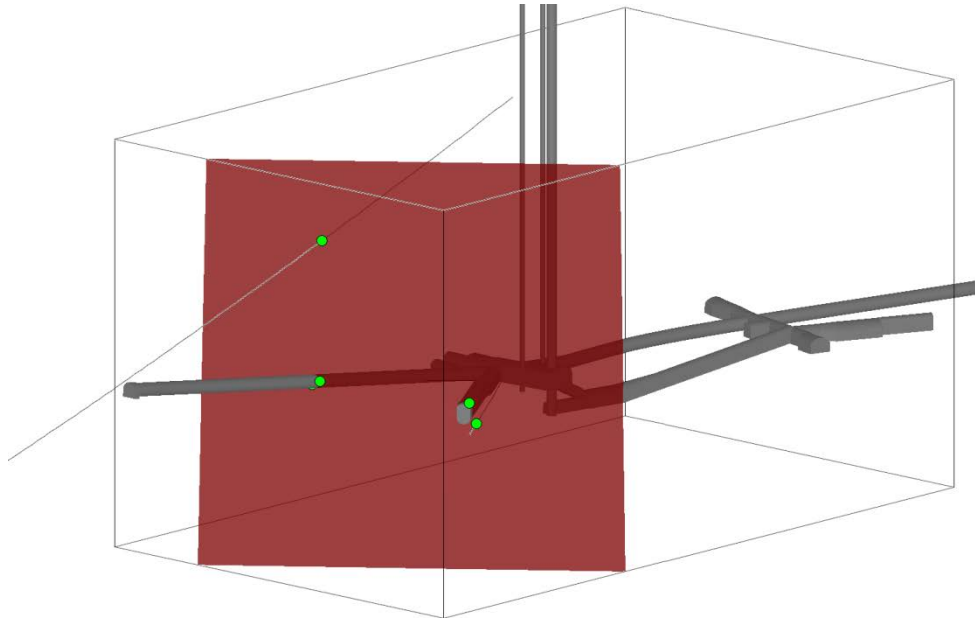


Figure A 21. 3D view of FASNW003 with observation points in green. View from NE.

If extrapolated upwards, in the north the modelled structure intersects TASA at section approximately 2/680 m in the lower tunnel turn in a mapped zone with high transmissivity. Same as FASNW006, FASNW005 and FASNW004. In the level above the structure intersects at approximately 1/750, where there are no corresponding water-bearing fractures, but a water bearing zone at 1/760 could fit reasonably well. Same as FASNW004. In the south the modelled structure intersects TASA far outside the model area.

Structure FASNW004

The basis of the interpretation of FASNW004 was connecting the mapped water-bearing fractures in the TBM-tunnel (TASA) and tunnel TASQ.

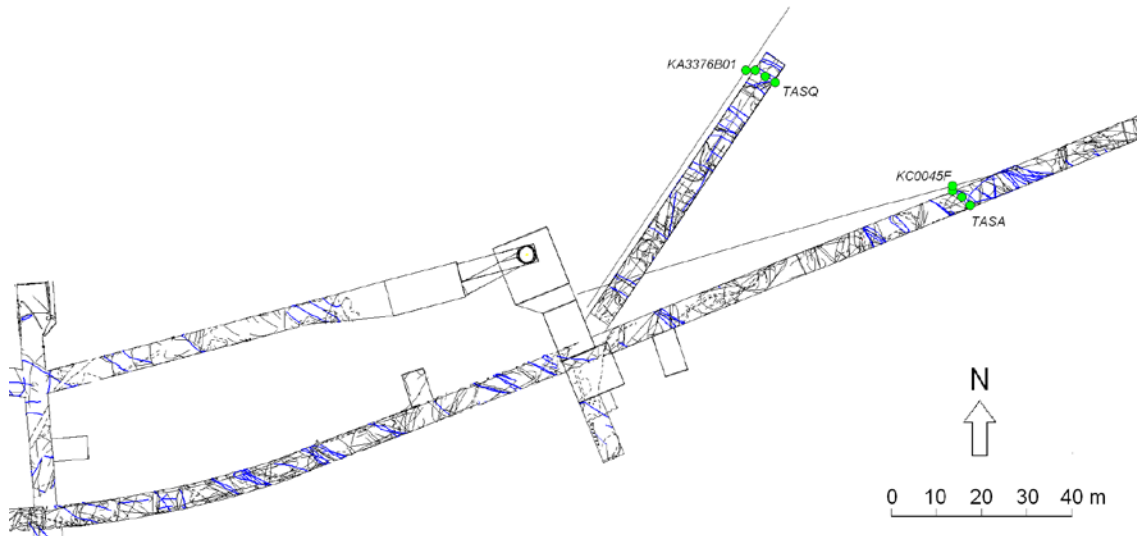


Figure A 22. Observation points used to model FASNW004 in tunnels and boreholes.

Structure FASNW004 was modelled with an orientation of $121^{\circ}/89^{\circ}$ (RT90).

The indications used to model structure FASNW004 were:

1. Tunnel mapping, water-bearing fracture 3304.8-06 in TASA (the TBM tunnel). Mapped with an orientation of RT90: $132^{\circ}/86^{\circ}$ ($130^{\circ}/86^{\circ}$ to magnetic north) /TMS/.
2. Tunnel mapping, water-bearing fracture 80-07 i TASQ mapped with an orientation of RT90: $306^{\circ}/85^{\circ}$ ($304^{\circ}/85^{\circ}$ to magnetic north) /TMS/.
3. Borehole KAS3376B01 at BH length 63 m. Reduced RQD value (73%) at BH length 63-64 m /rqd_rqd, SICADA/. Mapped open fracture at BH length 63.23 m oriented RT90: $309^{\circ}/57^{\circ}$ ($321^{\circ}/57^{\circ}$ Äspö96) /fract_core-ori_open, SICADA/. Inflow PFL at 63.4 m / Pöllänen and Rouhiainen, 2003/.
4. Borehole KC0045F at 94.5 m BH length. Rather low RQD value (56%) at BH length 94-95 m /rqd_rqd, SICADA/. Crush at 94.5 m /fract_crush-pclen, SICADA/. Crush (12) between 94-95 m /freq_1m-petrocor_crush, SICADA/. A radar reflector at BH length 95 m oriented RT90: $325^{\circ}/70^{\circ}$ /radar_direct-ori1, SICADA/. Inflow at 94 m BH length (24 l/min) /Olsson et al. 1994/.

The modelled fracture intersects the borehole KA3191F at a borehole length of about 100.3 m. There is no suitable oriented fracture here but in the SICADA tables there are some steeply dipping fractures mapped as broken between 99.5-100.6 m. This borehole is not included in the modelling of the structure.

This structure is classified as **probable**.

FASNW004 121°/89° (probable) - point table

ID	Object	Section (m)	Water	Fract RT90	Mineral	Width (mm)	RQD (%)	Freq (fr/m)	Crush	Radar RT90	Oth
1	TASA	3304-06	vv	132/86	Kl/Ka	-	-	-	-	-	Ox
2	TASQ	80-07	vv	306/85	Ka	1	-	-	-	-	
3	KA3376B01	63	PFL	309/57	Ka	1	73	12/2 ¹	0 ¹	-	BIPS
4	KC0045F	94.5	Infl	Crush	Ka/Kl	-	56	17/5 ¹	12 ¹	325/70	

The structure is trimmed by FASNS002 in the NW and FASNS001 in the SE. It is modelled only between z= -370 – -450 m.

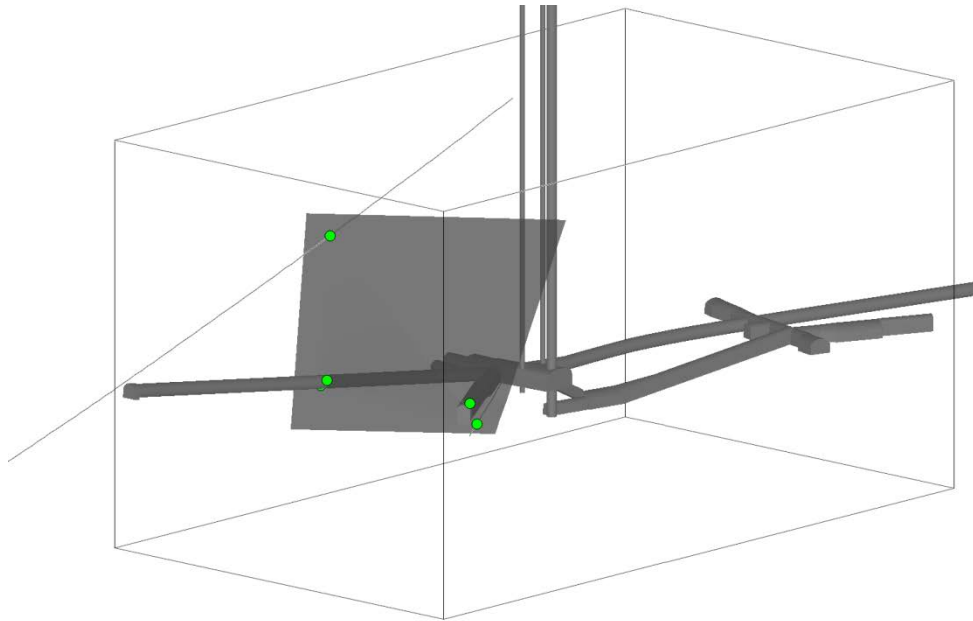


Figure A 23. 3D view of FASNW004 with observation points in green. View from NE.

If extrapolated upwards, in the north the modelled structure intersects TASA at section approximately 2/685 m in the lower tunnel turn in a mapped zone with high transmissivity. Same as FASNW006 and FASNW005. In the level above the structure intersects at approximately 1/760, where there is a mapped water bearing zone that could fit reasonably well.

In the south the modelled structure intersects TASA far outside the model area.

Structure FASNW005

The basis of the interpretation of FASNW005 was connecting the mapped water-bearing fractures in the TBM-tunnel (TASA) and tunnel TASQ.

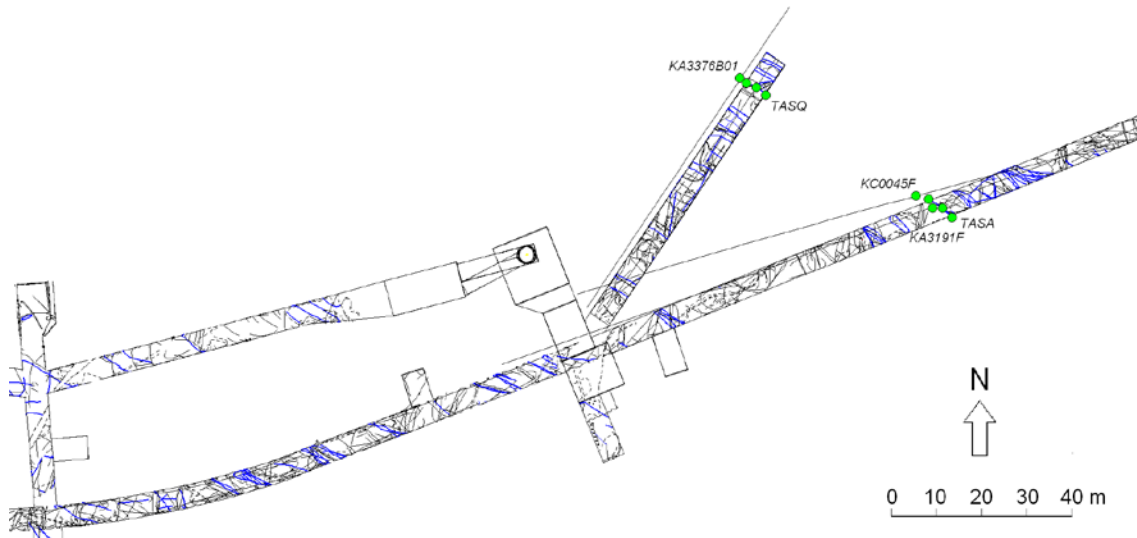


Figure A 24. Observation points used to model FASNW005 in tunnels and boreholes.

Structure FASNW005 was modelled with an orientation of $303^{\circ}/89^{\circ}$ (RT90).

The indications used to model structure FASNW005 were:

1. Tunnel mapping, water-bearing fracture 3304.8-01 in TASA (the TBM tunnel). Mapped with an orientation of RT90: $298^{\circ}/88^{\circ}$ ($296^{\circ}/88^{\circ}$ to magnetic north) /TMS/.
2. Tunnel mapping, water-bearing fracture 80-01 i TASQ mapped with an orientation of RT90: $124^{\circ}/86^{\circ}$ ($122^{\circ}/86^{\circ}$ to magnetic north) /TMS/.
3. Borehole KAS3376B01 at BH length 61 m. Mapped open fracture at BH length 61.07 m oriented RT90: $123^{\circ}/85^{\circ}$ ($135^{\circ}/85^{\circ}$ Äspö96) /fract_core-ori_open, SICADA/. Inflow PFL at 61.2 m /Pöllänen and Rouhiainen, 2003/.
4. Borehole KC0045F at 85 m BH length. Reduced RQD value (70%) at BH length 84-85 m /rqd_rqd, SICADA/. Inflow at 85 m BH length (12 l/min) /Olsson et al. 1994/. There are 9 natural fractures between 84-85 m /freq_1m_petrocor-natural, SICADA/. Same as FASNW006, point 4.
5. Borehole KA3191F at 107 m BH length. Crush zone at BH length 106.9 m /fract_crush-pklen SICADA/. Reduced RQD value (69%) at BH length 107-108 m /rqd_rqd, SICADA/. Crush (10) at 107-108 m /freq_1m_petrocor_crush, SICADA/.

This structure is classified as **probable**.

FASNW005 $303^{\circ}/89^{\circ}$ (probable) - point table

ID	Object	Section (m)	Water	Fract RT90	Mineral	Width (mm)	RQD (%)	Freq (fr/m)	Crush	Radar RT90	Oth
1	TASA	3304-01	vv	298/88	My/Ka	-	-	-	-	-	
2	TASQ	80-01	v	124/86	Kl/Ka	0.5	-	-	-	-	Ox
3	KA3376B01	61	PFL	123/85	Kl/Ka	1	96	2/1 ²	0 ²	-	BIPS
4	KC0045F	85	Infl	(315/89)	-	-	70	9/9 ¹	0 ¹	0	
5	KA3191F	107	0	Crush	Kl	-	69	12/1 ¹	10 ¹	-	

The structure is trimmed by FASNS002 in the NW and FASNS001 in the SE. It is modelled only between $z = -370 - -450$ m.

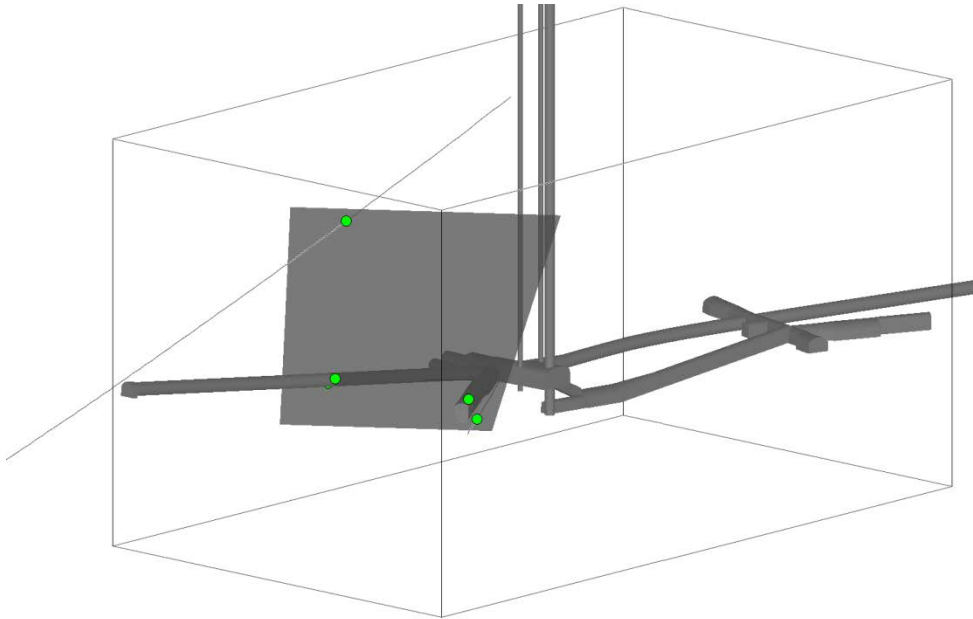


Figure A 25. 3D view of FASNW005 with observation points in green. View from NE.

If extrapolated upwards, the modelled structure intersects TASA at section approximately 2/685 in the lower tunnel turn in a mapped zone with high transmissivity. Same as FASNW006 and FASNW004.

Structure FASNW006

The basis of the interpretation of FASNW006 was connecting the mapped water-bearing fractures in the TBM-tunnel (TASA) and tunnel TASQ. The zone is mapped completely around TASQ but is not detected in the parallel borehole KAS3376B01, passing only 0.6 m outside the northern wall. During the pre grouting there was no water leakage in the position of this fracture /Emmelin et al. 2004/ but it is possible that it became water bearing after the other, more open fractures were grouted.

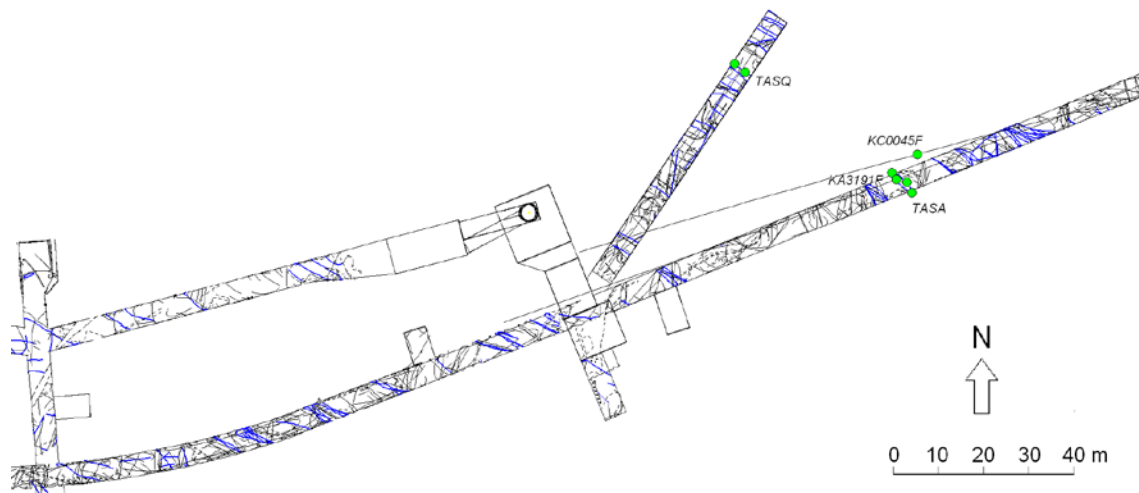


Figure A 26. Observation points used to model FASNW006 in tunnels and boreholes.

Structure FASNW006 was modelled with an orientation of $126^{\circ}/83^{\circ}$ (RT90).

The indications used to model structure FASNW006 were:

1. Tunnel mapping, water-bearing fracture 3319.6-01 in TASA (the TBM tunnel). Mapped with an orientation of RT90: $113^{\circ}/65^{\circ}$ ($111^{\circ}/65^{\circ}$ to magnetic north) /TMS/.
2. Tunnel mapping, water-bearing fracture 70-11 in TASQ mapped with an orientation of RT90: $104^{\circ}/72^{\circ}$ ($102^{\circ}/72^{\circ}$ to magnetic north) /TMS/.
3. Borehole KC0045F at 85 m BH length. Reduced RQD value (70%) at BH length 84-85 m /rqd_rqd, SICADA/. Inflow at 85 m BH length (12 l/min) /Olsson et al. 1994/. There is 9 Natural fractures between 84-85 m /freq_1m_petrocor-natural, SICADA/. Same as FASNW005, point 4.
4. (Weak) Borehole KA3191F at 116 m BH length. Slightly altered fracture, broken at 116.1 and 116.2 m BH length /p_fract_core, SICADA/. The orientation of this fracture is not mapped and hence it is missing in the RVS parameter fract_core-ori_all. The borehole was grouted during drilling between 10 – 135 m.

The modelled structure cannot be found in borehole KA3376B01 just outside the wall of TASQ on floor level. Also, since the mapped fracture in TASQ only exists above the $z=-442$, the modelled structure is cut off vertically at this level and is estimated to exist only above the borehole.

This structure is classified as **probable**.

FASNW006 126°/83° (probable) - point table

ID	Object	Section (m)	Water	Fract RT90	Mineral	Width (mm)	RQD (%)	Freq (fr/m)	Crush	Radar RT90	Oth
1	TASA	3319-01	vv	113/65	Ep/Kl	-	-	-	-	-	
2	TASQ	70-11	vv	104/72	Xz	0	-	-	-	-	
3	KC0045F	85	Infl	-	-	-	70	9/9 ¹	0 ¹	0	
4	KA3191F	116	-	-	-	-	100	2/2 ¹	0 ¹	0	

The structure is trimmed by FASNS002 in the NW and FASNS001 in the SE. It is modelled only above $z = -442$ m.

The modelled structure intersects KA2162B at approximately 63 m BH length, where a reduction in RQD (78%) is found at 65-66 m BH length /*rqd_rqd, SICADA/* and a radar reflector at 62 m BH length oriented 152°/76° (RT90), but this indication is located too far away to be included in the modelling.

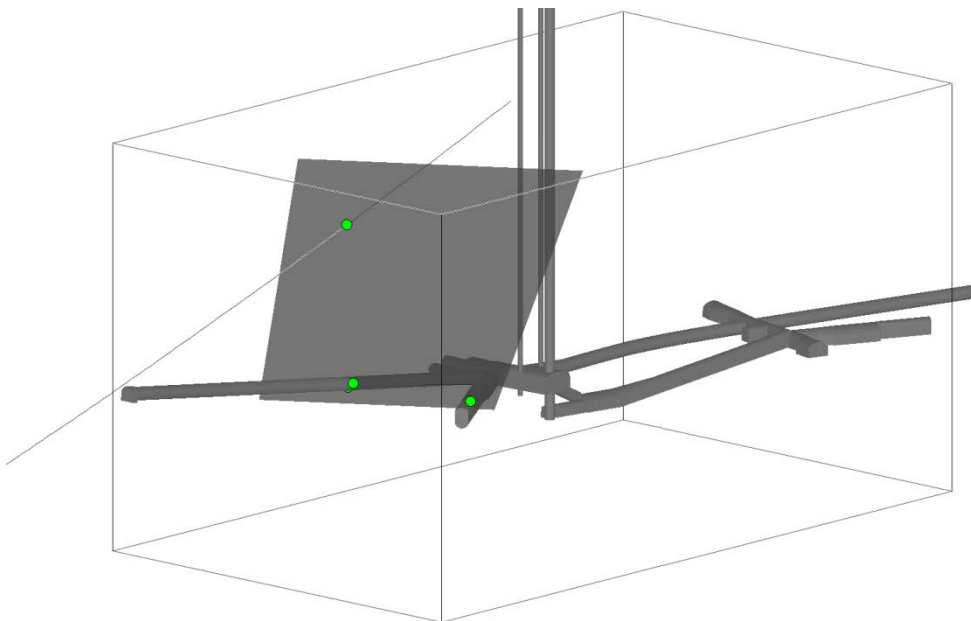


Figure A 27. 3D view of FASNW006 with observation points in green. View from NE.

If extrapolated upwards, the modelled structure intersects TASA at section approximately 2/685 m in the lower tunnel turn in a mapped zone with high transmissivity. *Same as FASNW005 and FASNW004.* In the level above the structure intersects at approximately 2/210, where there is a mapped water-bearing structure which corresponds well. In the top level there is no indication corresponding to the modelled structure.

Structure FASNW007

The basis of the interpretation of FASNW007 was connecting the mapped water-bearing fractures in the TBM-tunnel (TASA) and tunnel TASQ.

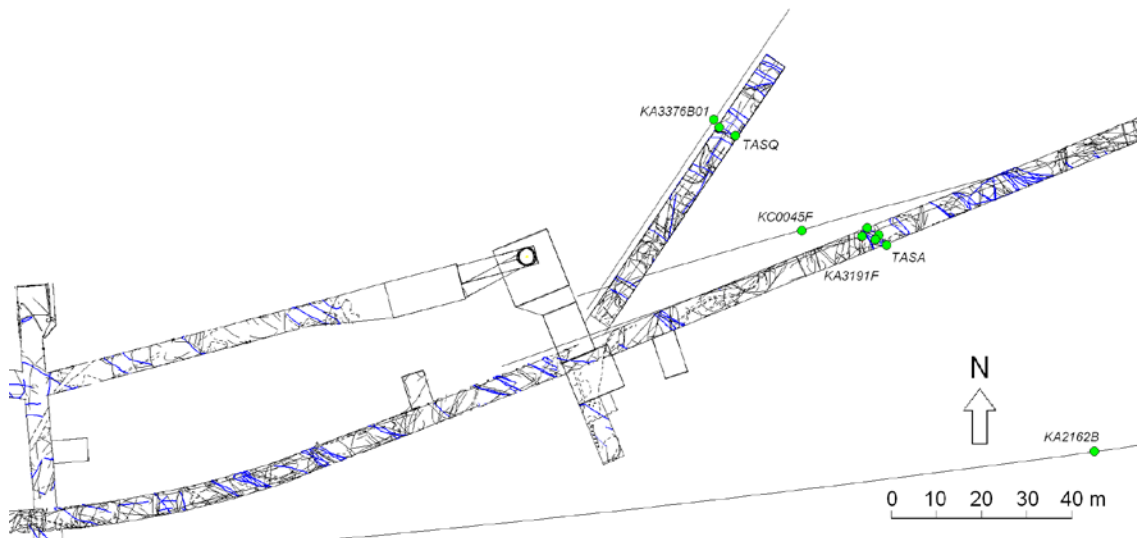


Figure A 28. Observation points used to model FASNW007 in tunnels and boreholes.

Structure FASNW007 was modelled with an orientation of $304^{\circ}/84^{\circ}$ (RT90).

The indications used to model structure FASNW007 were:

1. Tunnel mapping, water-bearing fracture 3319.6-04 in TASA (the TBM tunnel). Mapped with an orientation of RT90: $308^{\circ}/82^{\circ}$ ($306^{\circ}/82^{\circ}$ to magnetic north) /TMS/.
2. Tunnel mapping, water-bearing fracture 70-01 i TASQ mapped with an orientation of RT90: $123^{\circ}/84^{\circ}$ ($121^{\circ}/84^{\circ}$ to magnetic north) /TMS/.
3. Borehole KA3376B01 at BH length 50.5 m. Mapped open fracture at BH length 50.42 m oriented RT90: $114^{\circ}/86^{\circ}$ ($126^{\circ}/86^{\circ}$ Äspö96) /fract_core-ori_open, SICADA/. Significant inflow (over the range of measurement) at 50.5 m BH length /Pöllänen and Rouhiainen, 2003/. Slightly reduced RQD value (91%) at BH length 51-52 m /rqd_rqd, SICADA/.
4. Borehole KC0045F at 56 m BH length. Very low RQD value (0%) at BH length 55-56 m /rqd_rqd, SICADA/. Crush between 54.6-56.5 m /fract_crush-min1, SICADA/. No leakage detected in this point /Olsson et al. 1994/. Same as FASNW008, point 5.
5. Borehole KA3191F at 123.6 m BH length. Inflow of 110 l/min at 123.6 and 124.1 m, pressure responses with SA2240B, KAS02, KAS05 and KA2162B (maximum between 80.5-142 m) /Rhén et al., 1995/. Mapped open fracture at BH length 123.6 m oriented RT90: $310^{\circ}/77^{\circ}$ ($322^{\circ}/77^{\circ}$ Äspö96) /fract_core-ori_open, SICADA/. Reduced RQD value (86%) at BH length 123-124 m /rqd_rqd, SICADA/.
6. Borehole KA2162B at 111 m BH length. A radar reflector at BH length 111 m oriented RT90: $300^{\circ}/74^{\circ}$ /radar_direct-ori2, SICADA/. Slightly reduced RQD value (95%) at BH length 111-112 m. Oxidation between 107-111 m /rock_alter-type, SICADA/.

This structure is classified as **probable**.

FASNW007 304°/84° (probable) - point table

ID	Object	Section (m)	Water	Fract RT90	Mineral	Width (mm)	RQD (%)	Freq (fr/m)	Crush	Radar RT90	Oth
1	TASA	3319-04	wv	308/82	My/Ka/lj	-	-	-	-	-	
2	TASQ	70-01	wv	123/84	Ep/Ka/Kl	2	-	-	-	-	
3	KA3376B01	50.5	Infl	114/86	Ka/Kl	1	91	1/1 ²	0 ²	-	BIPS
4	KC0045F	56	0	Crush	Go/Ka	-	0	20/0 ¹	20 ¹	0	
5	KA3191F	123.6	resp	310/77	Ka/Ep/Kl	4	86	12/4 ¹	3 ¹	0	
6	KA2162B	111		-	-	-	95	6/5 ¹	0 ¹	300/74	Ox

The modelled structure intersects KAS02 at approximately 100 m BH length, where a clear reduction in RQD (27%) can be found at 99-100 m BH length /rqd_rqd, SICADA/, but this indication is weak and is located too far away to be included in the modelling.

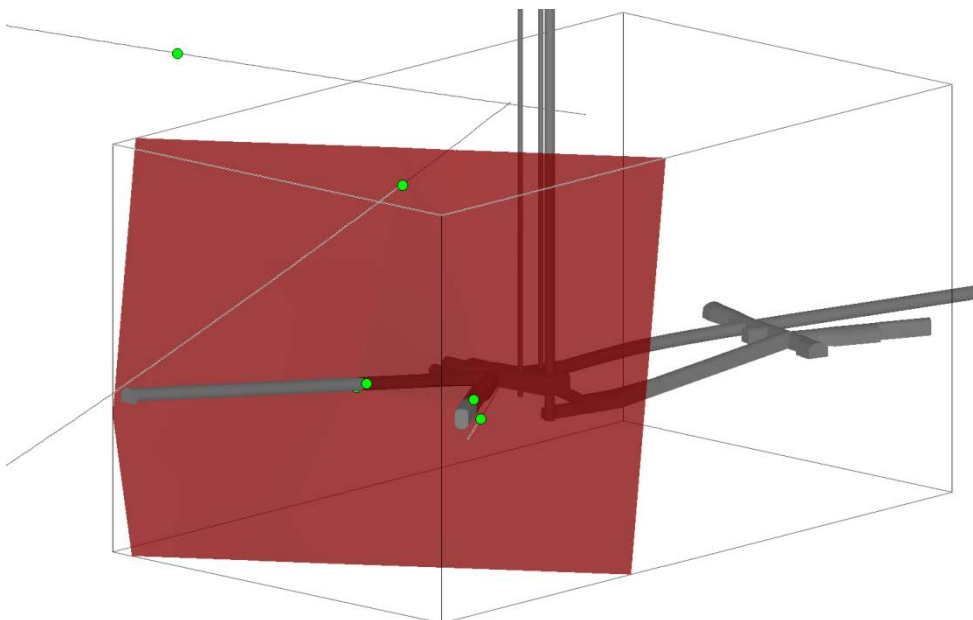


Figure A 29. 3D view of FASNW007 with observation points in green. View from NE.

If extrapolated upwards, the modelled structure intersects TASA at section approximately 2/663 in the lower tunnel turn. At the sections 2/666-69-70 there are mapped sub-parallel water-bearing fractures that corresponds well with the modelled structure.

Structure FASNW008

The basis of the interpretation of FASNW008 was connecting the mapped water-bearing fractures in the TBM-tunnel (TASA) and tunnel TASQ.

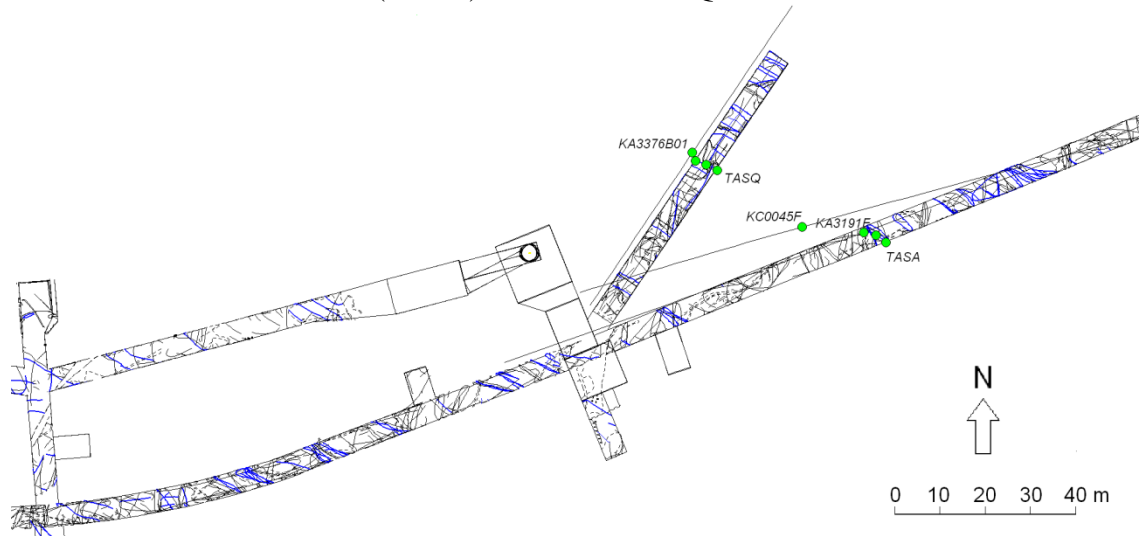


Figure A 30. Observation points used to model FASNW008 in tunnels and boreholes.

Structure FASNW008 was modelled with an orientation of $295^{\circ}/87^{\circ}$ (RT90).

The indications used to model structure FASNW008 were:

1. Tunnel mapping, water-bearing fracture 3319.6-10 in TASA (the TBM tunnel). Mapped with an orientation of RT90: $310^{\circ}/90^{\circ}$ ($308^{\circ}/90^{\circ}$ to magnetic north) /TMS/.
2. Tunnel mapping, water-bearing fracture 60-07 i TASQ mapped with an orientation of RT90: $292^{\circ}/90^{\circ}$ ($290^{\circ}/90^{\circ}$ to magnetic north) /TMS/.
3. Borehole KA3191F at 124.1 m BH length. Inflow of 110 l/min at 123.6 and 124.1 m, pressure responses with SA2240B, KAS02, KAS05 and KA2162B (maximum between 80.5-142 m) /Rhén et al., 1995/. Rather low RQD value (58%) at BH length 123-124 m /rqd_rqd, SICADA/. Crush between 124.1-124.2 m Oxidation between 124.1-124.4 m /rock_alter-type, SICADA/.
4. Borehole KC0045F at 56 m BH length. Very low RQD value (0%) at BH length 55-56 m /rqd_rqd, SICADA/. Crush between 54.6-56.5 m /fract_crush-min1, SICADA/. However, no leakage detected in this point /Olsson et al. 1994/. Same as FASNW007, point 4.
5. (Weak) Borehole KA3376B01 at BH length 40.7 m. Mapped fracture at BH length 40.7 m oriented RT90: $111^{\circ}/87^{\circ}$ ($123^{\circ}/87^{\circ}$ Äspö96) /fract_core-ori_all, SICADA/. NOTE, no hydraulic contact can be found between KA3376B01 and KF0069A01.

This structure is classified as **probable**.

FASNW008 295°/87° (probable) - point table

ID	Object	Section (m)	Water	Fract RT90	Mineral	Width (mm)	RQD (%)	Freq (fr/m)	Crush	Radar RT90	Oth
1	TASA	3319-10	vvv	310/90	Ka/lj	-	-	-	-	-	
2	TASQ	60-07	vv	292/90	Ka/lj	0.5	-	-	-	-	
3	KA3191F	124	Infl	Crush	Ka/Kl	-	58	15/7 ¹	5 ¹	(126)	Ox
4	KC0045F	56	0	-	Go/Ka	-	0	20/0 ¹	20 ¹	0	
5	KA3376B01	40.7	0	111/87	Kl/Ka	0	100	1/0 ²	0 ²	-	BIPS

The modelled structure intersects KA2162B at approximately 82 m BH length, here there is a radar reflector oriented 142°/78° (RT90) /radar_direct-ori2, SICADA/. The structure also intersects KAS06 at approximately 325 m BH length, where RQD (66%) is reduced at 325-326 m BH length /rqd_rqd, SICADA/. Both these indications are, however, weak and are located too far away to be included in the modelling.

The structure is trimmed by FASNS002 in the NW and FASNS001 in the SE. It is modelled only above z= -450 m.

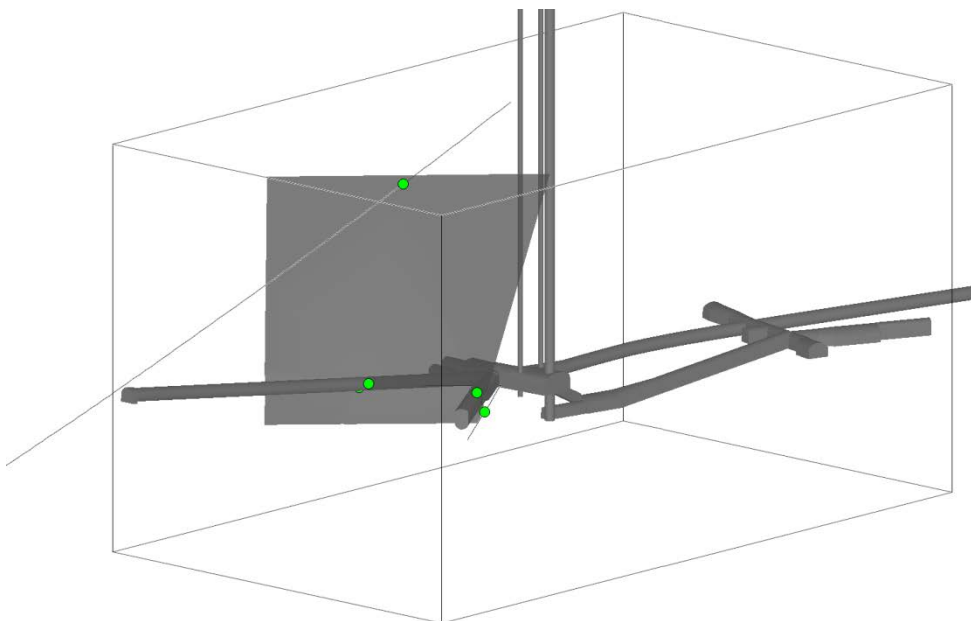


Figure A 31. 3D view of FASNW008 with observation points in green. View from NE.

If extrapolated upwards, in the north the structure intersects TASA at section approximately 2/647 in the lower tunnel turn and at approximately 1/710 m in the level above. On both places there are mapped sub-parallel water-bearing fractures that correspond well with the modelled structure.

Structure FASNW009

The basis of the interpretation of FASNW009 was a mapped water-bearing fracture in the TBM-tunnel (TASA). The structure cannot be found in tunnel TASQ.

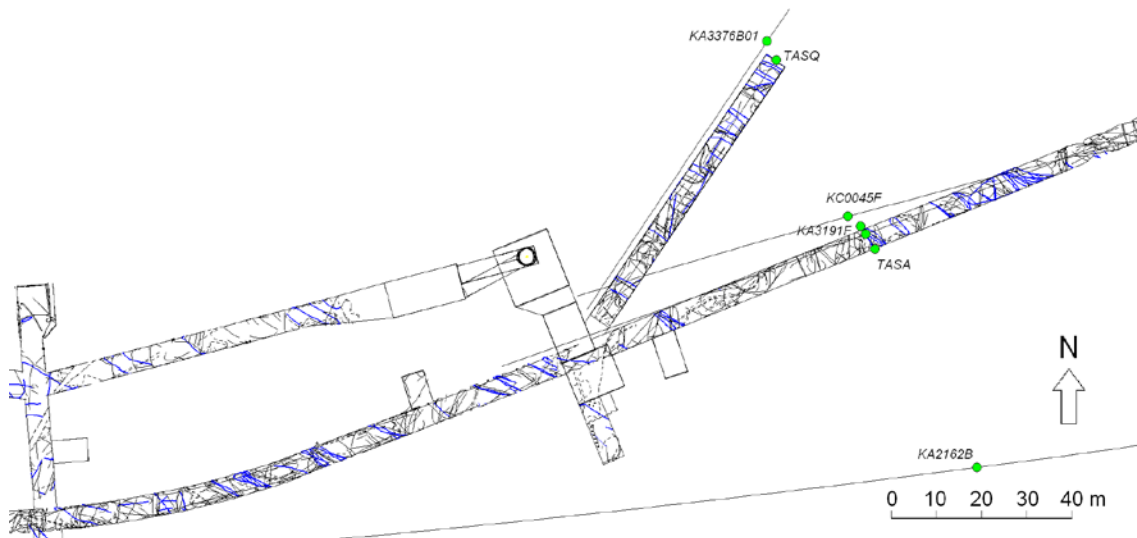


Figure A 32. Observation points used to model FASNW009 in tunnels and boreholes.

Structure FASNW009 was modelled with an orientation of $332^{\circ}/89^{\circ}$ (RT90).

The indications used to model structure FASNW009 were:

1. Tunnel mapping, water-bearing fracture 3319.6-06 in TASA (the TBM tunnel). Mapped with an orientation of RT90: $157^{\circ}/90^{\circ}$ ($155^{\circ}/90^{\circ}$ to magnetic north) /TMS/.
2. Tunnel mapping, water-bearing fracture 80F-12 in TASQ tunnel face mapped with an orientation of RT90: $321^{\circ}/80^{\circ}$ ($319^{\circ}/80^{\circ}$ to magnetic north) /TMS/. This fracture can, however, not be detected in the tunnel ceiling.
3. Borehole KA3191F at 123 m BH length. Inflow of 110 l/min at 123.6 and 124.1 m, pressure responses with SA2240B, KAS02, KAS05 and KA2162B (maximum between 80.5-142 m) /Rhén et al., 1995/. Rather low RQD value (58%) at BH length 122-123 m /rqd_rqd, SICADA/. Increased fracture frequency (8) between 122-123m /freq_1m-open_total, SICADA/. Crush between 122.8-123.1 m /fract_crush-pclen, SICADA/.
4. Borehole KC0045F at 68 m BH length. Rather low RQD value (53%) at BH length 68-69 m /rqd_rqd, SICADA/. Crush between 67.4-67.7 m /fract_crush-min1, SICADA/. Inflow between 67-72 m (24 l/min) /Olsson et al. 1994/.
5. Borehole KA2162B at 138 m BH length. Reduced RQD value (78%) at BH length 137-138 m /rqd_rqd, SICADA/. Increased fracture frequency between 138-139 m (5) and 139-140 m (9) /freq_1m-open_total, SICADA/. Crush at 138.2 and 139.8 m /fract_crush-min1, SICADA/.
6. Borehole KA3376B01 at 71 m BH length. Slightly reduced RQD value (89%) at BH length 69-70 m /rqd_rqd, SICADA/. Mapped open fracture at BH length 71.6 m oriented RT90: $311^{\circ}/76^{\circ}$ ($323^{\circ}/76^{\circ}$ Äspö96) /fract_core-ori_open, SICADA/. Measured inflow at 70.8 and 71.7 m /Pöllänen and Rouhiainen, 2003/.

This structure is classified as **probable**.

FASNW009 332°/89° (probable) - point table

ID	Object	Section (m)	Water	Fract RT90	Mineral	Width (mm)	RQD (%)	Freq (fr/m)	Crush	Radar RT90	Oth
1	TASA	3319-06	vv	157/90	Ep/Ka	-	-	-	-	-	Ox
2	TASQ	80F-12	v	321/80	Ep	0	-	-	-	-	*)
3	KA3191F	123	Infl	Crush	Ka/Kl	-	58	15/2 ¹	8 ¹	0	
4	KC0045F	68	Infl	-	-	-	53	18/5 ¹	13 ¹	0	
5	KA2162B	138		-	-	-	78	11/5 ¹	5 ¹	0	
6	KA3376B01	71	Infl	311/76	Ka	1	89	2/1 ²	0 ²	-	BIPS

*) Not detected in tunnel ceiling.

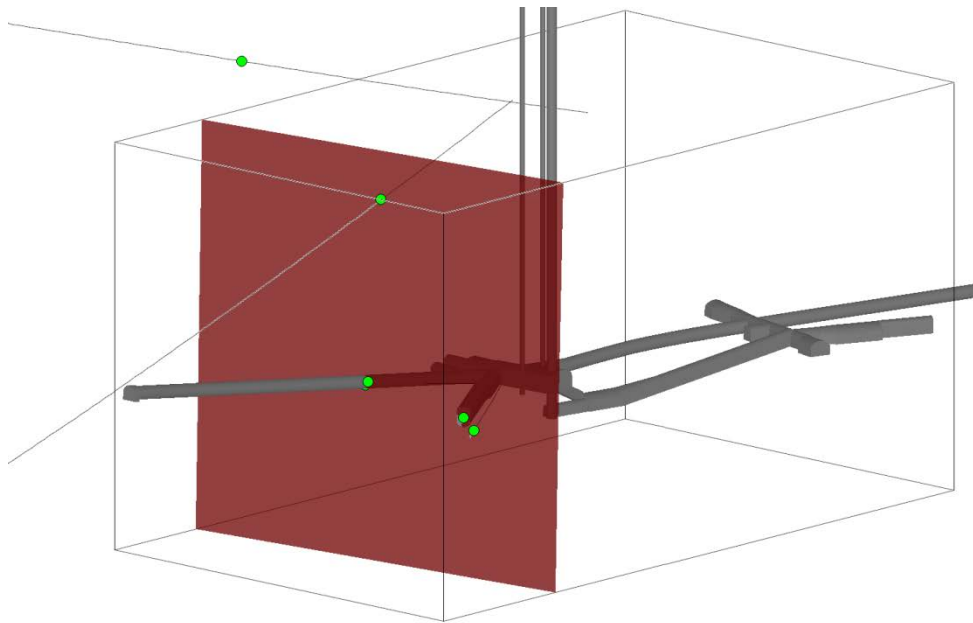


Figure A 33. 3D view of FASNW009 with observation points in green. View from NE.

The modelled structure intersects KAS07 at approximately 128 m BH length, here there is a reduction in RQD (64%) at 127-128 m BH length /rqd_rqd, SICADA/. The structure also intersects KAS06 at approximately 135 m BH length, where a reduction in RQD (74%) is found at 134-135 m BH length /rqd_rqd, SICADA/. Both these indications are, however, weak and are located high above the model area and are not included in the modelling. If extrapolated upwards, in the south the structure intersects TASA at section approximately 2/318 in the lower tunnel turn. At 2/305 and 2/315 m there are mapped sub-parallel water-bearing fractures that corresponds well with the modelled structure. In the north the modelled structure intersects the tunnel at approximately 2/740 in a mapped zon with high transmissivity and some sub-parallel water-bearing fractures that correspond well with the modelled structure. In the level above, the structure intersects at approximately 1/800 m. Here there is no corresponding mapped water-bearing fractures.

Structure FASNW010

The basis of the interpretation of FASNW010 was a mapped water-bearing fracture in the TASQ tunnel. The fracture is only indicated in the northern wall of the TBM-tunnel (TASA).

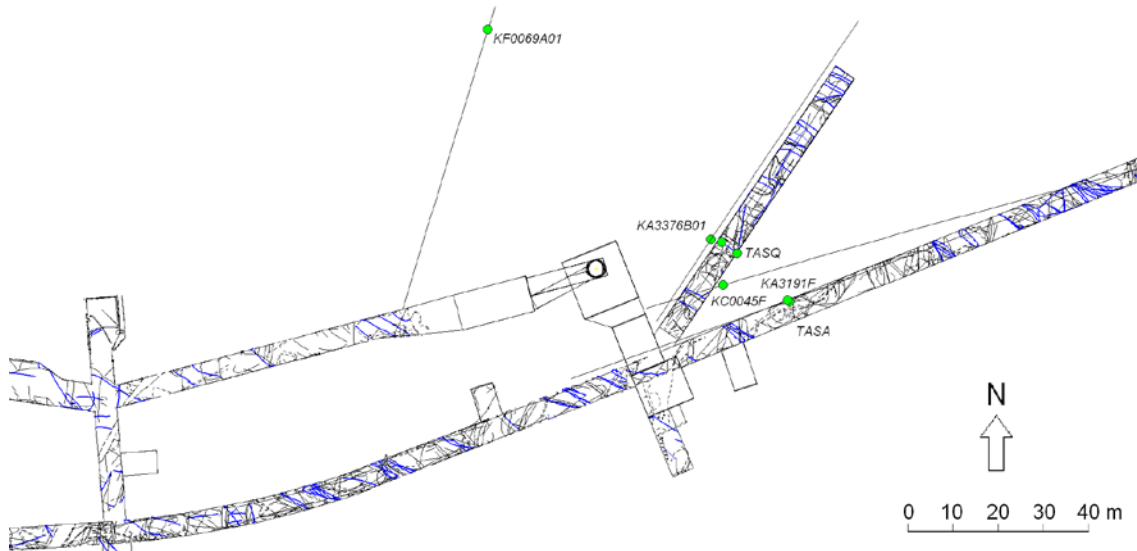


Figure A 34. Observation points used to model FASNW010 in tunnels and boreholes.

Structure FASNW010 was modelled with an orientation of $311^{\circ}/85^{\circ}$ (RT90).

The indications used to model structure FASNW010 were:

1. Tunnel mapping, water-bearing fractures 35-03 and -18 in TASQ mapped with the orientations RT90: $108^{\circ}/86^{\circ}$ and $107^{\circ}/90^{\circ}$ ($106^{\circ}/86^{\circ}$ and $105^{\circ}/90^{\circ}$ to magnetic north) /TMS/.
2. Tunnel mapping, water-bearing fracture 3364.1-01 in TASA (the TBM tunnel) only visible in the northern wall. Mapped with an orientation of RT90: $315^{\circ}/88^{\circ}$ ($313^{\circ}/88^{\circ}$ to magnetic north) /TMS/.
3. (Weak) Borehole KA3191F at 157 m BH length. Mapped fracture 'broken' at BH length 156.64 m oriented RT90: $296^{\circ}/85^{\circ}$ ($308^{\circ}/85^{\circ}$ Äspö96) /fract_core-ori_broken, SICADA/.
4. Borehole KC0045F at 19 m BH length. Some reduction of the RQD value (67%) at BH length 19-20 m /rqd_rqd, SICADA/. Crush (8 fractures) at BH length 19-20 m /freq_1m_petrocor-crush, SICADA/. However, no leakage or inflow detected /Olsson et al. 1994/.
5. Borehole KA3376B01 at 22 m BH length. Reduced RQD value (75%) at BH length 21-22 m /rqd_rqd, SICADA/. Increased fracture frequency (7) at 21-22 m /freq_1m-total, SICADA/. Mapped open fracture at BH length 21.87 m, however oriented RT90: $012^{\circ}/12^{\circ}$ ($024^{\circ}/12^{\circ}$ Äspö96) – (bad correspondence) /fract_core-ori_open, SICADA/. Water-bearing fracture from PFL logging at 21.8 m BH length /Pöllänen and Rouhiainen, 2003/.
6. Borehole KF0069A01 at BH length 65 m. Mapped open fracture at BH length 64.6 m oriented RT90: $278^{\circ}/81^{\circ}$ ($290^{\circ}/81^{\circ}$ Äspö96) /fract_core-ori_open, SICADA/. Inflow on drilling at 65 m BH length /Fransson, 2003/. Inflow from four fractures from PFL between 64 and 67m BH length /Pöllänen and Rouhiainen, 2002/.

This structure is classified as **probable**.

FASNW010 311°/85° (probable) - point table

ID	Object	Section (m)	Water	Fract RT90	Mineral	Width (mm)	RQD (%)	Freq (fr/m)	Crush	Radar RT90	Oth
1	TASQ	35-03 -18	v	108/86	Ka	0.5	-	-	-	-	
			v	107/90	lj	0.5	-	-	-	-	-
2	TASA	3364-01	wv	315/88	Ka	-	-	-	-	-	
3	KA3191F	157		296/85	Ka	0	100	2/1 ¹	0 ¹	115/86	
4	KC0045F	19	0	-	Kl/Ka	-	67	8/0 ¹	8 ¹	0	
5	KA3376B01	21.8	Infl	(012/12)	(Ka)	(1)	75	7/1 ²	0 ²	-	BIPS
6	KF0069A01	65	Infl	278/81	Py	1	100	0/0 ²	0 ²	-	BIPS

The structure is cut in the south at the northern wall of tunnel TASA. It is modelled only above z=-460 m.

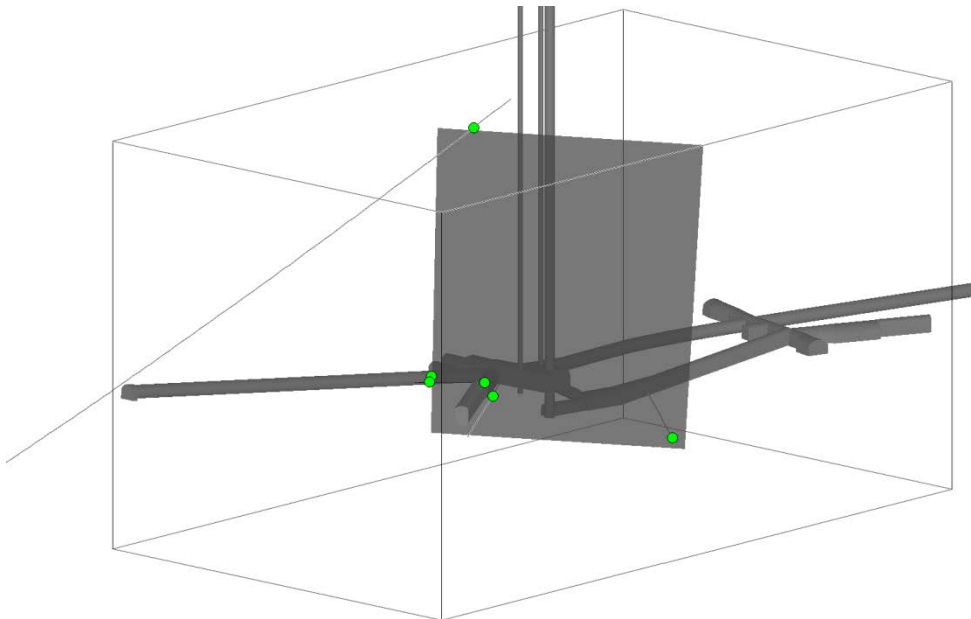


Figure A 35. 3D view of FASNW010 with observation points in green. View from NE.

If extrapolated upwards, the modelled structure intersects TASA at section approximately 2/642 in the lower tunnel turn and in the level above at approximately 1/705 m. In both places there are mapped sub-parallel water-bearing fractures corresponding with the modelled structure.

Structure FASNW011a

The basis of the interpretation of FASNW011a was connecting the mapped water-bearing fractures in the TBM-tunnel (TASA) and tunnel TASQ.

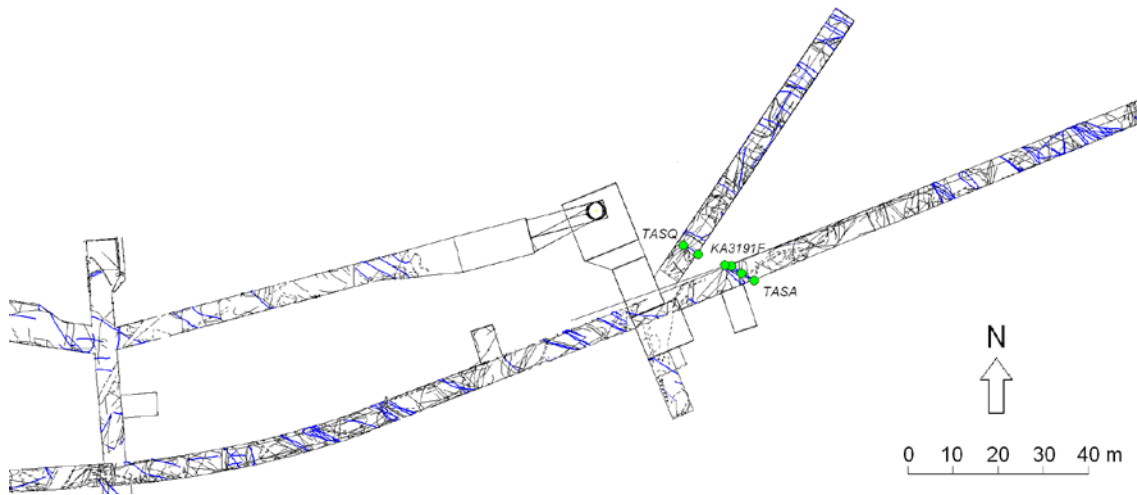


Figure A 36. Observation points used to model FASNW011a in tunnels and boreholes.

Structure FASNW011a was modelled with an orientation of $114^{\circ}/87^{\circ}$ (RT90).

The indications used to model structure FASNW011a were:

1. Tunnel mapping, water-bearing fracture 3364.1-07 in TASA (the TBM tunnel). Mapped with an orientation of RT90: $307^{\circ}/85^{\circ}$ ($305^{\circ}/85^{\circ}$ to magnetic north) /TMS/.
2. Tunnel mapping, water-bearing fracture 20-09 i TASQ mapped with an orientation of RT90: $107^{\circ}/80^{\circ}$ ($105^{\circ}/80^{\circ}$ to magnetic north) /TMS/.
3. Borehole KA3191F at BH length 173 m. Reduced RQD value (65%) at BH length 173-174 m /rqd_rqd, SICADA/. Mapped fracture 'broken' at BH length 172.3 m oriented RT90: $016^{\circ}/63^{\circ}$ ($028^{\circ}/63^{\circ}$ Äspö96) – (bad correspondence) /fract_core-ori_broken, SICADA/.

The modelled structure cannot be observed in KA3376B01 outside the left wall of the TASF tunnel. Furthermore, since the mapped fracture in TASF ends before the left wall, the modelled structure is cut in NW where the mapped fracture in TASF ends and is trimmed against FASNW009 in the SE. It is only modelled between $z = -390 - -490$ m.

This structure is classified as **probable**.

FASNW011a 114°/87° (probable) - point table

ID	Object	Section (m)	Water	Fract RT90	Mineral	Width (mm)	RQD (%)	Freq (fr/m)	Crush	Radar RT90	Oth
1	TASA	3364-07	vv	307/85	Ka	-	-	-	-	-	Ox
2	TASQ	20-09	v	107/80	Ka/Kl	0.2	-	-	-	-	
3	KA3191F	173		(016/63)	Kl	0	65	12/8 ¹	0 ¹	0	Ox

The modelled structure intersects KC0045F at approximately 14 m BH length, where a decrease of RQD appears between 15-16 m BH length but no leakage. This indication is too weak and too far away to be included in the modelling.

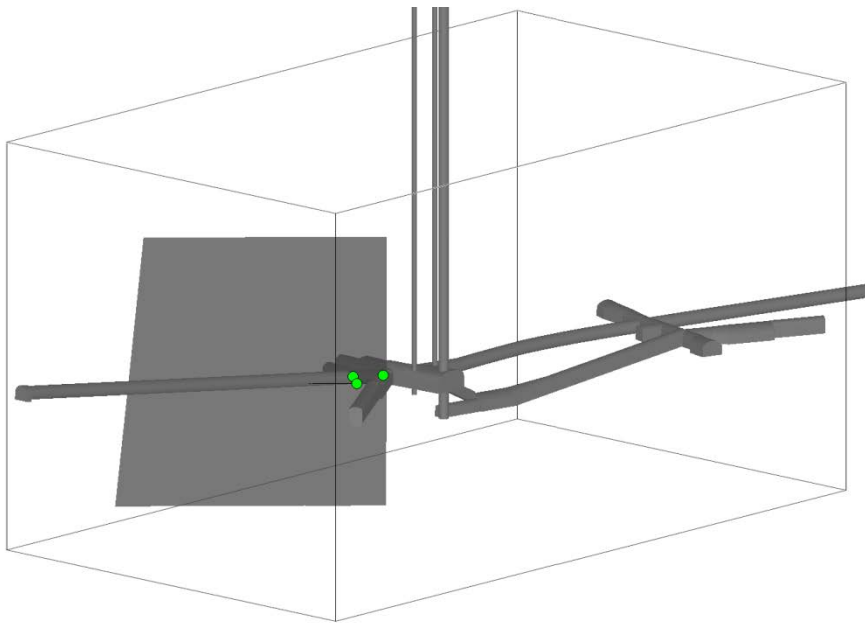


Figure A 37. 3D view of FASNW011a with observation points in green. View from NE.

If extrapolated upwards, the modelled structure intersects TASA at section approximately 2/620 in the lower tunnel turn. Here there is a smaller water-bearing fracture (08), mapped with an orientation of 300°/76° to magnetic north, corresponding well. In the level above the structure intersects at approximately 1/700 m follows the tunnel direction. Here there is a mapped water-bearing fracture (02), mapped with an orientation of 121°/74° to magnetic north.

Structure FASNW011b

The basis of the interpretation of FASNW011b was a mapped water-bearing fracture in the TBM-tunnel (TASA). The structure cannot be found in tunnel TASQ. The structure is modelled as a branch of FASNW011a.

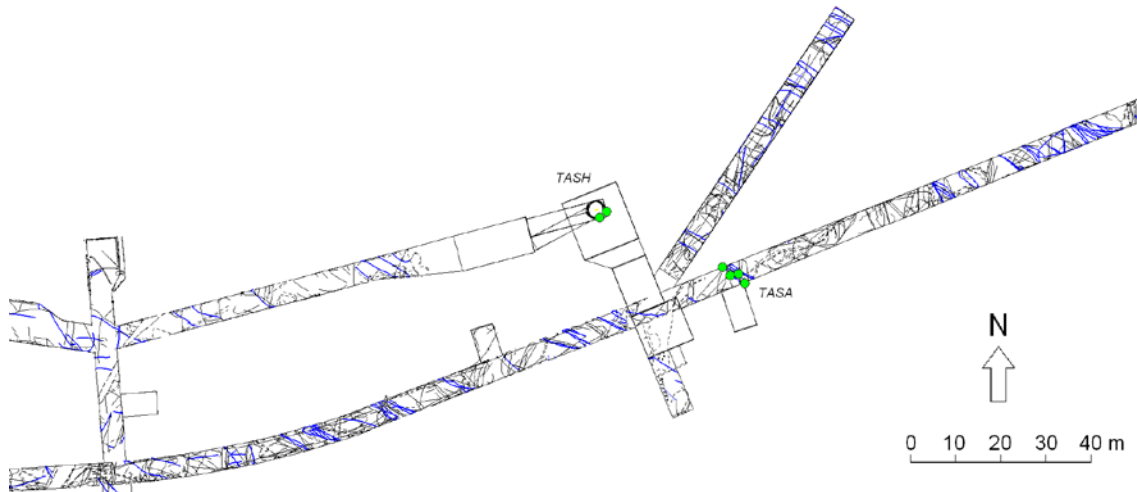


Figure A 38. Observation points used to model FASNW011b in tunnel and shaft.

Structure FASNW011b was modelled with an orientation of $307^{\circ}/82^{\circ}$ (RT90).

The only indication used to model structure FASNW011b was:

1. Tunnel mapping, water-bearing fracture 3364.1-08 in TASA (the TBM tunnel). Mapped with an orientation of RT90: $313^{\circ}/86^{\circ}$ ($311^{\circ}/86^{\circ}$ to magnetic north) /TMS/.
2. Elevator shaft mapping, fracture -400-25. Mapped with an orientation of RT90: $342^{\circ}/80^{\circ}$ ($340^{\circ}/80^{\circ}$ to magnetic north) /TMS/. Non water bearing.

This structure is classified as **possible**.

FASNW011b $307^{\circ}/82^{\circ}$ (possible) - point table

ID	Object	Section (m)	Water	Fract RT90	Mineral	Width (mm)	RQD (%)	Freq (fr/m)	Crush	Radar RT90	Oth
1	TASA	3364-08	vv	313/86	Ka	-	-	-	-	-	Ox
2	TASH (elev)	-400-25	No	342/80	Ep/KI	-	-	-	-	-	

The modelled structure intersects KA2162B at 285 m BH length, here there is a decrease in RQD and radar reflectors. The indication is, however outside the model area and is not included in the modelling. *Same as FASNW015, point 5.*

The indication in the elevator shaft is not water bearing and is only detected below $z=-397$ m. Hence, the modelled structured is cut above $z=-397$ m. It is modelled only down to $z = -480$ m.

The structure is not seen in tunnel TASQ and is considered to be a branch of FASN011a and is consequently trimmed towards FASNW011a in the NW. In the SE it is trimmed towards FASEW002c.

The extrapolated structure intersects the lower tunnel turn at approximately 2/625, where there is a mapped fracture zone, and the upper turn at approximately 1/668, where there are mapped water-bearing fractures corresponding well.

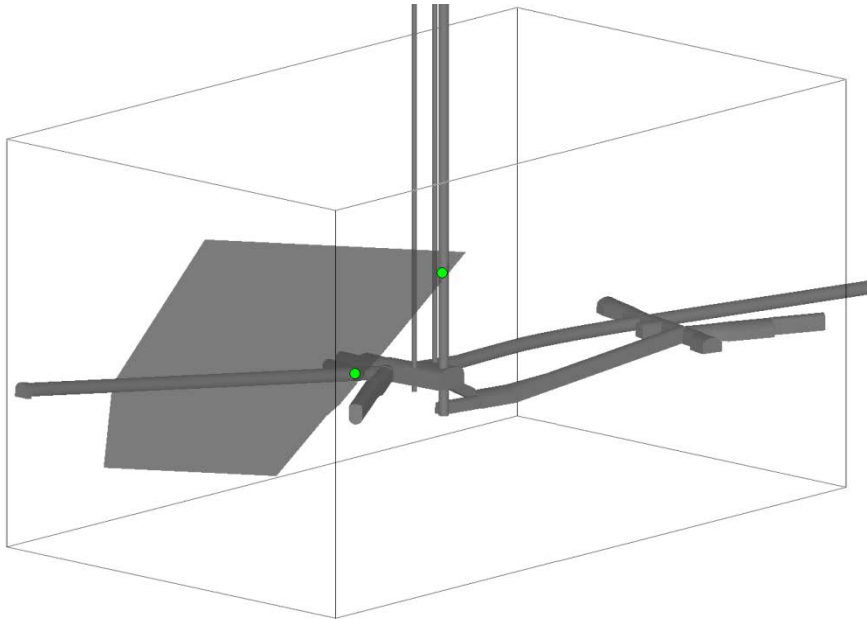


Figure A 39. 3D view of FASNW011b with observation points in green. View from NE.

Structure FASNW011c

The only basis of the interpretation of FASNW011c was a set of mapped water-bearing fractures in the TASQ tunnel. The structure cannot be found in tunnel TASA or in the borehole KA3376B01 just north of TASQ. Hence, the structure is only modelled as a limited plane around the TASQ tunnel, trimmed towards FASNS002 in the south. The structure is labelled as a branch of FASNW011a.

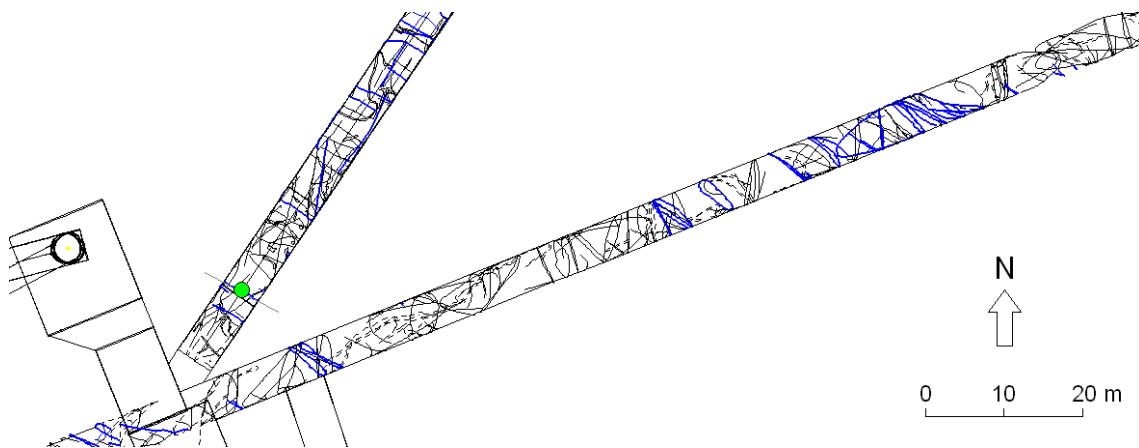


Figure A 40. Observation in A tunnel used to model FASNW011c.

Structure FASNW011c was modelled with an orientation of 295°/90° (RT90).

The indication used to model structure FASNW011c were:

1. Tunnel mapping, water-bearing fractures 30-03, -04 and -05 i TASQ mapped with orientations of RT90: 127°/80°, 092°/90° and 312°/80° (125°/80°, 090°/90° and 310°/80° to magnetic north) /TMS/.

This structure is classified as **possible**.

FASNW011c 295°/90° (possible) - point table

ID	Object	Section (m)	Water	Fract RT90	Mineral	Width (mm)	RQD (%)	Freq (fr/m)	Crush	Radar RT90	Oth
1	TASQ	30-03	wv	127/80	Kl/Ka/lj	0.7	-	-	-	-	
		-04	v	092/90	Ka	0.5	-	-	-	-	
		-05	vvv	312/80	lj/Ka	1.0	-	-	-	-	

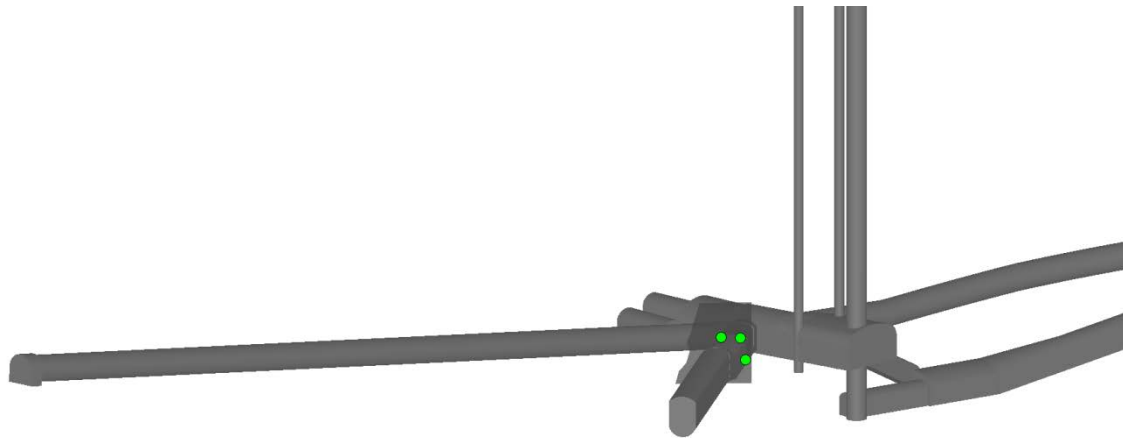


Figure A 41. 3D view of FASNW011c with observation points in green. View from NE.

Structure FASNW012

A steeply dipping structure with an orientation of 115°/84° (RT90) was modelled. The basis of the interpretation for this structure were the mapped water-bearing fractures in the TBM tunnel (TASA) and in TASF in combination with the large water inflow and pressure response that were monitored in KA3386A01 at 10-11 m BH length.

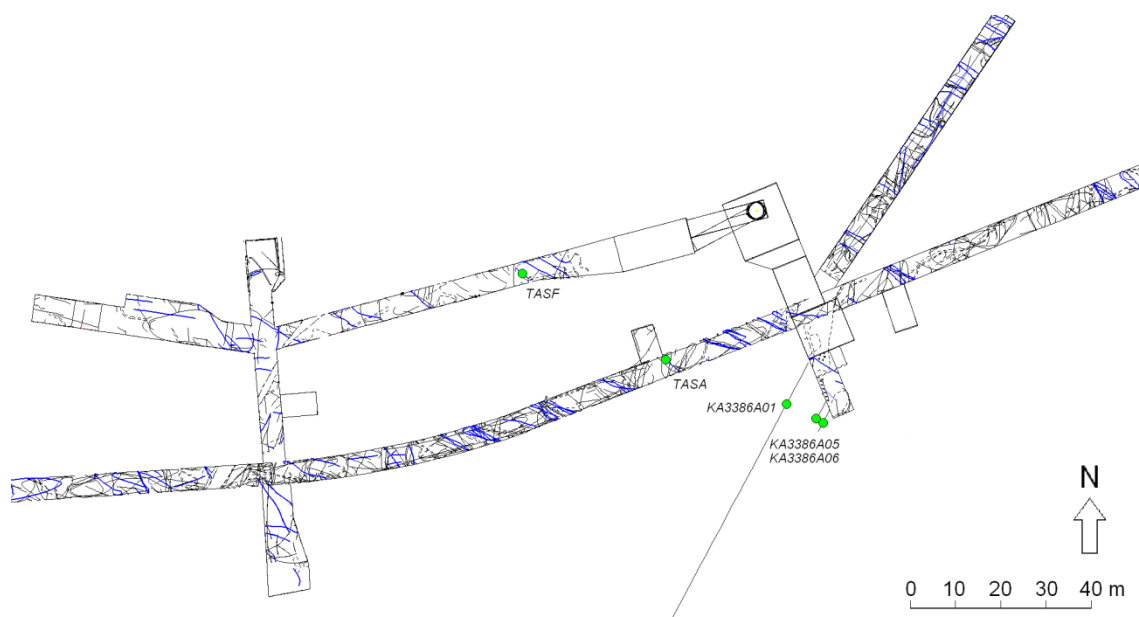


Figure A 42. Observation points used to model FASNW012 in tunnels and boreholes.

Recorded pressure responses in KA3386A04, KA3386A05 and KA3386A06 were checked where all except the first corresponded well with the assumed structure. Also, in all intersecting boreholes we have found some form of indication corresponding with the modelled structure.

The indications used to model structure FASNW012 were:

1. Tunnel mapping, water-bearing fracture 3420-08 in the TBM tunnel (TASA). Mapped with an orientation of RT90: $312^{\circ}/90^{\circ}$ ($310^{\circ}/90^{\circ}$ to magnetic north) /TMS/.
2. Tunnel mapping, water-bearing fracture 60-16 in the TASF tunnel. Mapped with an orientation of RT90: $127^{\circ}/90^{\circ}$ ($125^{\circ}/90^{\circ}$ to magnetic north) /TMS/.
3. Borehole KA3386A01 at BH length 10-11 m. Significant inflow on drilling between 9.48 and 10.90 m BH length /Fransson, 2003/. Significant inflow at BH length 9.5, 10.1 and 10.7 on flow logging /Pöllänen and Rouhiainen, 2002/. Mapped open fractures at BH length 10.05 m oriented RT90: $100^{\circ}/88^{\circ}$ ($112^{\circ}/88^{\circ}$ Äspö96) and 10.68 m oriented RT90: $097^{\circ}/73^{\circ}$ ($309^{\circ}/73^{\circ}$ Äspö96) /fract_core-ori_open, SICADA/. Slightly reduced RQD value (93%) at BH length 10-11 m /rqd_rqd, SICADA/.
4. Borehole KA3386A05 at 4.8 m BH length. Pressure response on drilling at BH length 4.8 m (hole bottom) in KA3385A, KA3386A01 and KA2598A /HMS, unpublished data/. Mapped open fracture at 4.8 m BH length with unknown strike and a dip of 70.5° /fract_core-ori_open, SICADA/.
5. Borehole KA3386A06 at 3.3 m BH length. BIPS indicated fracture at BH length 3.3 m /SICADA/. A mapped open fracture at BH length 3.21 m with a mapped orientation of RT90: $295^{\circ}/78^{\circ}$ ($307^{\circ}/78^{\circ}$ Äspö96) /fract_core-ori_open, SICADA/.

This structure is classified as **probable**.

FASNW012 115°/84° (probable) – point table

ID	Object	Section (m)	Water	Fract RT90	Mineral	Width (mm)	RQD (%)	Freq (fr/m)	Crush	Radar RT90	Oth
1	TASA	3420-08	v	312/90	Ep	-	-	-	-	-	
2	TASF	60-16	vv	127/90	Kl	-	-	-	-	-	
3	KA3386A01	10.5	Infl	97/73	Ka	2	93	4/3 ²	0 ²⁾	-	BIPS
4	KA3386A05	4.8	1)	??/71	Ka	0.5	93	2/1 ²	0 ²⁾	-	
5	KA3386A06	3.3	-	295/78	Pr	3.7	100	1/1 ²	0 ²⁾	-	

1) Pressure response in the borehole on drilling in NASA3384 (Mincan)

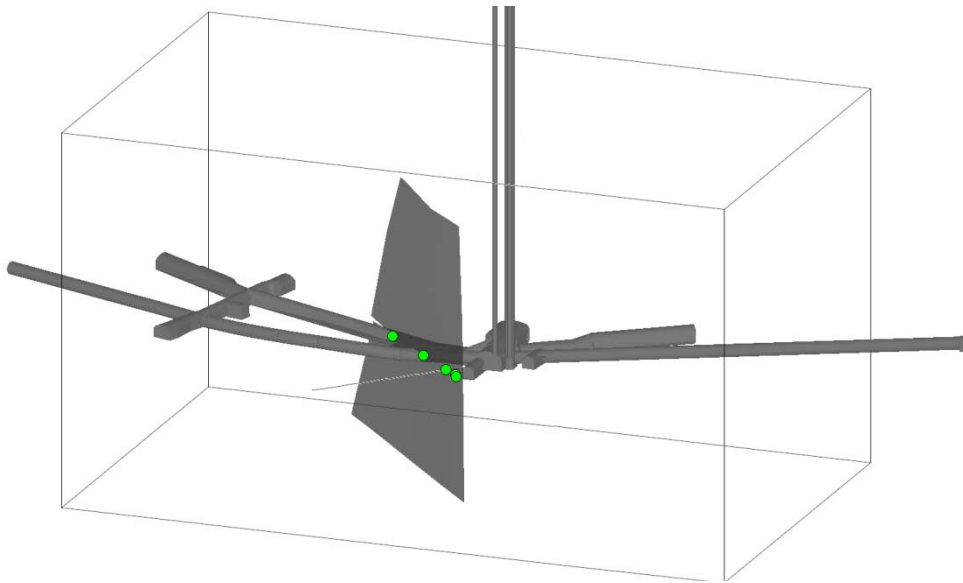


Figure A 43. 3D view of FASNW012 with observation points in green. View from SE.

The fracture is trimmed towards FASEW002c in the north and FASNS002 in the SE. It is modelled only between $z = -390 - -490$ m.

If the modelled fracture is extrapolated upwards, it will intersect the spiral tunnel TASA at about 2/585 and 1/665.

Between sections 2/575-2/585 there are a number of mapped water-bearing fractures, one of these are only one metre from the intersection between the tunnel and FASNW012 and it is sub-parallel to the modelled fracture.

At section 1/668 there is a mapped water-bearing fracture, sub-parallel to FASNW012 only two metres from the intersection between the tunnel and FASNW012.

This shows that also for this fracture there are, in both location of the TASA spiral tunnel above, mapped water-bearing fractures that corresponds very well with the position of the modelled structure. But also for these observations, no deeper analyses have been done.

Structure FASNW013

A steeply dipping structure with an orientation of 293°/85° (RT90) was modelled. The basis of the interpretation for this structure were the mapped water-bearing fractures in the TBM tunnel (TASA) and in TASF that can be connected to a structure with a supposed strike of 120° (300°) (Äspö 96).

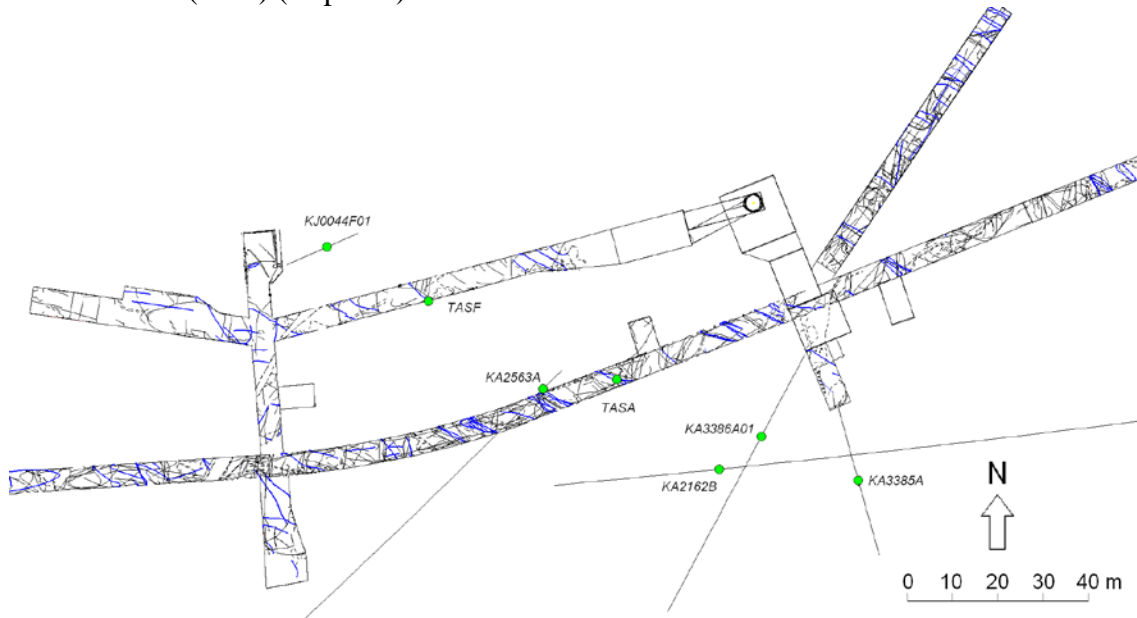


Figure A 44. Points used to model FASNW013 in tunnels and boreholes.

The indications used to model structure FASNW013 were:

1. Tunnel mapping, water-bearing fractures 03 and 04 in map cell 3433.2 in the TBM-tunnel. Mapped with an orientation of RT90: 289°/82° and 293°/85° (287°/82° and 291°/85° to magnetic north) /TMS/. The inflow monitored in these fractures in the tunnel is directly correlated to the ground water pressure in the Mini-Can area.
2. Tunnel mapping, water-bearing fracture 45-03 in the TASF tunnel. Mapped with an orientation of RT90: 311°/85° (309°/85° to magnetic north) /TMS/.
3. Borehole KA3386A01 at BH length 20 m. Flow logging inflow at 19.0 and 20.7 m /Pöllänen and Rouhiainen, 2002/. Three mapped open fractures, at BH length 19.02 m oriented RT90: 134°/87° (146°/87° Äspö96), at BH length 19,07 m oriented RT90: 118°/78° (130°/78° Äspö96) and at BH length 20.59 m oriented RT90: 285°/70° (297°/70° Äspö96) /fract_core-ori_open, SICADA/. Slightly reduced RQD value (94%) at BH length 19-20 m /rqd_rqd, SICADA/.
4. Borehole KJ0044F01 at 10 m BH length. A mapped open fracture at BH length 9.82 m with unknown strike and a mapped dip of 60° /fract_core-ori_open, SICADA/.
5. (Weak) Borehole KA2162B at BH length 252 m. Pressure response in the borehole mainly at BH length >200m when drilling in NASA3384 (Mini-Can) /HMS, unpublished data/. Water inflow between 252-254 m /SICADA/. Slightly reduced RQD value (92%) at BH length 251-252 m /rqd_rqd, SICADA/. Same as FASNS002, point 9.
6. (Weak) Borehole KA2563A at BH length 8 m. Slightly reduced RQD value (92%) at BH length 8-9 m /rqd_rqd, SICADA/. Four water-bearing fractures between 7.5-9.3 m with max inflow at 8.2 m /Rouhiainen and Heikkinen, 2002/.
7. Borehole KA3385A at BH length 17 m. Water inflow of 100 l/min in the section 16.1–18.6 m /PETROCORE, SICADA/. Reduced RQD value (69%) at BH length 17-18 m /rqd_rqd, SICADA/.

The modelled structure also intersects the boreholes KJ0050F01 (at 1.8 m depth), KJ0052F01 (at 4.3 m depth), KJ0052F02 (at 1.6 m depth) and KJ0052F03 (at 2.3 m depth) in the J-tunnel. KJ0050F01 is not mapped at that borehole depth. In the KJ0052 holes there are observations of broken or healed fractures near the intersection points. However, no orientation data are available for these observations and they are considered too weak to be included in the modelling. Hence, the existence of FASNW013 NW of the NEHQ3 structure is very uncertain and it could as well be cut against NEHQ3.

This structure is classified as **probable**.

FASNW013 293°/85° (probable) - point table

ID	Object	Section (m)	Water	Fract RT90	Mineral	Width (mm)	RQD (%)	Freq (fr/m)	Crush	Radar RT90	Oth
1	TASA	3433-03 04	wv wv	289/82 293/85	Ep/Ka Qz/Ka/Ep	-	-	-	-	-	Ox
2	TASF	45-03	wv	311/85	Ka/Kl/Cy	-	-	-	-	-	
3	KA3386A01	20	Infl	285/70	Ka	1	94	3/2 ²	0 ²	-	BIPS
4	KJ0044F01	10	0	??/60	Ka	2	100	1/1 ²	0 ²	-	
5	KA2162B	251	Wloss	-	-	-	92	2/2 ¹	0 ¹	0	
6	KA2563A	8	Infl	-	-	-	92	3/3 ¹	0 ¹	0	BIPS
7	KA3385A	17	Infl	-	-	-	69	7/7 ¹	0 ¹	0	BIPS

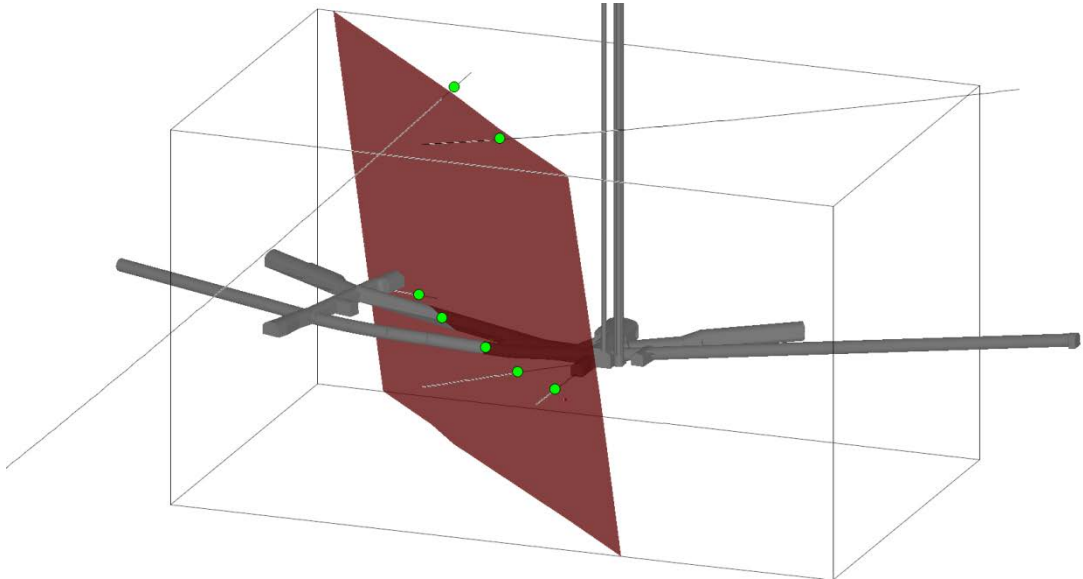


Figure A 45. 3D view of FASNW013 with observation points in green. View from SE.

The fracture is modelled with an upper limitation at Z=-350 m, which is the upper boundary of the model volume. If the modelled fracture is extrapolated upwards, it will intersect the spiral tunnel TASA at about 2/557 and 1/615.

At section 2/557 there is no mapped water-bearing fracture that directly corresponds with FASNW013. There is a water-bearing fracture at section 2/550 with a mapped orientation of 247°/67° to magnetic north but this does not correspond particularly well with the modelled structure.

At section 1/615 there is, however, a smaller mapped water-bearing fracture in the right wall, mapped with an orientation of 123°(303°)/90° to magnetic north.

Therefore, for this structure there is no mapped water-bearing fractures in the tunnel TASA above that corresponds with the geometry of the modelled structure, other than a very weak indication in the upper turn.

Structure FASNW014a

A number of adjacent, sub-parallel, steeply dipping structures with an orientation of 308°-309°/86°-87° (Äspö96) were identified. These were modelled as separate fracture planes but were named FASNW014a, b and c to indicate that they are part of one swarm or "zone". In this area there are some probe holes with a high measured transmissivity.

The basis of the interpretation of FASNW014a were the mapped water-bearing fractures in the TBM-tunnel (TASA) and in TASF combined with the significant water inflow and pressure response that were monitored in KA3386A01 at 32-33 m BH length.

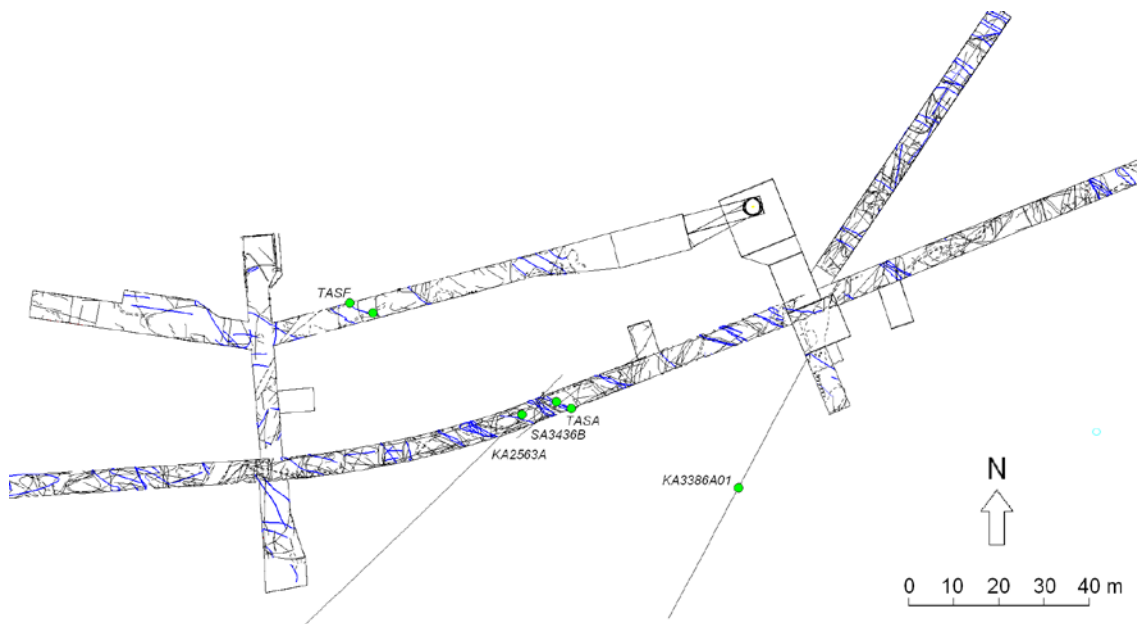


Figure A 46. Points used to model FASNW014a in tunnels and boreholes.

Structure FASNW014a was modelled with an orientation of 295°/86° (RT90).

The indications used to model structure FASNW014a were:

1. Tunnel mapping, water-bearing fractures 3448.1-01, 05 and 06 in TASA (the TBM tunnel). Mapped with an orientation of RT90: 286°/84°, 112°/90° and 112°/90° (284°/84°, 110°/90° and 110°/90° to magnetic north) /TMS/.
2. Tunnel mapping, water-bearing fracture 30-11 in the TASF-tunnel. Mapped with an orientation of RT90: 129°/86° (127°/86° to magnetic north) /TMS/.
3. Borehole KA3386A01 at BH length 32-33 m. Significant inflow on drilling (30 l/min) at 32-33.5 m BH length /Fransson, 2003/. Pressure responses when drilling from >33 m in the boreholes KG0021A01 and KG0048A01 (Fransson, 2003). Significant inflow and low resistance of rock at 32.4 m on flow logging /Pöllänen and Rouhiainen, 2002/. A mapped open fracture at BH length 32.34 m oriented RT90: 290°/70° (302°/70° Äspö96) /fract_core-ori_open, SICADA/.
4. Borehole KA2563A at BH length 17 m. Reduced RQD value (67%) at BH length 16-17 m. /rqd_rqd, SICADA/. A radar reflector at BH length 17 m oriented RT90: 292°/79° /radar_direct-ori1, SICADA/. Chloritization between 16.2-16.9 m BH length /rock_alter-type, SICADA/. PFL anomaly at 17.05 m /Rouhiainen and Heikkinen, 2002/.
5. Probe hole SA3436B. Inflow 22 l/min, transmissivity $4.1 \cdot 10^{-6} \text{ m/s}^2$.

This structure is classified as **probable**.

FASNW014a 295°/86° (probable) - point table

ID	Object	Section (m)	Water	Fract RT90	Mineral	Width (mm)	RQD (%)	Freq (fr/m)	Crush	Radar RT90	Oth
1	TASA	3448-01	vvv	286/84	My/Ka/Ep	-	-	-	-	-	
		-05	wv	112/90	Ep/Kl	-	-	-	-	-	
		-06	vvv	112/90	Ep/Kl/Ka	-	-	-	-	-	
2	TASF	30-11	v	129/86	Ka/lj	-	-	-	-	-	
3	KA3386A01	32.3	Infl	290/70	Ka/Kl	2	100	1/1 ²	0 ²	-	BIPS
4	KA2563A	17	PFL	-	-	-	67	8/8 ¹	0 ¹	292/79	Cl*, BIPS
5	SA3436B	??	Infl	-	-	-	-	-	-	-	

*) Chloritization

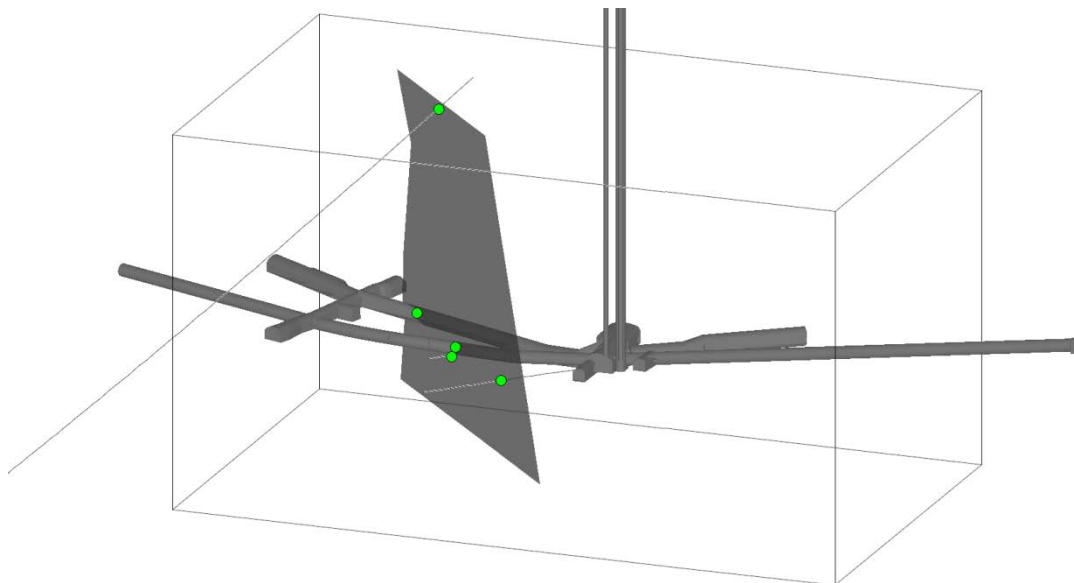


Figure A 47. 3D view of FASNW014a with observation points in green. View from SE.

Northwest of the F-tunnel, up towards the boreholes at the end of the J-tunnel, there are no direct indications supporting the modelled structure. Therefore, the structure is trimmed towards the structure NEHQ3 in the NW immediately north of the F-tunnel and in SE it is trimmed towards FASNS002. It is modelled only between z= -350 – -480 m.

If the modelled FASNW014 structures a, b and c, are extrapolated upwards, they will intersect the spiral tunnel TASA at about 2/542-2/549 and 1/600-1/609.

At section 2/545 there is a mapped water-bearing fracture zone, sub-parallel to the modelled group of structures.

There are, however, no mapped water-bearing fractures or zone near section 1/605 that fits to the modelled group of structures.

This means that for this group of modelled structures there is a water-bearing fracture zone in the lower, closest levels of the TASA tunnel that corresponds well with the position of the modelled structures.

Structure FASNW014b

The basis for the modelling of FASNW014b was the mapped water-bearing fractures in the TBM-tunnel (TASA) and in TASF in combination with a measured water inflow in KA3386A01 at 36.3 m BH length.

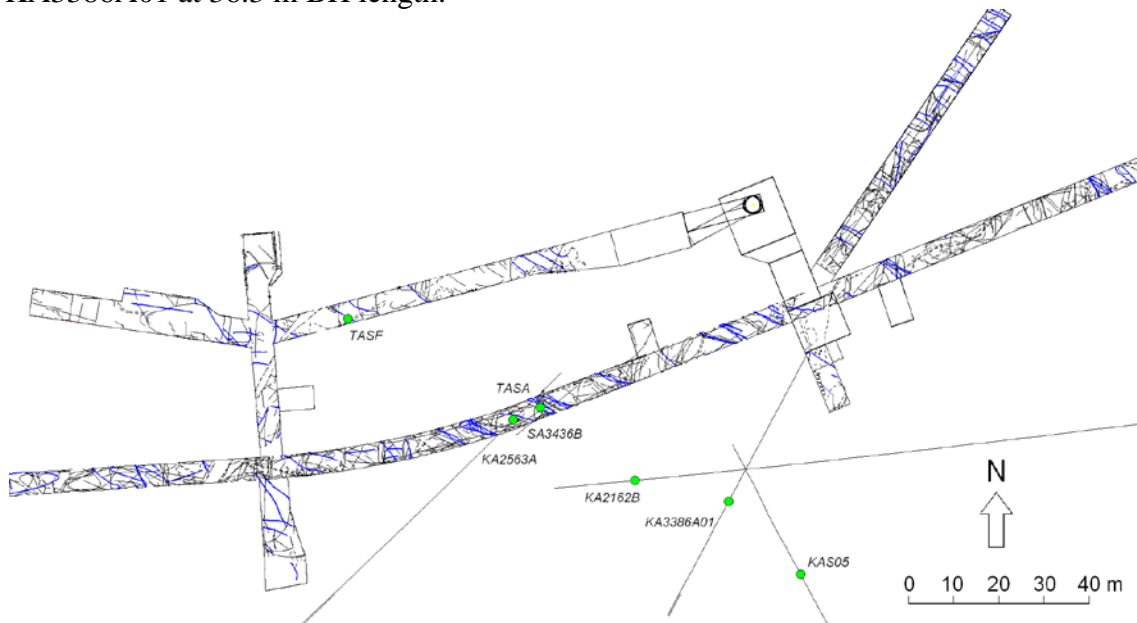


Figure A 48. Observation points used to model FASNW014b in tunnels and boreholes.

Structure FASNW014b was modelled with an orientation of $296^{\circ}/87^{\circ}$ (RT90).

The indications used to model structure FASNW014b were:

1. Tunnel mapping, water-bearing fractures 3448.1-15 and 16 in TASA (the TBM tunnel). Mapped with an orientation of RT90: $321^{\circ}/84^{\circ}$ and $283^{\circ}/82^{\circ}$ ($319^{\circ}/84^{\circ}$ and $281^{\circ}/82^{\circ}$ to magnetic north) /TMS/.
2. Tunnel mapping, water-bearing fractures 30-05, 06 and 32 in the TASF-tunnel. Mapped with an orientation of RT90: $280^{\circ}/90^{\circ}$, $308^{\circ}/90^{\circ}$ and $112^{\circ}/83^{\circ}$ ($278^{\circ}/90^{\circ}$, $306^{\circ}/90^{\circ}$ and $110^{\circ}/83^{\circ}$ to magnetic north) /TMS/.
3. Borehole KA3386A01 at BH length 36.3 m. Reduced inflow when drilling at 36.3 m BH length /Fransson, 2003/. Inflow at BH length 36.3 m when flow logging / Pöllänen and Rouhiainen, 2002/. A mapped open fracture at BH length 36.27 m oriented RT90: $294^{\circ}/72^{\circ}$ ($306^{\circ}/72^{\circ}$ Äspö96) /fract_core-ori_open, SICADA/. Reduced or slightly reduced RQD values at BH length 34-35 m (81%), 35-36 m (94%) and 36-37 m (85%) m /rqd_rqd, SICADA/.
4. Borehole KAS05 at BH length 321 m. Very high hydraulic conductivity between 319-324 m BH length /transient injection test, SICADA/. Crush zone between 320.6-321.1 m BH length /fract_crush_pcelen, SICADA/. Rather low RQD value (49%) at BH length 320-321 m /rqd_rqd, SICADA/.
5. (Weak) Borehole KA2162B at BH length 269.5 m. Reduced RQD value (87%) at BH length 269-270 m /rqd_rqd, SICADA/. Measured inflow of 35 l/min at 270-271 m BH length on spinner measurements, /SKB, 1994/. Same as FASNW016, point 3.
6. (Weak) Borehole KA2563A at BH length 20.5 m. Reduced RQD value (75%) at BH length 20-21 m /rqd_rqd, SICADA/.
7. Probe hole SA3436B. Inflow 22 l/min, transmissivity $4.1 \cdot 10^{-6} \text{ m}^2/\text{s}$ /Markström and Erlström, 1996/.

This structure is classified as **probable**.

FASNW014b 296°/87° (probable) - point table

ID	Object	Section (m)	Water	Fract RT90	Mineral	Width (mm)	RQD (%)	Freq (fr/m)	Crush	Radar RT90	Oth
1	TASA	3448-15 -16	vv vv	321/84 283/82	Ka/Kl/Ep Ka/Kl/Ep	- -	- -	- -	- -	- -	
2	TASF	30-05 -06 -32	vv vv vv	280/90 308/90 112/83	Ka Ka/lj Ka	- - -	- - -	- - -	- - -	- - -	
3	KA3386A01	36.3	Infl	294/72	Ka/Kl/Py	2	85	5/1 ²	0 ²	-	BIPS
4	KAS05	321	Cond	Crush	La/Ka/Kl	2	49	14/5 ¹	6 ¹	-	
5	KA2162B	269.5	Infl	-	-	-	87	6/6 ¹	0 ¹	0	
6	KA2563A	20.5	0	-	-	-	75	9/9 ¹	0 ¹	0	BIPS
7	SA3436B	??	Infl	-	-	-	-	-	-	-	

Just as FASNW014a the structure is trimmed towards NEHQ3 in NW immediately north of the F-tunnel.

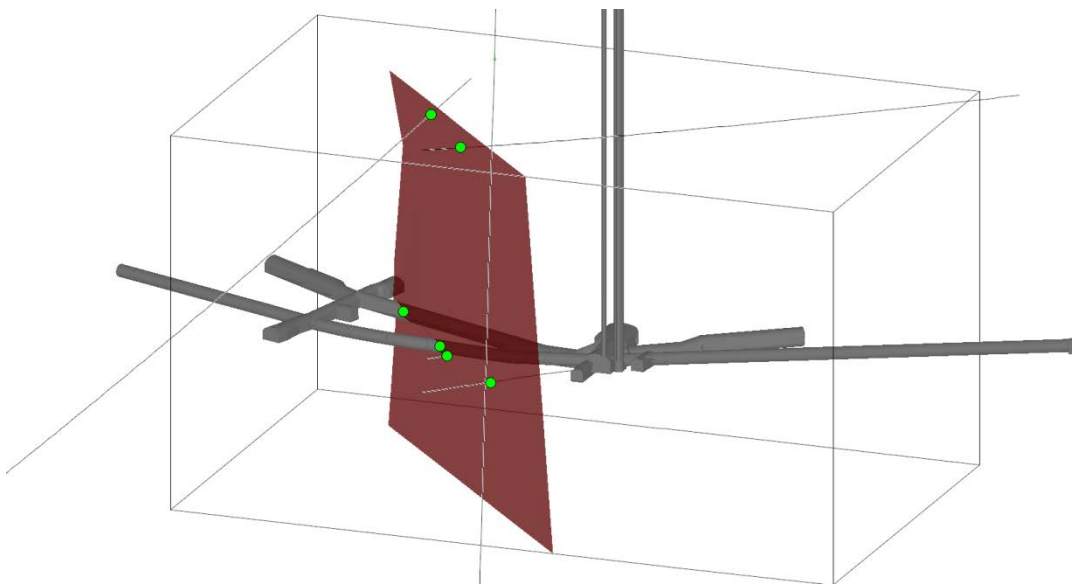


Figure A 49. 3D view of FASNW014b with observation points in green. View from SE.

The structure is modelled with an upper limitation at Z=-350 m, which is the upper boundary of the model volume. Regarding intersections with the tunnel above, see Structure FASNW014a above, where the FASNW014x structures are analyzed as a group.

Structure FASNW014c

The basis for the modelling of FASNW014c was the mapped water-bearing fractures in the TBM-tunnel (TASA) and in TASF combined with a measured significant water inflow in KA3386A01 at 41 m BH length.

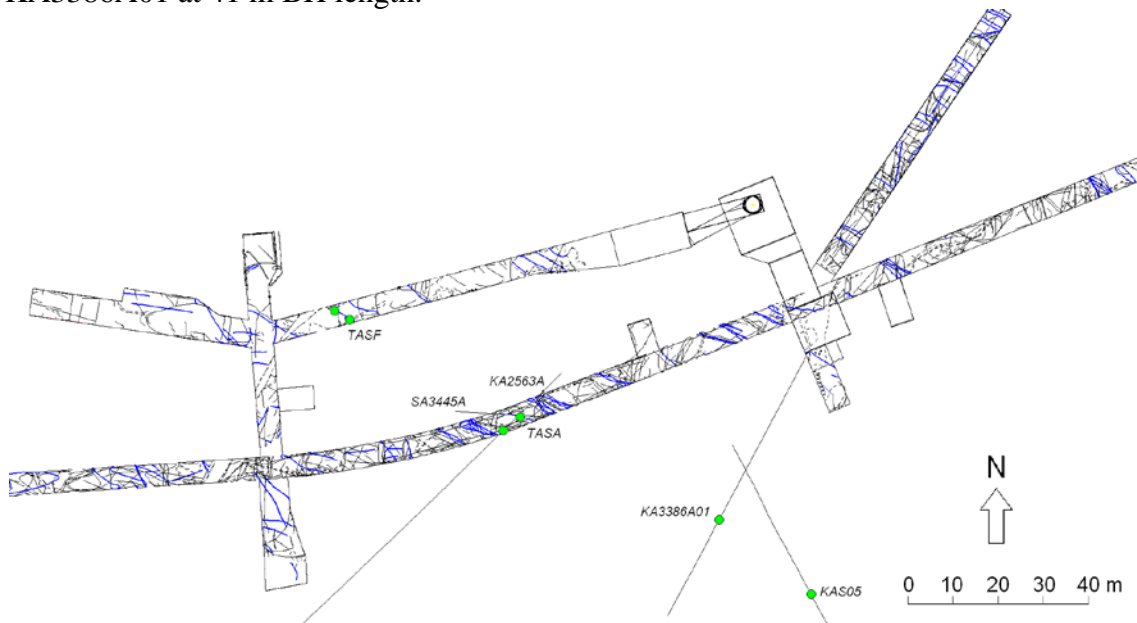


Figure A 50. Observation points used to model FASNW014c in tunnels and boreholes.

Structure FASNW014c was modelled with an orientation of $298^{\circ}/87^{\circ}$ (RT90).

The indications used to model structure FASNW014c were:

1. Tunnel mapping, water-bearing fracture 3463,0-09 in TASA (the TBM tunnel). Mapped with an orientation of RT90: $107^{\circ}/87^{\circ}$ ($105^{\circ}/87^{\circ}$ to magnetic north) /TMS/.
2. Tunnel mapping, water-bearing fractures 30-05, 06 and 32 in the TASF tunnel. Mapped with an orientation of RT90: $280^{\circ}/90^{\circ}$, $308^{\circ}/90^{\circ}$ and $112^{\circ}/83^{\circ}$ ($278^{\circ}/90^{\circ}$, $306^{\circ}/90^{\circ}$ and $110^{\circ}/83^{\circ}$ to magnetic north) /TMS/.
3. Borehole KA3386A01 at BH length 41 m. Large inflow on drilling on a BH length between 40.2-41.7 m /Fransson, 2003/. Inflow and decreased resistivity at BH length 40-42 m on PFL flow logging /Pöllänen and Rouhiainen, 2002/. A number of mapped open fractures at BH lengths between 40.2-41.7 m oriented RT90: 288° - $298^{\circ}/65^{\circ}$ - 85° (300° - $310^{\circ}/65^{\circ}$ - 85° Äspö96) /fract_core-ori_open, SICADA/. Reduced RQD value (84%) at BH length 40-41 m /rqd_rqd, SICADA/.
4. Borehole KAS05 at BH length 363 m. High hydraulic conductivity between 361-367 m BH length /transient injection test, SICADA/. Crush zone between 362.4-363.1 m BH length /fract_crush_pcelen, SICADA/. Low RQD value (41%) at BH length 362-363 m /rqd_rqd, SICADA/.
5. (Weak) Borehole KA2563A at BH length 24.5 m. Slightly decreased RQD value (88%) at BH length 24-25 m /rqd_rqd, SICADA/. PFL-anomaly at 24.1 m /Rouhiainen and Heikkinen, 2002/.
6. Probe hole SA3445A. Inflow 0.5 l/min, transmissivity $6.5 \cdot 10^{-7} \text{ m}^2/\text{s}$ /Markström and Erlström, 1996/.

This structure is classified as **probable**.

FASNW014c 298°/87° (probable) - point table

ID	Object	Section (m)	Water	Fract RT90	Mineral	Width (mm)	RQD (%)	Freq (fr/m)	Crush	Radar RT90	Oth
1	TASA	3463-09	vvv	107/87	Ka/Kl	-	-	-	-	-	
2	TASF	30-05 -06 -32	vv vv vv	280/90 308/90 112/83	Ka Ka/lj Ka	- - -	- - -	- - -	- - -	- - -	
3	KA3386A01	41	Infl	293/75	Ka/Kl/Py	1-3	84	5/1 ²	0 ²	-	a), BIPS
4	KAS05	363	Cond	Crush	He/Ka/Kl	-	41	18/1 ¹	15 ¹	-	
5	KA2563A	24.5	PFL	-	-	-	88	4/4 ¹	0 ¹	0	BIPS
6	SA3445A	??	Infl	-	-	-	-	-	-	-	

a) Low resistivity at 41-42 m.

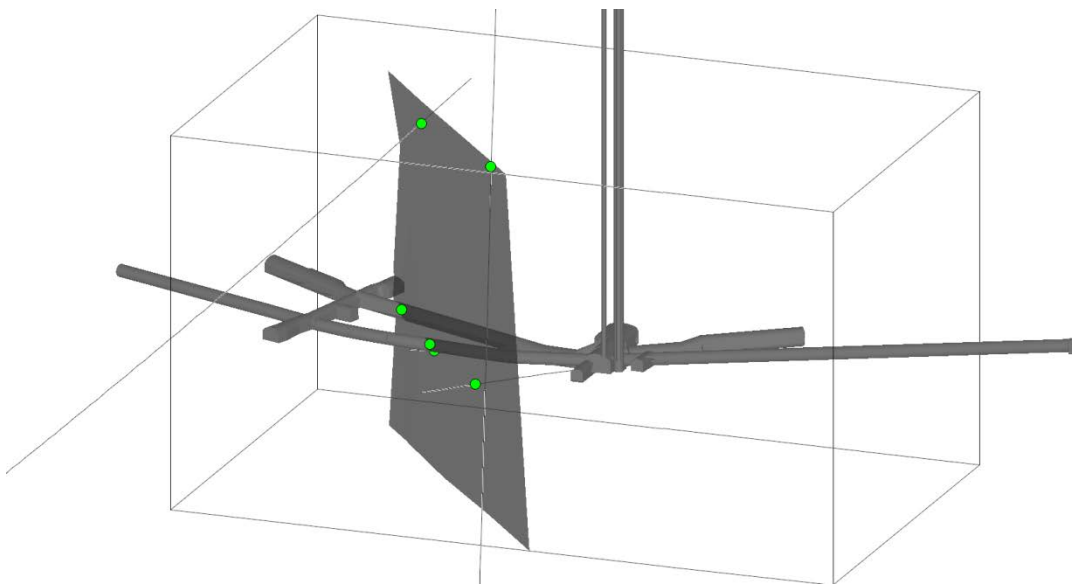


Figure A 51. 3D view of FASNW014c with observation points in green. View from SE.

The structure FASNW014c, that is a part of the fracture set FASNW014, is trimmed towards the structure NEHQ3 in the NW immediately north of the F-tunnel.

The structure is modelled with an upper limitation at Z=-350 m, which is the upper boundary of the model volume. Regarding intersections with the tunnel above, see Structure FASNW014a above, where the FASNW014x structures are analyzed as a group.

Structure FASNW015

A steeply dipping structure with an orientation of $297^{\circ}/87^{\circ}$ (RT90) was modelled. The basis of the interpretation for this structure were the mapped water-bearing fractures in the TBM tunnel (TASA) and in TASF that can be connected to a structure with a supposed strike of $\sim 120^{\circ}$ (300°) (Äspö 96).

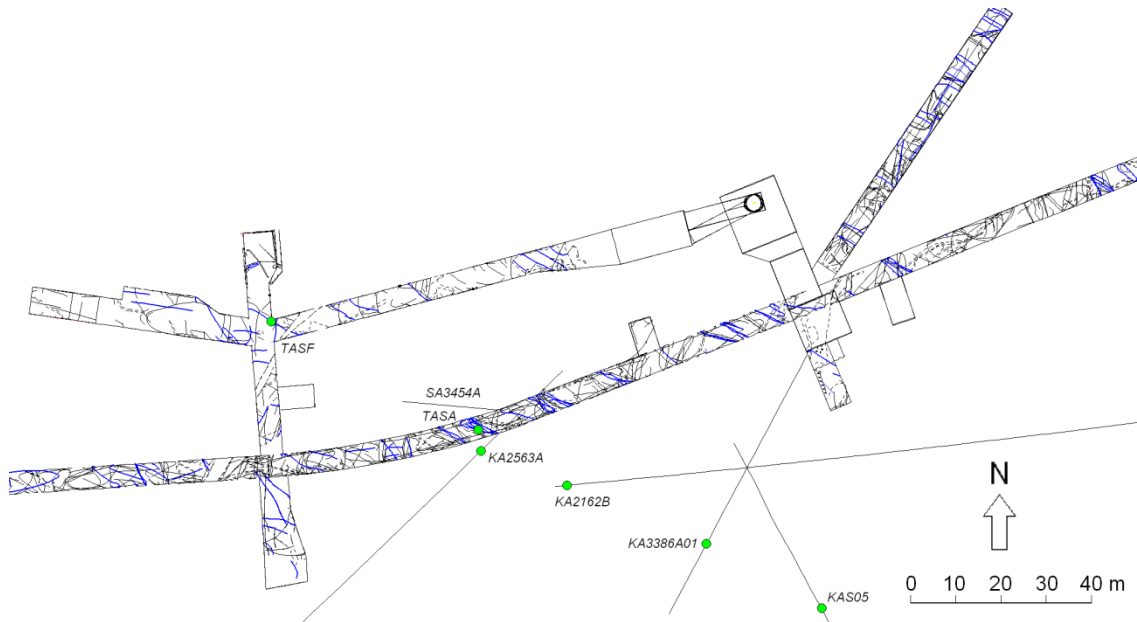


Figure A 52. Observation points used to model FASNW015 in tunnels and boreholes.

The indications used to model structure FASNW015 were:

1. Tunnel mapping, water-bearing fractures 3463,0-14, 15, 18, 20 and 22 in TASA (the TBM tunnel). Mapped with an orientation of RT90: $114^{\circ}/88^{\circ}$, $114^{\circ}/88^{\circ}$, $294^{\circ}/61^{\circ}$, $127^{\circ}/83^{\circ}$ and $114^{\circ}/88^{\circ}$ ($112^{\circ}/88^{\circ}$, $112^{\circ}/88^{\circ}$, $292^{\circ}/61^{\circ}$, $125^{\circ}/83^{\circ}$ and $112^{\circ}/88^{\circ}$ to magnetic north) /TMS/.
2. Tunnel mapping, water-bearing fractures 15-06 in TASF/TASF and 11 in the TASF-tunnel. Mapped with an orientation of RT90: $328^{\circ}/82^{\circ}$ and $121^{\circ}/90^{\circ}$ ($326^{\circ}/82^{\circ}$ and $119^{\circ}/90^{\circ}$ to magnetic north) /TMS/.
3. Borehole KAS05 at BH length 400 m. High hydraulic conductivity between 397-400 m BH length /transient injection test, SICADA/. Crush zone between 399.9-400.3 m BH length /fract_crush_pcelen, SICADA/. Reduced RQD value (52%) at BH length 400-401 m /rqd_rqd, SICADA/.
4. Borehole KA3386A01 at BH length 47 m. Inflow at BH length 47-48 m on flow measurements /flow_logging-flow, SICADA/. A mapped fracture 'broken' at BH length 46.83 m oriented $311^{\circ}/76^{\circ}$ (Äspö96) (RT90: $299^{\circ}/76^{\circ}$) /fract_core-ori_broken, SICADA/.
5. (Weak) Borehole KA2162B at BH length 285 m. Slightly decreased RQD value (84%) at BH length 285-286 m /rqd_rqd, SICADA/. Same as FASNW011b.
6. (Weak) Borehole KA2563A at BH length 34 m. Slightly decreased RQD value (93%) at BH length 34-35 m /rqd_rqd, SICADA/. Same as FASNW017, point 2.
7. Probe hole SA3454A. Inflow 0.2 l/min, transmissivity $2 \cdot 10^{-8} \text{ m}^2/\text{s}$ /Markström and Erlström, 1996/.

This structure is classified as **probable**.

FASNW015 297°/87° (probable) - point table

ID	Object	Section (m)	Water	Fract RT90	Mineral	Width (mm)	RQD (%)	Freq (fr/m)	Crush	Radar RT90	Oth
1	TASA	3463-14	vv	114/88	Ep/Ka/Kl	-	-	-	-	-	Ox
		-15	v	114/88	Ka/Ep	-	-	-	-	-	
		-18	vvv	294/61	Kl	-	-	-	-	-	
		-20	vvv	127/83	Ep	-	-	-	-	-	
		-22	vvv	114/88	Ka/lj	-	-	-	-	-	
2	TASF	15-06	vv	328/82	Ka/lj	-	-	-	-	-	
		-11	vv	121/90	Fl/Ka/lj	-	-	-	-	-	
3	KAS05	400	Cond	Crush	Ka/Kl/Cy	-	52	14/3 ¹	10 ¹	-	
4	KA3386A01	47	Infl	299/76	Kl	1	100	1/0 ²	0 ²	-	BIPS
5	KA2162B	285	Infl*	-	-	-	84	4/4 ¹	0 ¹	0	
6	KA2563A	34	0	-	-	-	93	2/2 ¹	0 ¹	0	BIPS
7	SA3454A	??	Infl	-	-	-	-	-	-	-	

*) Increased inflow after 270 m

In addition to the tunnel observations there are weak anomalies in the intersecting boreholes that can be connected to the geometry of the modelled structure.

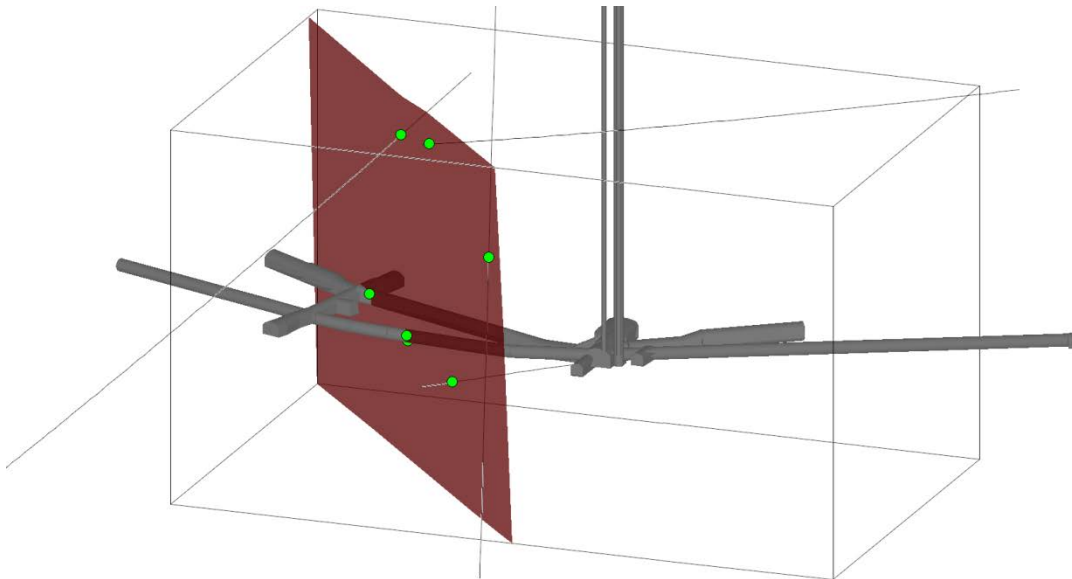


Figure A 53. 3D view of FASNW015 with observation points in green. View from SE.

The structure is modelled with an upper limitation at Z=-350 m, which is the upper boundary of the model volume. If the modelled structure is extrapolated upwards, it will intersect the spiral tunnel TASA at abt 2/536 and 1/590.

At neither of these sections are there any mapped water-bearing fractures or zone corresponding to the modelled structure.

Structure FASNW016

A steeply dipping structure with an orientation of $116^{\circ}/82^{\circ}$ (RT90) was modelled. The basis of the interpretation for this structure was a mapped water-bearing fracture in the TBM tunnel (TASA) that possibly can be connected to an observation in borehole KA3386A01 approx. 50 m southeast of the tunnel observation. The structure can, however, not be observed in TASF or TASJ.

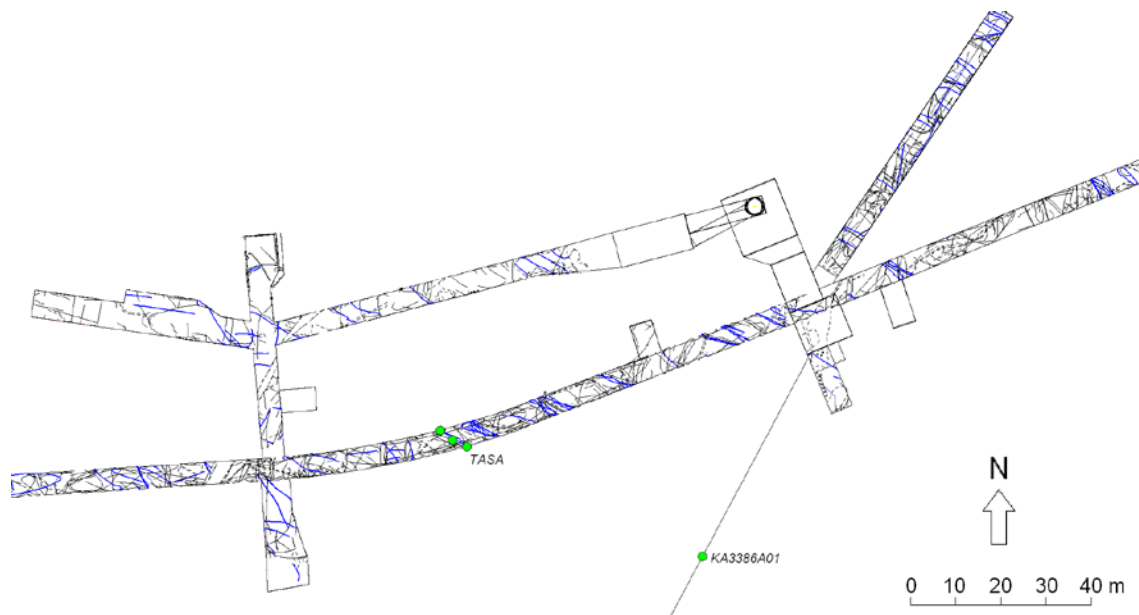


Figure A 54. Observation points used to model FASNW016 in A tunnel and boreholes.

The indications used to model structure FASNW016 were:

1. Tunnel mapping, water-bearing fracture 3478.1-02 in TASA (the TBM tunnel). Mapped with an orientation of RT90: $118^{\circ}/82^{\circ}$ ($116^{\circ}/82^{\circ}$ to magnetic north) /TMS/.
2. Borehole KA3386A01 at BH length 50 m. Inflow at BH length 49.9 m on flow measurements /flow_logging-flow, SICADA/. Mapped fractures 'broken' at BH length 49.85 m oriented RT90: $292^{\circ}/89.6^{\circ}$ ($304^{\circ}/89.6^{\circ}$ Äspö96) and BH length 50.29 m oriented RT90: $298^{\circ}/85.4^{\circ}$ ($310^{\circ}/85.4^{\circ}$ Äspö96) /fract_core-ori_broken, SICADA/.

This structure is classified as **possible**.

Structure FASNW017

A vertical structure with an orientation of $322^{\circ}(142^{\circ})/90^{\circ}$ (RT90) was modelled. The basis of the interpretation for this structure was a mapped water-bearing fracture in the TBM tunnel (TASA), more N-S striking than the other modelled fractures.

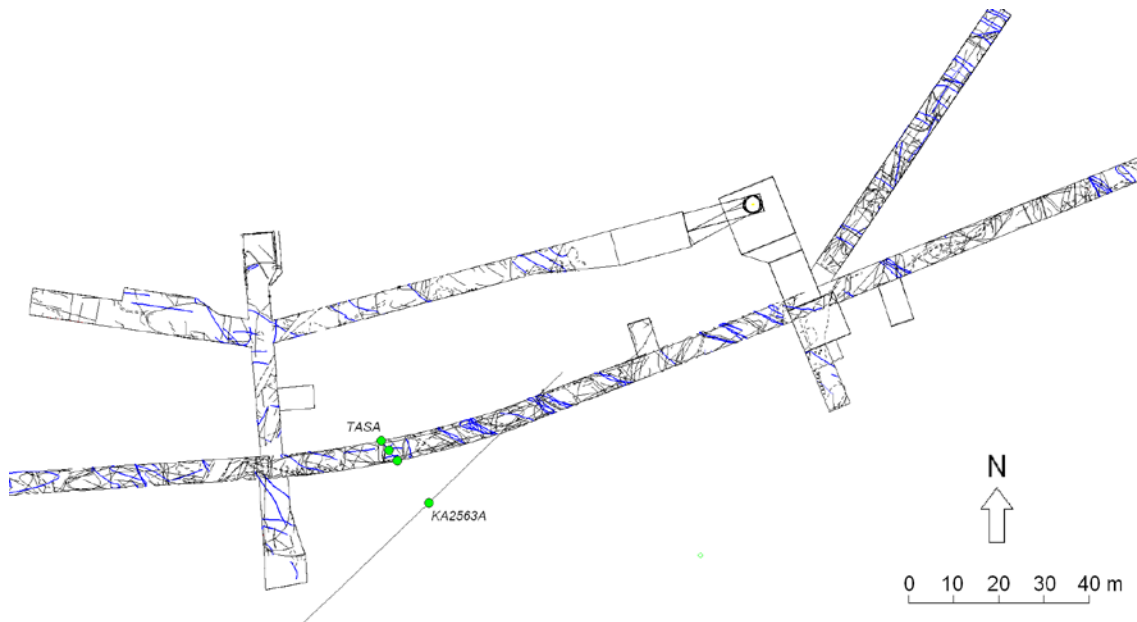


Figure A 56. Observation points used to model FASNW017 in A tunnel and boreholes.

This observation can possibly be connected to an observation in borehole KA2563A approx. 70 m above the tunnel observation.

The indications used to model structure FASNW017 were:

1. Tunnel mapping, water-bearing fracture 3492.9-03 in TASA (the TBM tunnel). Mapped with an orientation of RT90: $231^{\circ}/87^{\circ}$ ($229^{\circ}/87^{\circ}$ to magnetic north) /TMS/. This fracture is drawn parallel to fracture 05 that has a given orientation of (RT90: $148^{\circ}/88^{\circ}$ ($146^{\circ}/88^{\circ}$ to magnetic north). This orientation corresponds better with the drawn objects and is therefore considered to be more reliable.
2. (Weak) Borehole KA2563A at BH length 56.1 m. Reduced RQD value (46%) at BH length 56-57 m /rqd_rqd, SICADA/.

This structure is classified as **possible**.

FASNW017 322°(142°)/90° (possible) - point table

ID	Object	Section (m)	Water	Fract RT90	Mineral	Width (mm)	RQD (%)	Freq (fr/m)	Crush	Radar RT90	Oth
1	TASA	3493-03	wv	231*/87	Ep/Kl/Ka	-	-	-	-	-	
2	KA2563A	56.1	0	-	-	4	46	14/13 1	0 ¹	0	BIPS

*) Given value of strike corresponds poorly with the drawn geometry.

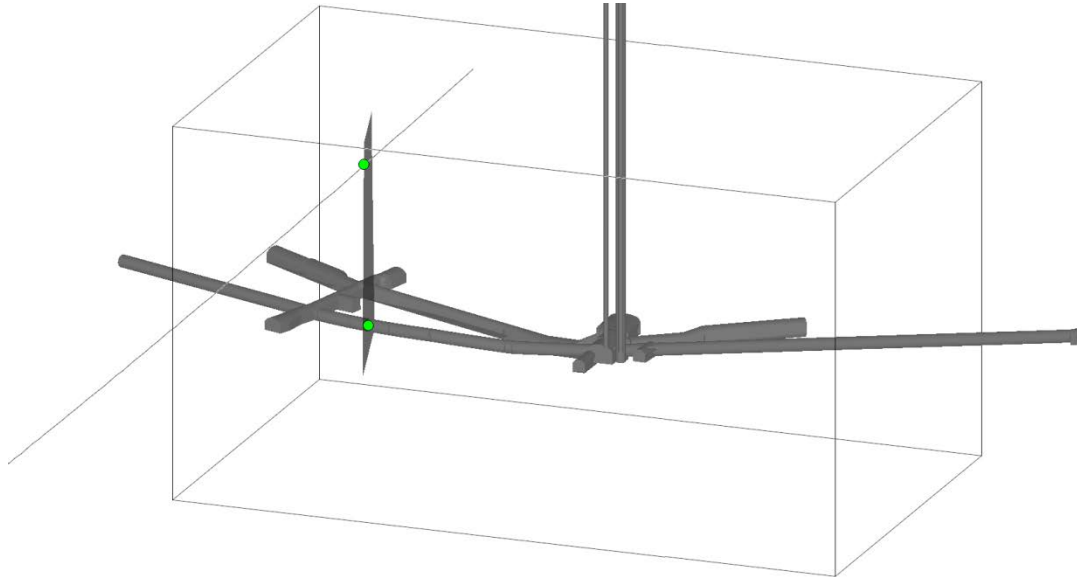


Figure A 57. 3D view of FASNW017 with observation points in green. View from SE.

The structure crosses over all other modelled structures but is trimmed towards the two closest; FASNW015 and FASNW018. It is modelled only between $z = -370 - -460$ m.

Structure FASNW018

A steeply dipping structure with an orientation of $116^\circ/87^\circ$ (RT90) was modelled.

The basis of the interpretation for this structure were mapped water-bearing fractures in the TBM tunnel (TASA) and TASJ, that can be connected to observations in boreholes south of the tunnel. The fracture just misses TASG.

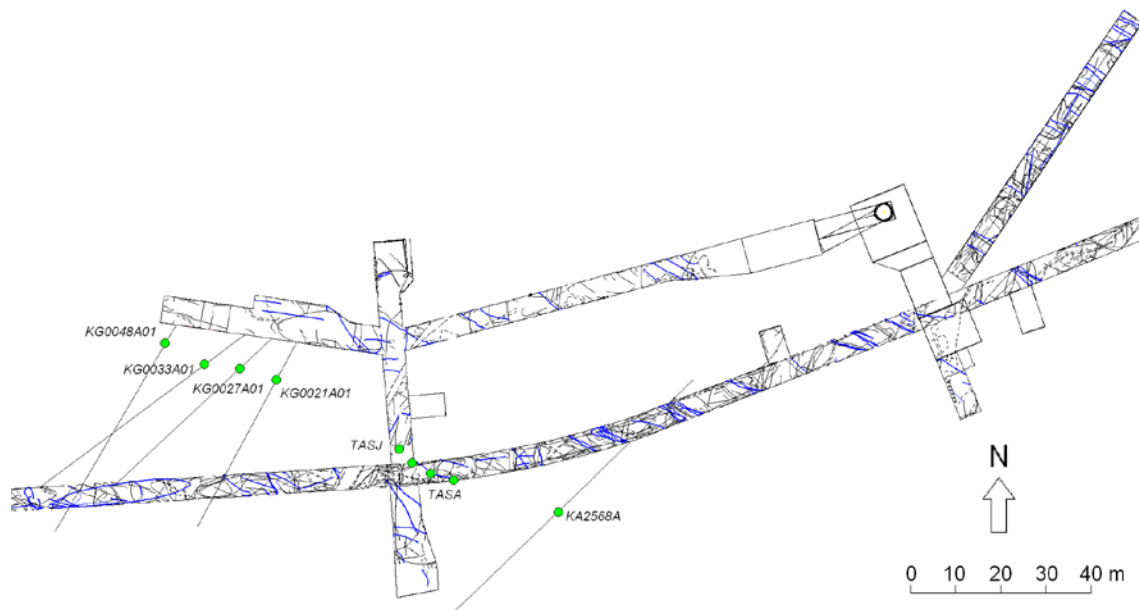


Figure A 58. Observation points used to model FASNW018 in tunnels and boreholes.

The indications used to model structure FASNW018 were:

1. Tunnel mapping, water-bearing fractures in TASA (the TBM tunnel) 3507.7-14 mapped with an orientation of RT90: $118^{\circ}/82^{\circ}$ ($116^{\circ}/82^{\circ}$ to magnetic north) and 3507.7-08 mapped with an orientation of RT90: $114^{\circ}/89^{\circ}$ ($112^{\circ}/89^{\circ}$ to magnetic north) /TMS/.
2. Tunnel mapping, water-bearing fracture 27-08 in the TASJ-tunnel. Mapped with an orientation of RT90: $114^{\circ}/79^{\circ}$ ($112^{\circ}/79^{\circ}$ to magnetic north) /TMS/.
3. Borehole KA2563A at BH length 57.8 m. Reduced RQD value at BH length 56-57 m (46%) at BH length 57-58 m (99) and at BH length 58-59 m (91) /rqd_rqd, SICADA/. PFL flow anomaly 57.8 and 58.2 m BH length / Rouhiainen and Heikkinen, 2002/. Oxidation at BH length 56.3-57.2 m /rock_alter-type, SICADA/.
4. Borehole KG0048A01 at BH length 5 m. Mapped open fracture at BH length 5.64 m oriented RT90: $115^{\circ}/77^{\circ}$ ($127^{\circ}/77^{\circ}$ Äspö96) /fract_core-ori_open, SICADA/. Inflow during drilling at 5.5–7.0 m /SICADA/. Inflow at flow logging and high hydraulic conductivity at 5–8 m BH length /Forsmark and Rhén, 2000/.
5. Borehole KG0021A01 at BH length 10 m. Mapped fracture ‘broken’ at BH length 10.98 m oriented RT90: $293^{\circ}/89^{\circ}$ ($305^{\circ}/89^{\circ}$ Äspö96) /fract_core-ori_broken, SICADA/. Inflow during drilling at 7-10 m BH length /SICADA/. High hydraulic conductivity at 10-13 m BH length /Forsmark and Rhén, 2000/.
6. (Weak) Borehole KG0027A01 at BH length 9.1 m. High hydraulic conductivity at 7-11 m BH length. Inflow at 8.1–9.9 m during drilling /Forsmark and Rhén, 2001/.
7. (Weak) Borehole KG0033A01 at BH length 11.4 m. High hydraulic conductivity at 9-13 m BH length. Inflow at 7.9–10.7 m during drilling /Forsmark and Rhén, 2001/.

This structure is classified as **probable**.

There is also an indication where the structure intersects KA3542G02, at 29.49 m BH length where there is a mapped fracture oriented RT90: $103^{\circ}/89^{\circ}$ ($115^{\circ}/89^{\circ}$ Äspö96) but this indication is considered to be too weak to be included in the modelling of the structure. The structure also intersects KG0023A01 but cannot be detected there.

FASNW018 116°/87° (probable) - point table

ID	Object	Section (m)	Water	Fract RT90	Mineral	Width (mm)	RQD (%)	Freq (fr/m)	Crush	Radar RT90	Oth
1	TASA	3507-14 -08	vv vv	118/82 114/89	Ka At	- -	- -	- -	- -	- -	
2	TASJ	27-08	vv	114/79	Kl/Ka	-	-	-	-	-	
3	KA2563A	57.8	Infl	-	-	-	91	14/13 ¹	0 ¹	0	Ox, BIPS
4	KG0048A01	5	Inf/Kon	115/77	Ep/Kl	3	90	1/1 ²	0 ²	-	BIPS
5	KG0021A01	10	Inf/Kon	293/89	Ka/Py	0	100	0/0 ²	0 ²	-	BIPS
6	KG0027A01	9.5	Cond	-	-	-	-	-	-	-	BIPS
7	KG0033A01	11	Cond	-	-	-	-	-	-	-	BIPS

The structure is modelled with an upper limitation at Z=-350 m, which is the upper boundary of the model volume.

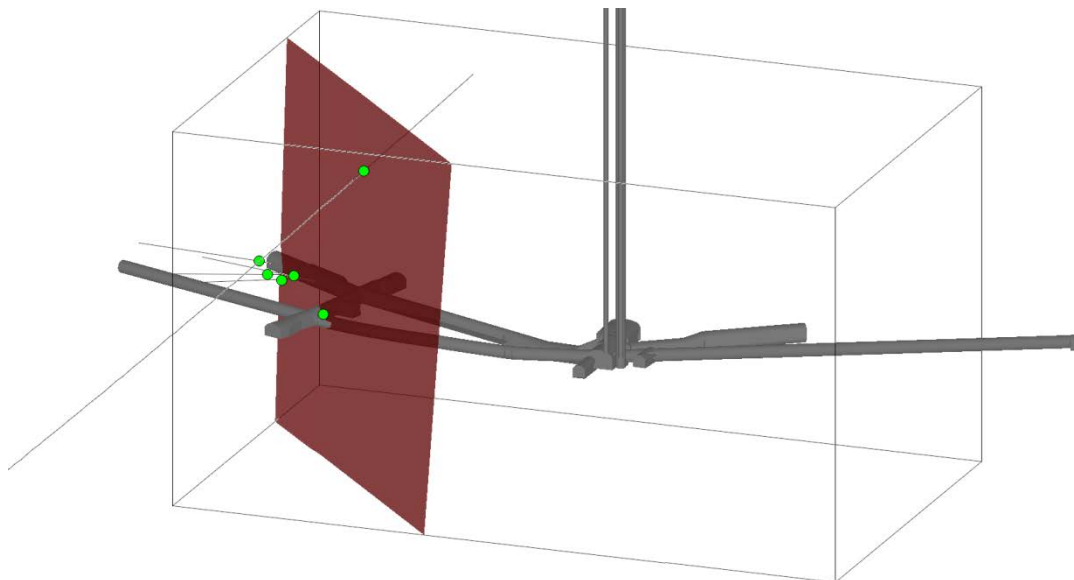


Figure A 59. 3D view of FASNW018 with observation points in green. View from SE.

If the modelled structure is extrapolated upwards, it will intersect the spiral tunnel TASA at about 2/505. At section 2/506 there is a mapped water-bearing fracture (04), mapped with an orientation of 160°/88° to magnetic north, which corresponds well with the modelled structure.

In the tunnel turn above the structure intersects TASA at section approximately 1/560. At section 1/564 there is a mapped water-bearing fracture (15), mapped with an orientation of 108°/86° to magnetic north and located approximately 10 m from the modelled FASNW018.

Structure FASNW019n

The basis of the interpretation of FASNW019n was a mapped water-bearing fracture in tunnel TASG.

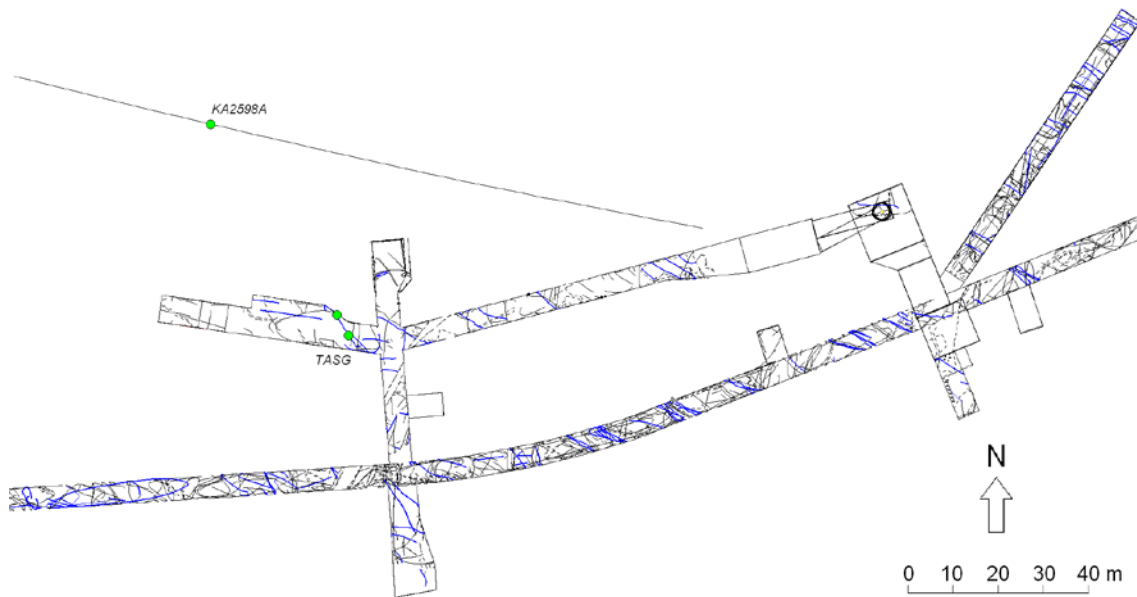


Figure A 60. Observation points used to model FASNW019n in tunnel and borehole.

Structure FASNW019n was modelled with an orientation of $329^{\circ}/86^{\circ}$ (RT90).

The indications used to model structure FASNW019n were:

1. Tunnel mapping, water-bearing fracture 16-16 in TASG. Mapped with an orientation of RT90: $322^{\circ}/72^{\circ}$ ($320^{\circ}/72^{\circ}$ to magnetic north) /TMS/.
2. Borehole KA2598A at BH length 132,0 m. Reduced RQD value (81%) at BH length 132-133 m /rqd_rqd, SICADA/. Water-bearing fracture detected on flow logging at 132.0 m /Rouhiainen and Heikkinen, 2003/. Mapped fracture 'broken' at BH length 131.9 m oriented RT90: $295^{\circ}/64^{\circ}$ ($307^{\circ}/64^{\circ}$ Äspö96) /fract_core-ori_broken, SICADA/.

This structure is classified as **possible**.

FASNW019n 329°/86° (possible) - point table

ID	Object	Section (m)	Water	Fract RT90	Mineral	Width (mm)	RQD (%)	Freq (fr/m)	Crush	Radar RT90	Oth
1	TASG	16-16	vv	322/72	Ka/Kl	-	-	-	-	-	Ox
2	KA2598A	132	Infl	295/64	Ka	-	81	6/6 ¹	0 ¹	0	

The structure FASNW019n is estimated to exist only north of NEHQ3. It is modelled only between $z = -380 - -460$ m.

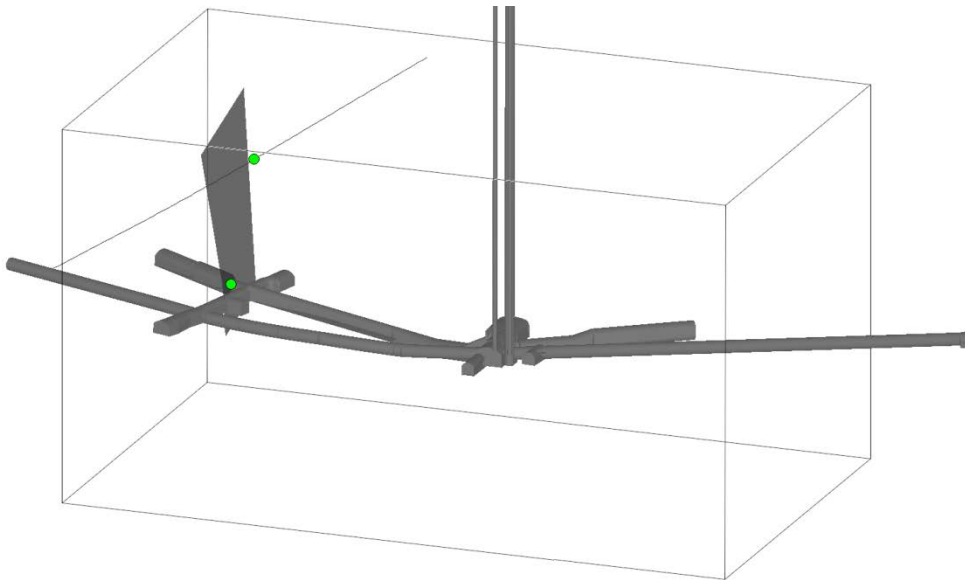


Figure A 61. 3D view of FASNW019n Observation points shown as green dots.

Structure FASNW019s

The basis of the interpretation of FASNW019s was a mapped water-bearing fracture in tunnel TASI.



Figure A 62. Observation points used to model FASNW019s in the TASI tunnel and boreholes.

Structure FASNW019s was modelled with an orientation of $151^{\circ}/86^{\circ}$ (RT90).

The indications used to model structure FASNW019s were:

1. Tunnel mapping, water-bearing fracture 15.5-02 in the TASI tunnel. Mapped with an orientation of RT90: $148^{\circ}/82^{\circ}$ ($146^{\circ}/82^{\circ}$ to magnetic north) /TMS/.
2. Borehole KA2563A at BH length 94.4 m. Slightly lowered RQD value (96%) at BH length 94-95 m /rqd_rqd, SICADA/. Small inflow PFL at 94.4 m /Rouhiainen and Heikkinen, 2002/. A radar reflector at BH length 93 m oriented RT90: $127^{\circ}/82^{\circ}$ /radar_direct-ori1, SICADA/.
3. Borehole KA2511A at BH length 52.5 m. Slightly reduced RQD value (89%) at BH length 52-53 m /rqd_rqd, SICADA/. Water-bearing fractures between 52-53 m, one inflow at 51.9 m BH length and a larger inflow at 52.5 m BH length /Rouhiainen and Heikkinen, 2002/. Mapped fracture at BH length 52.2 m oriented RT90: $143^{\circ}/85^{\circ}$ ($155^{\circ}/85^{\circ}$ Äspö96) /fract_core-ori_all, SICADA/. The section between 50-55 m has the highest transmissivity in the entire borehole.

This structure is classified as **possible**.

FASNW019s 151°/86° (possible) - point table

ID	Object	Section (m)	Water	Fract RT90	Mineral	Width (mm)	RQD (%)	Freq (fr/m)	Crush	Radar RT90	Oth
1	TASI	15-02	v	148/82	Kl	-	-	-	-	-	
2	KA2563A	94.4	PFL	-	-	-	96	6/6 ¹	0 ¹	127/82	BIPS
3	KA2511A	52.2	Infl	143/85	Ka/Kl	-	89	7/7 ¹	0 ¹	0	BIPS

Structure FASNW019s is estimated to exist only south of the structure FASNW020. It is modelled only between z= -360 – -460 m.

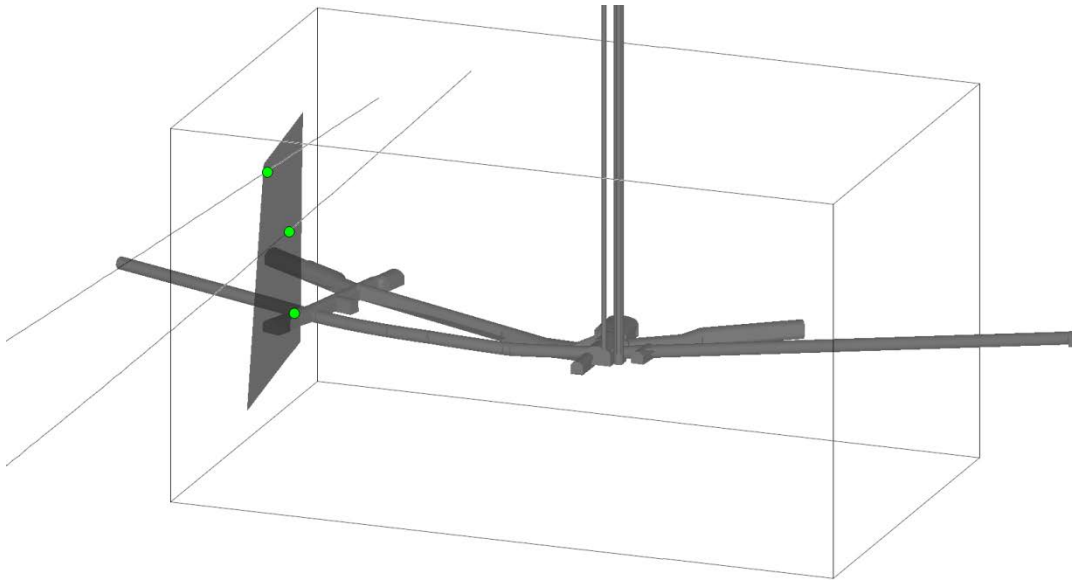


Figure A 63. 3D view of FASNW019s with observation points in green. View from SE.

Structure FASNW020

Two adjacent, steeply dipping structures with an orientation of 130° - $150^{\circ}/83^{\circ}$ (Äspö96) were identified south of structure FASNW018.

The basis of the interpretation of FASNW020 was a mapped water-bearing fracture in tunnel TASI. The extrapolated fracture intersects tunnel TASG and boreholes KG0021A01, KG0023A01, KG0027A01 and KG0033A01 but no indications can be found here.



Figure A 64. Observation points used to model FASNW020 in the TASI tunnel and boreholes.

Structure FASNW020 was modelled with an orientation of $306^{\circ}/88^{\circ}$ (RT90)

The indications used to model structure FASNW020 were:

1. Tunnel mapping, water-bearing fracture 15.5-03 in the tunnel TASI. Mapped with an orientation of RT90: $123^{\circ}/83^{\circ}$ ($121^{\circ}/83^{\circ}$ to magnetic north) /TMS/.
2. Borehole KA2563A at BH length 82 m. Slightly lowered RQD value (93%) at BH length 82-83 m /rqd_rqd, SICADA/. Small inflow PFL at 82.4 m BH length /Rouhiainen and Heikkinen, 2002/. Oxidation at BH length 79.3-81.8 m /rock_alter-type, SICADA/. Fracture mapped as 'broken' at 82.3 m BH length /p_fract_core, SICADA/, oriented RT90: $291^{\circ}/77^{\circ}$ ($303^{\circ}/77^{\circ}$ Äspö96) /BIPS, SICADA/.
3. Borehole KA2511A at BH length 20.6 m. Slightly lowered RQD value (93%) at BH length 20-21 m /rqd_rqd, SICADA/. PFL anomaly at 20.6 m BH length /Rouhiainen and Heikkinen, 2002/. Mapped fracture at BH length 20.6 m oriented RT90: $299^{\circ}/78^{\circ}$ ($311^{\circ}/78^{\circ}$ Äspö96) /fract_core-ori_all, SICADA/.
4. Borehole SA3509F at approximately 2 m BH length. Inflow on drilling between 0-3 m 1.5 l/min.

This structure is classified as **possible**.

FASNW020 306°/88° (possible) - point table

ID	Object	Section (m)	Water	Fract RT90	Mineral	Width (mm)	RQD (%)	Freq (fr/m)	Crush	Radar RT90	Oth
1	TASI	15-03	vv	123/83	Ka/Kl	-	-	-	-	-	
2	KA2563A	82	PFL	291/77	-	2	93	6/5 ¹	0 ¹	0	Ox, BIPS
3	KA2511A	20.6	Infl	299/78	Ka	-	93	3/3 ¹	0 ¹	0	BIPS
4	SA3509F	2	Infl	-	-	-	-	-	-	-	

Structure FASNW020 is estimated to exist only south of NEHQ3. It is modelled only between z= -360 – -480 m.

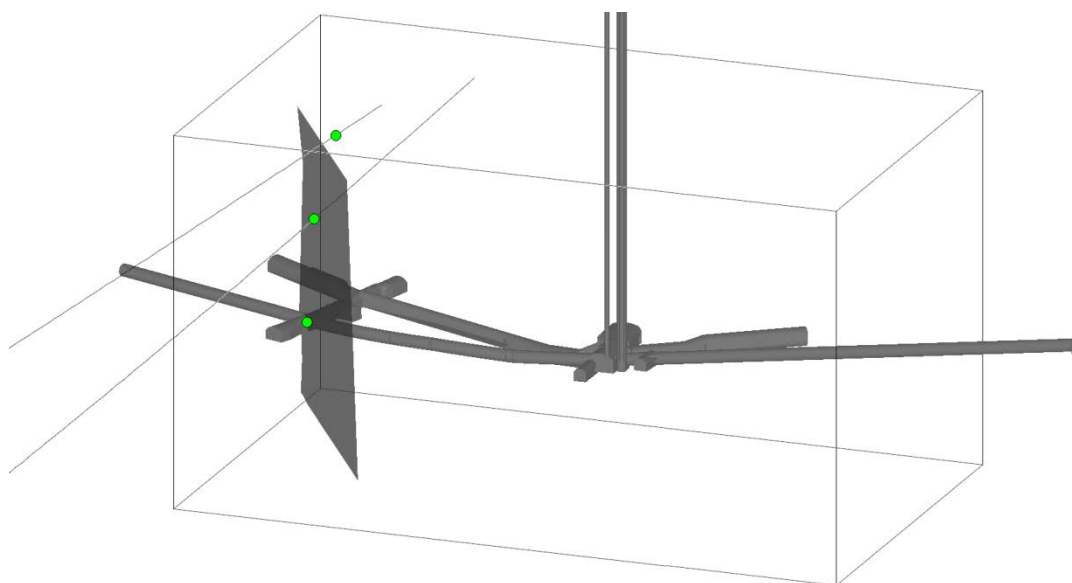


Figure A 65. 3D view of FASNW020 with observation points in green. View from SE.

Structure FASNW021a

A number of adjacent, sub-parallel, steeply dipping structures with an orientation of 123-125°/81° (Äspö96) were identified. These were modelled as separate fracture planes but were named FASNW021a, b and c to indicate that they are part of one "zone".

The basis of the interpretation of FASNW021a was connecting the mapped water-bearing fractures in the TBM-tunnel (TASA) and tunnel TASI.



Figure A 66. Observation points used to model FASNW021a in tunnels and boreholes.

Structure FASNW021a was modelled with an orientation of 114°/81° (RT90).

The indications used to model structure FASNW021a were:

1. Tunnel mapping, water-bearing fracture 3537.6-01 in TASA (the TBM tunnel). Mapped with an orientation of RT90: 288°/84° (286°/84° to magnetic north) /TMS/.
2. Tunnel mapping, water-bearing fracture 15.5-13 in TASI mapped with an orientation of RT90: 106°/82° (104°/82° to magnetic north) /TMS/.
3. Borehole KA3510A at BH length 11 m. Two 4 mm wide, open fractures at 11.5 and 11.7 m BH length /fract_core-width, SICADA/ and another open fracture at 11.1 m BH length. /fract_core-width, SICADA/. RQD value (99%) between 10-11 m /rqd_rqd, SICADA/.
4. Borehole KG0021A01 at BH length 28 m. Mapped open fractures at BH length 28.04 m oriented RT90: 299°/77° (311°/77° Äspö96) and at BH length 28.05 m oriented RT90: 297°/80° (309°/80° Äspö96) /fract_core-ori_open, SICADA/. Inflow at 26-30 m BH length with a maximum between 26-27 m /Forsmark and Rhén, 2000/. High hydraulic conductivity between 27-29 m BH length /Forsmark and Rhén, 2000/.
5. Borehole KA3542G02 at BH length 5 m. Mapped open fracture at BH length 5.06 m oriented RT90: 099°/90° (111°/90° Äspö96) /fract_core-ori_open, SICADA/. Inflow on drilling at 4.4–5.1 m BH length /core drilling record, SICADA/. Inflow according to flow log at 5-6 m BH length /Forsmark and Rhén, 2000/.

6. (Weak) Borehole KA3554G02 at BH length 12.65 m. Mapped fracture 'broken' at BH length 12.65 m oriented RT90: 126°/82° (138°/82° Äspö96) /fract_core-ori_broken, SICADA/. Inflow according to flow log at 11-18 m BH length /Forsmark and Rhén, 2000/. High hydraulic conductivity between 12-18 m BH length /Forsmark and Rhén, 2000/.
7. Borehole KA2563A at BH length 68.5 m. Very low RQD (0%) between 68-69 m /rqd_rqd, SICADA/. Increased fracture frequency (33) between 68-69 m /freq_1m-open_crush, SICADA/. Crush between 68-69 m /fract_crush-min1, SICADA/. A radar reflector at BH length 69 m oriented RT90: 167°/79° /radar_direct-ori1, SICADA/. Water-bearing fractures from PFL between 68.1-70.0 m /Rouhiainen and Heikkinen, 2002/. *Same as FASNW021b, point 6.*
8. Borehole KG0048A01 at BH length 21 m. Mapped fracture 'broken' at BH length 20.5 m oriented RT90: 314°/74° (326°/74° Äspö96) /fract_core-ori_broken, SICADA/. Inflow and maximum for conductivity between 20-23 m, 24-25 m and 27-28 m. Increased hydraulic conductivity between 20-25 m BH length /Forsmark and Rhén, 2000/.
9. Borehole KG0027A01 at BH length 29 m. Three open fractures visible in BIPS image, intersecting the borehole almost perpendicularly at 28.8-28.9 m depth /BIPS/.
10. Borehole KG0033A01 at BH length 29 m. Two open fractures visible in BIPS image, intersecting the borehole almost perpendicularly at 28.7 m depth /BIPS/.
11. (Weak) Borehole KA3566G02 at BH length 20 m. Mapped fracture 'broken' at BH length 19.9 m oriented RT90: 331°/78° (343°/78° Äspö96) /fract_core-ori_broken, SICADA/. Slightly lowered RQD (92%) between 20-21 m /rqd_rqd, SICADA/.
12. 12-13 The structure intersects probe hole SA3526F at a BH length of approximately 7 m, the inflow to the borehole has increased from approximately 5 l/min to 10 l/min between 4-15 m BH length. The fracture also intersects SA3509F at approximately 24 m BH length (near hole end), here there is no measured inflow /probeobs, SICADA/.

This structure is classified as **probable**.

FASNW021a 114°/81° (probable) - point table

ID	Object	Section (m)	Water	Fract RT90	Mineral	Width (mm)	RQD (%)	Freq (fr/m)	Crush	Radar RT90	Oth
1	TASA	3537-01	vv	288/84	Ep/Kl	0	-	-	-	-	
2	TASI	15-13	v	106/82	Ka/Kl	-	-	-	-	-	
3	KA3510A	11	0	-	-	-	99	7/3 ¹	0 ¹	(13m)	
4	KG0021A01	28	Inf/Kon	297/80	Ka/Kl/Py	1	99	0/0 ²	0 ²	-	
5	KA3542G02	5	Infl	099/90	Ka	-	88	1/1 ²	0 ²	-	
6	KA3554G02	12.65	Inf/Kon	126/82	Kl	0	100	0/0 ²	0 ²	-	
7	KA2563A	68.5	Infl	Crush	Kl/Ep/Ka	-	0	33/0 ¹	33 ¹	167/79	Ox
8	KG0048A01	21	Inf/Cond	314/74	Ep/Ka/Kl	0	100	0/0 ²	0 ²	-	
9	KG0027A01	29		Bips	-	-	-	-	-	-	
10	KG0033A01	29		Open	-	-	-	-	-	-	
11	KA3566G02	20		331/78	Kl/Ka	3	92	0/0 ²	0 ²	-	
12	SA3526F	7	Infl	-	-	-	-	-	-	-	Inj
13	SA3509F	24	0	-	-	-	-	-	-	-	

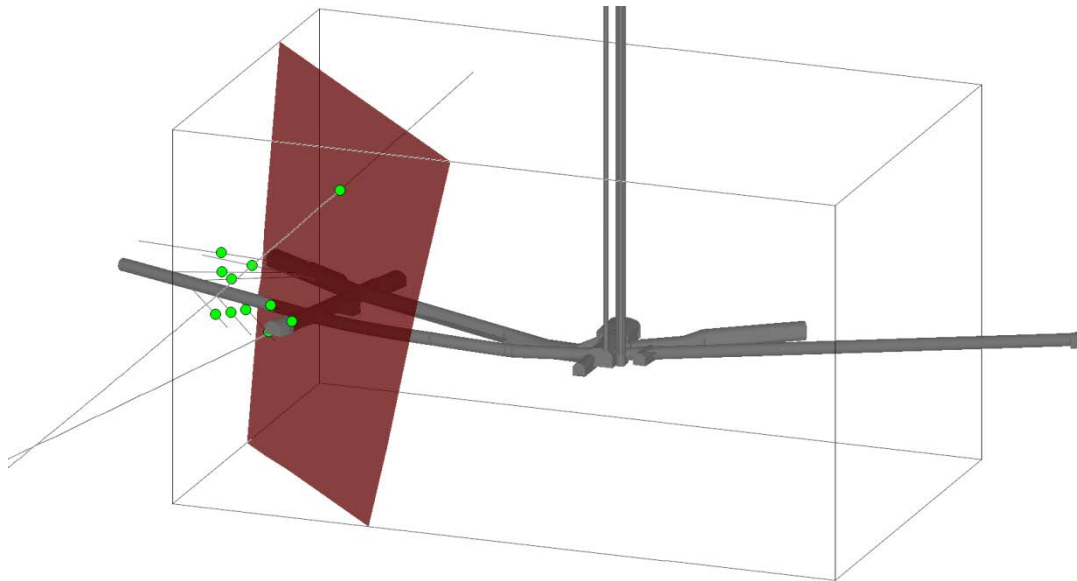


Figure A 67. 3D view of FASNW021a with observation points in green. View from SE.

This structure is an alternative interpretation of Prototyp WTRSTD7 and TRUE #2 fracture. The structure is modelled with an upper limitation at Z=-350 m, which is the upper boundary of the model volume.

Structure FASNW021b

The basis of the interpretation of FASNW021b was connecting the mapped water-bearing fractures in the TBM-tunnel (TASA) and tunnel TASI.

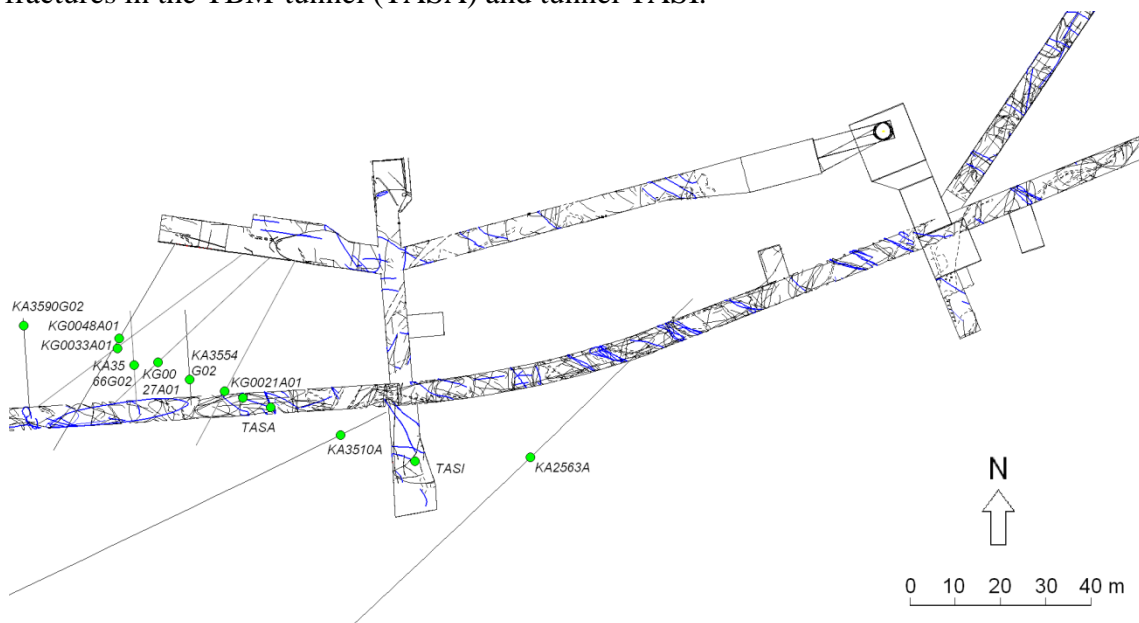


Figure A 68. Observation points used to model FASNW021b in tunnels and boreholes.

Structure FASNW021b was modelled with an orientation of 111°/81° (RT90).

The indications used to model structure FASNW021b were:

1. Tunnel mapping, water-bearing fracture 3552.7-05 in TASA (the TBM tunnel). Mapped with an orientation of RT90: 299°/77° (297°/77° to magnetic north) /TMS/.
2. Tunnel mapping, water-bearing fracture 15.5-23 in the tunnel TASI mapped with an orientation of RT90: 098°/84° (096°/84° to magnetic north) /TMS/.
3. (Weak) Borehole KA3554G02 at BH length 8.08 m. Mapped open fracture at BH length 8.08 m oriented RT90: 112°/85° (124°/85° Äspö96) /fract_core-ori_open, SICADA/. Slightly lowered RQD value (98%) between 8-9 m /rqd_rqd, SICADA/.
4. (Weak) Borehole KA3590G02 at BH length 27.83 m. Mapped open fracture at BH length 27.83 m oriented RT90: 128°/80° (140°/80° Äspö96) /fract_core-ori_open, SICADA/. Increased hydraulic conductivity after 24 m BH length /Forsmark and Rhén, 2000/. Slightly lowered RQD (92%) between 28-29 m /rqd_rqd, SICADA/.
5. Borehole KA3510A at BH length 13 m. Radar reflector at 13 m BH length oriented RT90: 293°/90° /radar_direct-ori1, SICADA/. PFL anomaly at 15 m BH length /Rouhiainen and Heikkinen, 2003/. Slightly lowered RQD value (94%) between 12-13 m /rqd_rqd, SICADA/. Oxidation at BH length 13.63 m /rock_alter-type, SICADA/.
6. Borehole KA2563A at BH length 68.5 m. Very low RQD (0%) between 68-69 m /rqd_rqd, SICADA/. Increased fracture frequency (33) between 68-69 m /freq_1m-open_crush, SICADA/. Crush between 68-69 m /fract_crush-min1, SICADA/. A radar reflector at BH length 69 m oriented RT90: 167°/79° /radar_direct-ori1, SICADA/. Water-bearing fractures between 68.1-70.0 m / Rouhiainen and Heikkinen, 2002/. *Same as FASNW021a, point 7.*
7. Borehole KG0048A01 at BH length 25 m. Mapped fracture at BH length 24.51 m oriented RT90: 271°/76° (283°/76° Äspö96) /fract_core-ori_all, SICADA/. Inflow and higher conductivity between 20-23 m, 24-25 m and 27-28 m, maximum at 24–25 m. Smaller inflow at 23-24 m BH length / Forsmark and Rhén, 2000/.
8. Borehole KG0027A01 at BH length 34 m. An open fracture visible in BIPS image, intersecting the borehole almost perpendicularly at 33.5 m depth /BIPS/.
9. (Weak) Borehole KG0033A01 at BH length 35 m. An open fracture visible in BIPS image, intersecting the borehole with a small angle at 34.9 m depth /BIPS/.
10. Borehole KG0021A01 at BH length 35.5 m. Mapped open fracture at BH length 35.51 m oriented RT90: 314°/69° (326°/69° Äspö96)/fract_core-ori_open, SICADA/. Inflow between 34-35 m BH length /Forsmark and Rhén, 2000/. Increased hydraulic conductivity between 35-36 m BH length /Forsmark and Rhén, 2000/. Slightly lowered RQD value (97%) at BH length 35-36 m /rqd_rqd, SICADA/. *Near FASNW021c, point 3.*
11. (Weak) Borehole KA3566G02 at BH length 13.3 m. Mapped fracture ‘broken’ at BH length 13.3 m oriented RT90: 304°/79° (316°/79° Äspö96) /fract_core-ori_broken, SICADA/. Slightly lowered RQD (79%) between 13-14 m /rqd_rqd, SICADA/.
12. The structure intersects probe hole SA3526F at a BH length of approximately 13 m, the inflow to the borehole has increased from approximately 5 l/min to 10 l/min between 4-15 m BH length /probeobs, SICADA/.

The structure also intersects the sub-vertical boreholes KA3542G02 and KA3543G01 at a small angle. No evidence of the structure can be found here, but the structure is very steeply dipping and can easily miss the sub-vertical boreholes with a few cm.

It also intersects the borehole KA3548D01 very near the hole start. No evidence of the structure can be found here but it is possible that the structure misses the borehole completely.

This structure is classified as **probable**.

FASNW021b 111°/81° (probable) - point table

ID	Object	Section (m)	Water	Fract RT90	Mineral	Width (mm)	RQD (%)	Freq (fr/m)	Crush	Radar RT90	Oth
1	TASA	3552-05	vv	299/77	KI	-	-	-	-	-	
2	TASI	15-23	vv	098/84	Ka/KI	-	-	-	-	-	
3	KA3554G02	8		112/85	Ka	2	98	1/1 ²	0 ²	-	
4	KA3590G02	28	Cond	128/80	Ka/KI/Py	2	92	0/0 ²	0 ²	-	
5	KA3510A	13	Infl	-	-	-	94	3/3 ¹	0 ¹	293/90	Ox
6	KA2563A	68.5	Infl	Crush	KI/Ep/Ka	-	0	33/0 ¹	33 ¹	167/79	Ox
7	KG0048A01	25	Inf/Kon	271/76	KI/Ka	0	100	-	-	-	
8	KG0027A01	34		open	-	-	-	-	-	-	bips
9	KG0033A01	35		open	-	-	-	-	-	-	bips
10	KG0021A01	35.51	Inf/Kon	314/69	KI/Ka	1	97	2/2 ²	0 ²	-	
11	KA3566G02	13.3		304/79	KI/Ka	1	79	0/0 ²	0 ²	-	
12	SA3526F	13	Infl	-	-	-	-	-	-	-	Inj

This structure is an alternative interpretation of Prototyp WTRSTD6 and TRUE #4 fracture. The structure is regarded as a splay from FASNW021a and is trimmed towards FASNW021a in the SE. Since FASNW021b is detected far outside the boundary cube it is judged to have a lateral extent that motivates that it may not be limited horizontally.

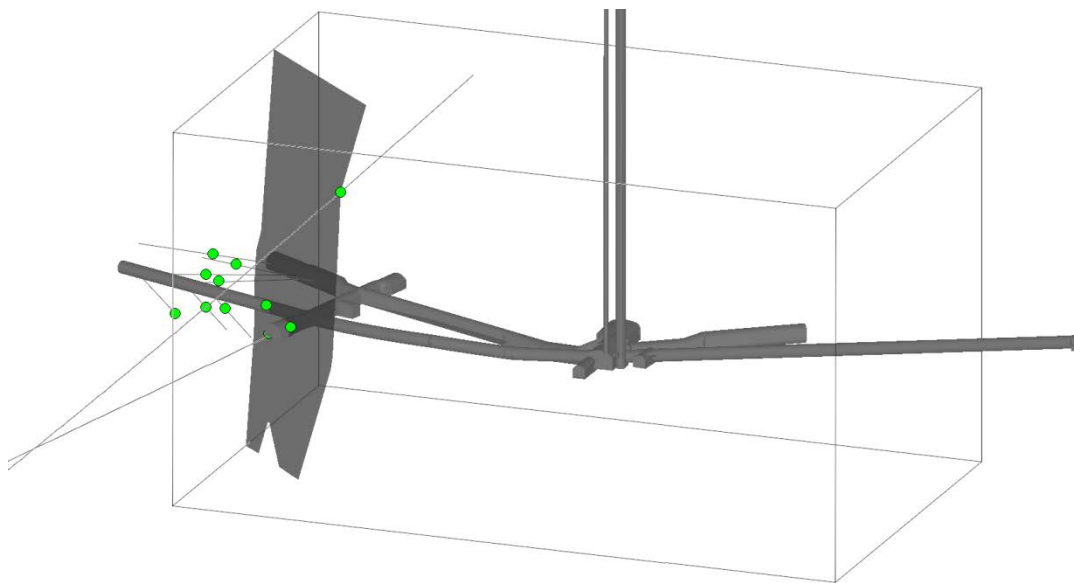


Figure A 69. 3D view of FASNW021b with observation points in green. View from SE.

The structure is modelled with an upper limitation at Z=-350 m, which is the upper boundary of the model volume. Regarding intersections with the tunnel above, see Structure FASNW021c below, where the FASNW021x structures are analyzed as a group.

Structure FASNW021c

The basis of the interpretation of FASNW021c was connecting the mapped water-bearing fractures in the TBM-tunnel (TASA) and tunnel TASI.

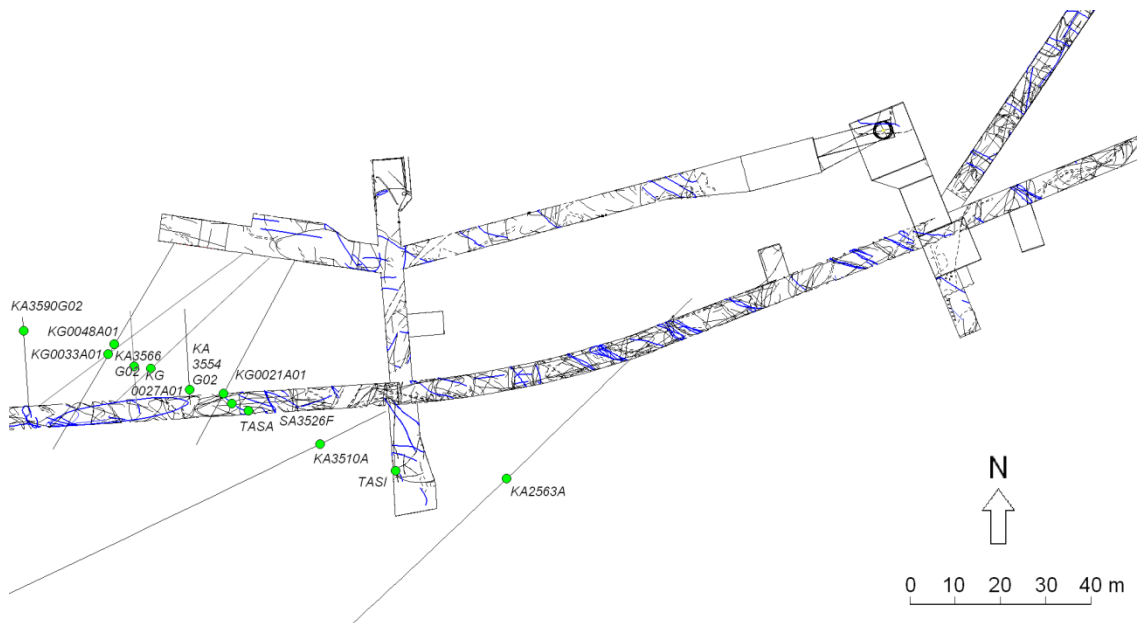


Figure A 70. Observation points used to model FASNW021c in tunnels and boreholes.

Structure FASNW021c was modelled with an orientation of $112^{\circ}/81^{\circ}$ (RT90).

The indications used to model structure FASNW021c were:

1. Tunnel mapping, water-bearing fracture 3552.7-10 in TASA (the TBM tunnel). Mapped with an orientation of RT90: $122^{\circ}/88^{\circ}$ ($120^{\circ}/88^{\circ}$ to magnetic north) /TMS/.
2. Tunnel mapping, water-bearing fracture 15.5-02 in tunnel TASI mapped with an orientation of RT90: $328^{\circ}/68^{\circ}$ ($326^{\circ}/68^{\circ}$ to magnetic north) /TMS/.
3. Borehole KG0021A01 at BH length 35.5 m. Mapped open fracture at BH length 35.54 m oriented RT90: $305^{\circ}/77^{\circ}$ ($317^{\circ}/77^{\circ}$ Äspö96) /fract_core-ori_open, SICADA/. Inflow between 34-35 m BH length /Forsmark and Rhén, 2000/. Increased hydraulic conductivity between 35-36 m BH length /Forsmark and Rhén, 2000/. Slightly lowered RQD value (97%) at BH length 35-36 m /rqd_rqd, SICADA/. Near FASNW021b, point10.
4. (Weak) Borehole KA3590G02 at BH length 25.74 m. Mapped open fracture at BH length 25.74 m oriented RT90: $126^{\circ}/77^{\circ}$ ($138^{\circ}/77^{\circ}$ Äspö96) /fract_core-ori_open, SICADA/. Higher hydraulic conductivity after 24 m BH length /Forsmark and Rhén, 2000/.
5. (Weak) Borehole KA3510A at BH length 19 m. Radar reflector at 19 m BH length oriented RT90: $122^{\circ}/87^{\circ}$ /radar_direct-ori1, SICADA/. PFL anomaly at 20.5 m and 22.2 m /Rouhiainen and Heikkinen, 2003/. Slightly reduced RQD value (90-92%) at BH length 18-20 m /rqd_rqd, SICADA/.
6. (Weak) Borehole KA3554G02 at BH length 4.53 m. Mapped fracture at BH length 4.53 m oriented RT90: $102^{\circ}/78^{\circ}$ ($114^{\circ}/78^{\circ}$ Äspö96) /fract_core-ori_all, SICADA/. RQD value (99%) at BH length 5-6 m /rqd_rqd, SICADA/. Small inflow at 3.5 m BH length /Forsmark and Rhén, 2000/.

7. Borehole KG0048A01 at BH length 27 m. Mapped fracture 'broken' at BH length 27.16 m oriented RT90: 092°/82° (104°/82° Äspö96) /fract_core-ori_broken, SICADA/. Inflow and maximum conductivity at 20-23 m, 24-25 m and 27-28 m /Forsmark and Rhén, 2000/.
8. Borehole KA2563A at BH length 78 m. Water-bearing fractures at BH length 73, 75.9 and 78 m BH length /Rouhiainen and Heikkinen, 2002/. Mapped fracture at BH length 77.9 m oriented RT90: 275°/78° (287°/78° Äspö96) /BIPS, SICADA/.
9. (Weak) Borehole KG0027A01 at BH length 36 m. A healed fracture visible in BIPS image, intersecting the borehole almost perpendicularly at 35.5 m depth /BIPS/.
10. (Weak) Borehole KG0033A01 at BH length 35 m. An open fracture visible in BIPS image, intersecting the borehole with a small angle at 34.9 m depth /BIPS/.
11. (Weak) Borehole KA3566G02 at BH length 13.2 m. Mapped fracture 'broken' at BH length 13.2 m oriented RT90: 120°/87° (132°/87° Äspö96) /fract_core-ori_broken, SICADA/. Slightly lowered RQD (79%) between 13-14 m /rqd_rqd, SICADA/.
12. The structure intersects probe hole SA3526F at a BH length of approximately 19 m, the inflow to the borehole has increased with approximately 13 l/min between 16.8-22.2 m BH length /probeobs, SICADA/.

This structure is classified as **probable**.

FASNW021c 112°/81° (probable) - point table

ID	Object	Section (m)	Water	Fract RT90	Mineral	Width (mm)	RQD (%)	Freq (fr/m)	Crush	Radar RT90	Oth
1	TASA	3552-10	v	122/88	Ka/Kl	-	-	-	-	-	
2	TASI	15-02	wv	328/68	Qz/Kl	-	-	-	-	-	
3	KG0021A01	35.54	Inf/Kon	305/77	Kl/Ka	1	97	2/2 ²	0 ²	-	
4	KA3590G02	26	Cond	126/77	Kl/Ka	1	100	0/0 ²	0 ²	-	Ox
5	KA3510A	19	Infl	-	-	-	90	6/3 ¹	0 ¹	122/87	
6	KA3554G02	4.5	(Infl)	102/78	Kl/Ka	0	99	0/0 ²	0 ²	-	
7	KG0048A01	27	Inf/Kon	092/82	Ka/Kl	0	100	0/0 ²	0 ²	-	
8	KA2563A	78	Infl	275/78		3	100	1/1 ¹	0 ¹	0	
9	KG0027A01	36		open	-	-	-	-	-	-	bips
10	KG0033A01	37		open	-	-	-	-	-	-	bips
11	KA3566G02	13.2		120/87	Kl/Ka	1	79	0/0 ²	0 ²	-	
12	SA3526F	19	Infl	-	-	-	-	-	-	-	Inj

The structure is regarded as a splay from FASNW021a and is trimmed towards FASNW021a in the SE. Since FASNW021c is detected far outside the boundary cube it is judged to have a lateral extent that motivates that it may not be limited horizontally.

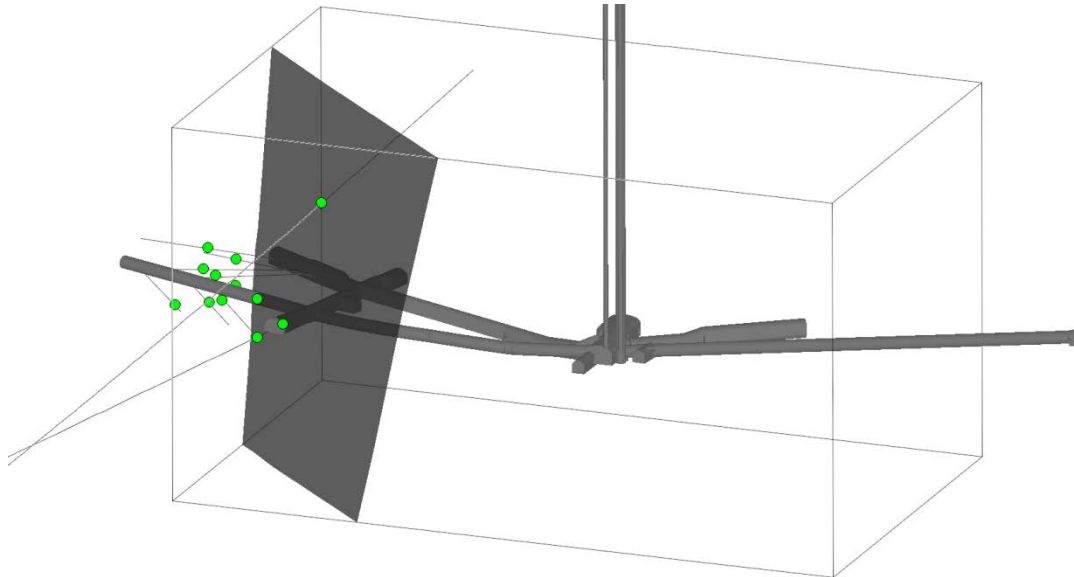


Figure A 71. 3D view of FASNW021c with observation points in green. View from SE.

The structure also intersects the sub-vertical boreholes KA3542G01, KA3543I01, KA3544G02, KA3545G05, KA3545G06, KA3546G01, KA3546G03 and KA3548G01 at a small angle, often near the hole start or end. No evidence of the structure can be found here, but the structure is very steeply dipping and can easily miss the sub-vertical boreholes with a few cm.

If the three modelled FASNW021-structures are extrapolated upwards, they will intersect the spiral tunnel TASA at about 2/505. At section 2/506 there is a mapped water-bearing fracture (04), mapped with an orientation of $160^{\circ}/88^{\circ}$ to magnetic north, which corresponds well with the modelled structure. This is the same indication that fits with structure FASNW018.

Structure FASSH001

The basis of the interpretation of FASSH001 was a mapped water-bearing fracture in the TBM-tunnel (TASA). The structure does not intersect TASQ.

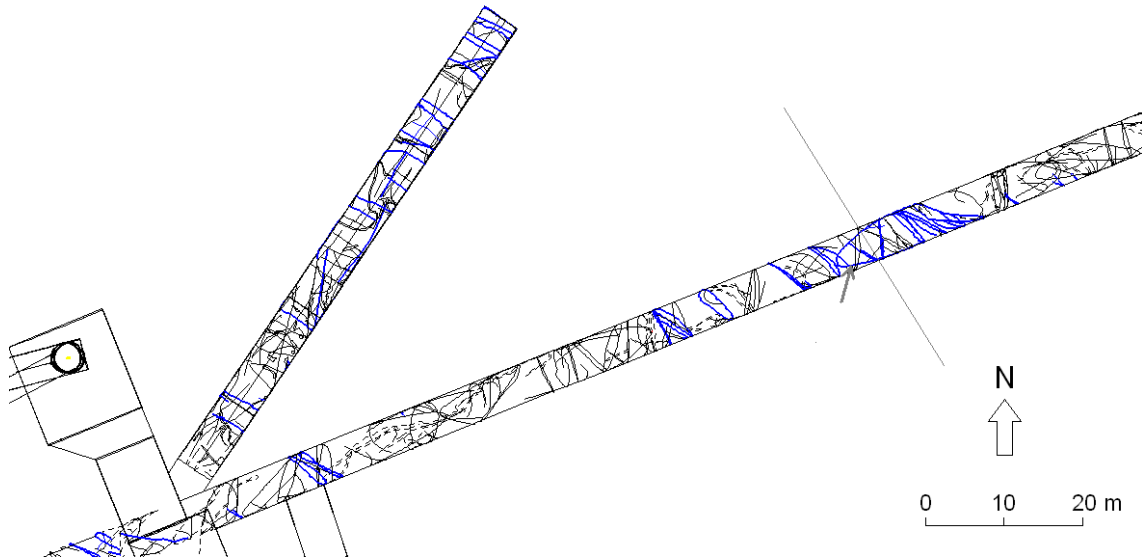


Figure A 72. Observation in A tunnel used to model FASSH001.

Structure FASSH001 was modelled with an orientation of $016^{\circ}/10^{\circ}$ (RT90).

The indications used to model structure FASSH001 were:

1. Tunnel mapping, water-bearing fracture 3290.0-06 in TASA (the TBM tunnel). Mapped with an orientation of RT90: $354^{\circ}/02^{\circ}$ ($352^{\circ}/02^{\circ}$ to magnetic north) /TMS/.
2. (Weak) Borehole KAS02 at 429 m BH length. Oxidation at BH length 429 m /rock_alter-type, SICADA/. Mapped fracture 'broken' at BH length 429 m oriented RT90: $352^{\circ}/1^{\circ}$ ($004^{\circ}/1^{\circ}$ Äspö96) /fract_core-ori_broken, SICADA/.

This structure is classified as **possible**.

FASSH001 016°/10° (possible) – point table

ID	Object	Section (m)	Water	Fract RT90	Mineral	Width (mm)	RQD (%)	Freq (fr/m)	Crush	Radar RT90	Oth
1	TASA	3290-06	vv	354/02	Kl/Ka	-	-	-	-	-	Ox
2	KAS02	429		352/01	Kl/Ka	-	100	5/1 ¹	0 ¹	-	Ox

The structure is not identified in the shaft and is trimmed by FASNS002 in the W, east of the shaft. The lateral extension is limited to 100 m.

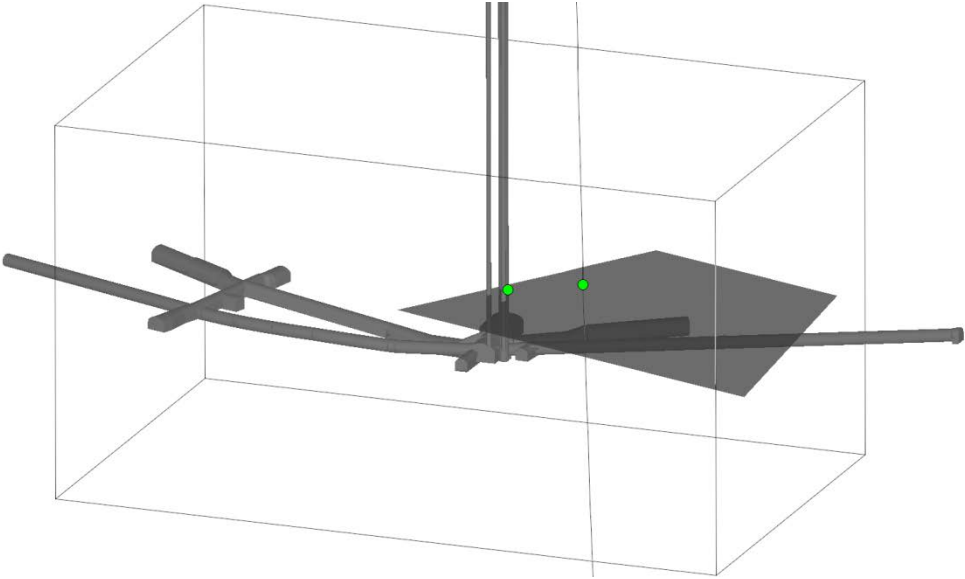


Figure A 73. 3D view of FASSH001 with observation points in green. View from SE.

Table of points, all points used in boreholes

Borehole	BH Length (m)	Structure
KA2162B	111	FASNW007
KA2162B	129	FASNS001
KA2162B	138	FASNW009
KA2162B	163	FASEW002c
KA2162B	224	FASEW003
KA2162B	252	FASNW013, FASNS002
KA2162B	269.5	FASNW014b
KA2162B	285	FASNW015
KA2511A	20.6	FASNW020
KA2511A	52.2	FASNW019s
KA2563A	8	FASNW013
KA2563A	17	FASNW014a
KA2563A	20.5	FASNW014b
KA2563A	24.5	FASNW014c
KA2563A	34	FASNW015
KA2563A	56	FASNW017
KA2563A	57.8	FASNW018
KA2563A	68.5	FASNW021a, FASNW021b
KA2563A	78	FASNW021c
KA2563A	82.4	FASNW020
KA2563A	94.4	FASNW019s
KA2598A	37.1	FASEW002c
KA2598A	132	FASNW019n
KA3191F	85	FASEW001
KA3191F	87	FASNW002
KA3191F	89	FASNW001
KA3191F	92	FASNS001
KA3191F	96	FASNW003
KA3191F	107	FASNW005
KA3191F	116	FASNW006
KA3191F	123	FASNW009
KA3191F	123.6	FASNW007
KA3191F	124	FASNW008
KA3191F	157	FASNW010
KA3191F	173	FASNW011
KA3191F	174	FASNS002
KA3191F	203.5	FASEW002a
KA3191F	209.5	FASEW002b
KA3375A05	2.8	FASEW002a
KA3376B01	21.8	FASNW010
KA3376B01	40.7	FASNW008
KA3376B01	43.4	FASNS002
KA3376B01	47.7	FASEW001
KA3376B01	50.5	FASNW007
KA3376B01	61	FASNW005
KA3376B01	63	FASNW004
KA3376B01	65	FASNW003

Borehole	BH Length (m)	Structure
KA3376B01	65.6	FASNW002
KA3376B01	71	FASNW009
KA3378A01	4.6	FASEW002b
KA3385A	7	FASNS002
KA3385A	17	FASNW013
KA3385A	25	FASNW013
KA3386A01	10.5	FASNW012
KA3386A01	20	FASNW013
KA3386A01	32.3	FASNW014a
KA3386A01	36.3	FASNW014b
KA3386A01	41	FASNW014c
KA3386A01	47	FASNW015
KA3386A01	50	FASNW016
KA3386A05	4.8	FASNW012
KA3386A06	3.3	FASNW012
KA3510A	11	FASNW021a
KA3510A	13	FASNW021b
KA3510A	19	FASNW021c
KA3542G02	5	FASNW021a
KA3554G02	4.5	FASNW021c
KA3554G02	8	FASNW021b
KA3554G02	12.65	FASNW021a
KA3566G02	13.2	FASNW021c
KA3566G02	13.3	FASNW021b
KA3566G02	20	FASNW021a
KA3590G02	26	FASNW021c
KA3590G02	28	FASNW021b
KAS02	405	FASEW003
KAS02	429	FASSH001
KAS02	464	FASNS002
KAS05	321	FASNW014b
KAS05	363	FASNW014c
KAS05	400	FASNW015
KAS05	491	FASNS002
KC0045F	19	FASNW010
KC0045F	56	FASNW008, FASNW007
KC0045F	68	FASNW009
KC0045F	86	FASNW006, FASNW005
KC0045F	94.5	FASNW004
KC0045F	99	FASNW003
KC0045F	102	FASNS001
KC0045F	113	FASNW002
KC0045F	114	FASNW001
KC0045F	131	FASEW001
KF0069A01	65	FASNW010
KG0021A01	10	FASNW018
KG0021A01	28	FASNW021a
KG0021A01	35.51	FASNW021b

Borehole	BH Length (m)	Structure
KG0021A01	35.54	FASNW021c
KG0027A01	9.5	FASNW018
KG0027A01	29	FASNW021a
KG0027A01	34	FASNW021b
KG0027A01	36	FASNW021c
KG0033A01	11	FASNW018
KG0033A01	29	FASNW021a
KG0033A01	35	FASNW021b
KG0033A01	37	FASNW021c
KG0048A01	5	FASNW018
KG0048A01	21	FASNW021a
KJ0044F01	10	FASNW013
KJ0050F01	12.7	FASEW002c
KJ0052F01	12.9	FASEW002c
KJ0052F02	9.1	FASEW002c
KJ0052F03	9.2	FASEW002c
KQ0053A01	6	FASEW001
KQ0053A02	6	FASEW001
KQ0053A03	6	FASEW001
KQ0053A04	6	FASEW001
SA3436B	??	FASNW014a
SA3436B	??	FASNW014b
SA3445A	??	FASNW014c
SA3454A	??	FASNW015
SA3509F	2	FASNW020
SA3509F	24	FASNW021a
SA3526F	7	FASNW021a
SA3526F	13	FASNW021b

Table of observation in BIPS

Structure FASEW001

Borhole ID	BIPS logging	Visible in BIPS	BIPS quality
KC0045F	No	No	
KA3376B01	Yes	Yes	Good
KQ0053A01	No	No	
KQ0053A02	No	No	
KQ0053A03	No	No	
KQ0053A04	No	No	
KA3191F	No	No	

Structure FASEW002a

Borhole ID	BIPS logging	Visible in BIPS	BIPS quality
KA3191F	No	No	
KA3375A05	Yes	Yes	Good

Structure FASEW002b

Borhole ID	BIPS logging	Visible in BIPS	BIPS quality
KA3378A01	Yes	Yes	Acceptable
KA3191F	No	No	

Structure FASEW002c

Borhole ID	BIPS logging	Visible in BIPS	BIPS quality
KJ0050F01	Yes	Yes	Acceptable
KJ0052F02	Yes	Yes	Acceptable
KJ0052F03	Yes	Yes	Good
KJ0052F01	Yes	Yes	Acceptable
KA2598A	No	No	
KA2162B	No	No	

Structure FASEW002d

Borhole ID	BIPS logging	Visible in BIPS	BIPS quality
No borehole			

Structure FASEW003

Borhole ID	BIPS logging	Visible in BIPS	BIPS quality
KAS02	No	No	
KA2162B	No	No	

Structure FASNS001

Borhole ID	BIPS logging	Visible in BIPS	BIPS quality
KC0045F	No	No	
KA2162B	No	No	
KA3191F	No	No	

Structure FASNS002

Borhole ID	BIPS logging	Visible in BIPS	BIPS quality
KA3376B01	Yes	Yes	Acceptable
KAS02	No	No	
KA3191F	No	No	
KA3385A	Yes	Yes	Bad
KAS05	No	No	
KA2162B	No	No	

Structure FASNW001			
Borhole ID	BIPS logging	Visible in BIPS	BIPS quality
KA3191F	No	No	
KC0045F	No	No	
Structure FASNW002			
Borhole ID	BIPS logging	Visible in BIPS	BIPS quality
KA3191F	No	No	
KC0045F	No	No	
KA3376B01	Yes	Yes	Good
Structure FASNW003			
Borhole ID	BIPS logging	Visible in BIPS	BIPS quality
KA3376B01	Yes	Yes	Good
KC0045F	No	No	
KA3191F	No	No	
Structure FASNW004			
Borhole ID	BIPS logging	Visible in BIPS	BIPS quality
KA3376B01	Yes	Yes	Good
KC0045F	No	No	
Structure FASNW005			
Borhole ID	BIPS logging	Visible in BIPS	BIPS quality
KA3376B01	Yes	Yes	Acceptable
KC0045F	No	No	
KA3191F	No	No	
Structure FASNW006			
Borhole ID	BIPS logging	Visible in BIPS	BIPS quality
KC0045F	No	No	
KA3191F	No	No	
Structure FSNW007			
Borhole ID	BIPS logging	Visible in BIPS	BIPS quality
KA3376B01	Yes	Yes	Good
KC0045F	No	No	
KA3191F	No	No	
KA2162B	No	No	
Structure FASNW008			
Borhole ID	BIPS logging	Visible in BIPS	BIPS quality
KA3191F	No	No	
KC0045F	No	No	
KA3376B01	Yes	Yes, weak	Acceptable
Structure FASNW009			
Borhole ID	BIPS logging	Visible in BIPS	BIPS quality
KA3191F	No	No	
KC0045F	No	No	
KA2162B	No	No	
KA3376B01	Yes	Yes	Good

Structure FASNW010			
Borhole ID	BIPS logging	Visible in BIPS	BIPS quality
KA3191F	No	No	
KC0045F	No	No	
KA3376B01	Yes	Yes	Good
KF0069A01	Yes	Yes	Good
Structure FASNW011a			
Borhole ID	BIPS logging	Visible in BIPS	BIPS quality
KA3191F	No	No	
Structure FASNW011b			
Borhole ID	BIPS logging	Visible in BIPS	BIPS quality
No borehole			
Structure FASNW011c			
Borhole ID	BIPS logging	Visible in BIPS	BIPS quality
No borehole			
Structure FASNW012			
Borhole ID	BIPS logging	Visible in BIPS	BIPS quality
KA3386A01	Yes	Yes	Good
KA3386A05	No	No	
KA3386A06	Yes	No	
KA2162B	No	No	
Structure FASNW013			
Borhole ID	BIPS logging	Visible in BIPS	BIPS quality
KA3386A01	Yes	Yes	Good
KJ0044F01	Yes	No	very bad
KA2162B	No	No	
KA2563A	Yes	Yes	Acceptable
KA3385A	Yes	Yes	Bad
Structure FASNW014a			
Borhole ID	BIPS logging	Visible in BIPS	BIPS quality
KA3386A01	Yes	Yes	Good
KA2563A	Yes	Yes	Good
SA3436B	No	No	
Structure FASNW014b			
Borhole ID	BIPS logging	Visible in BIPS	BIPS quality
KA3386A01	Yes	Yes	Good
KS05	No	No	
KA2162B	No	No	
KA2563A	Yes	Yes	Good
SA3436B	No	No	
Structure FASNW014c			
Borhole ID	BIPS logging	Visible in BIPS	BIPS quality
KA3386A01	Yes	Yes	Good
KAS05	No	No	
KA2563A	Yes	Yes	Good
SA3445A	No	No	

Structure FASNW015			
Borhole ID	BIPS logging	Visible in BIPS	BIPS quality
KAS05	No	No	
KA3386A01	Yes	Yes	Good
KA2162B	No	No	
KA2563A	Yes	Yes	Acceptable
SA3454A	No	No	
Structure FASNW016			
Borhole ID	BIPS logging	Visible in BIPS	BIPS quality
KA3386A01	Yes	Yes	Good
Structure FASNW017			
Borhole ID	BIPS logging	Visible in BIPS	BIPS quality
KA2563A	Yes	Yes	Acceptable
Structure FASNW018			
Borhole ID	BIPS logging	Visible in BIPS	BIPS quality
KA2563A	Yes	Yes	Acceptable
KG0048A01	Yes	Yes	Acceptable
KG0021A01	Yes	Yes	Acceptable
KG0027A01	Yes	Yes	Good
KG0033A01	Yes	Yes	Acceptable
Structure FASNW019n			
Borhole ID	BIPS logging	Visible in BIPS	BIPS quality
2598A	No	No	
Structure FASNW019s			
Borhole ID	BIPS logging	Visible in BIPS	BIPS quality
KA2563A	Yes	Yes	Acceptable
KA2511A	Yes	Yes	Good
Structure FASNW020			
Borhole ID	BIPS logging	Visible in BIPS	BIPS quality
KA2563A	Yes	Yes	Acceptable
KA2511A	Yes	Yes	Good
Structure FASNW021a			
Borhole ID	BIPS logging	Visible in BIPS	BIPS quality
KA3510A	Yes	Yes	Acceptable
KG0021A01	Yes	Yes	Acceptable
KA3542G02	Yes	Yes	Good
KA3554G02	Yes	Yes	Good
KA2563A	Yes	Yes	Acceptable
KG0048A01	Yes	Yes	Acceptable
KG0027A01	Yes	Yes	Acceptable
KG0033A01	Yes	Yes	Acceptable
KA3566G02	Yes	Yes	Good
KG0023A01	Yes		
SA3526F	No	No	
SA3509F	No	No	

Structure FASNW021b

Borhole ID	BIPS logging	Visible in BIPS	BIPS quality
KA3554G02	Yes	Yes	Good
KA3590G02	Yes	Yes	Good
KA3510A	Yes	Yes	Acceptable
KA2563A	Yes	Yes	Good
KG0048A01	Yes	Yes	Acceptable
KG0027A01	Yes	Yes	Acceptable
KG0033A01	Yes	Yes	Acceptable
KG0021A01	Yes	Yes	Acceptable
KA3566G02	Yes	Yes	Good
SA3526F	No	No	

Structure FASNW021c

Borhole ID	BIPS logging	Visible in BIPS	BIPS quality
KG0021A01	Yes	Yes	Acceptable
KA3590G02	Yes	Yes	Good
KA3510A	Yes	Yes	Acceptable
KA3554G03	Yes	Yes	Good
KG0048A01	Yes	Yes	Acceptable
KA2563A	Yes	Yes	Bad
KG0027A01	Yes	Yes	Acceptable
KG0033A01	Yes	Yes	Acceptable
KA3566G02	Yes	Yes	Good
SA3526F	No	No	

Structure FASSH001

Borhole ID	BIPS logging	Visible in BIPS	BIPS quality
KAS02	No	No	